

Copyright is owned by the Author of the thesis. Permission is given for a copy to be downloaded by an individual for the purpose of research and private study only. The thesis may not be reproduced elsewhere without the permission of the Author.

**SEDIMENTOLOGY AND PALEOENVIRONMENTAL ANALYSIS OF
CASTLECLIFFIAN STRATA IN THE DANNEVIRKE BASIN**

A thesis presented
in partial fulfilment of the requirements
for the degree
of Master of Science in
Quaternary Science at
Massey University

**FRANCIS WILLIAM KRIEGER
1992**

*Copied from microfiche.
Best copy available.*

ABSTRACT

Castlecliffian deposits of the Mangatarata Formation are widespread in the Dannevirke Basin, a fault angle depression on the east coast of North Island, New Zealand. The basin is 80km long and 19-24km wide, is bounded to the east by the upthrust Waewaepa-Oruawharo High and to the west by the upthrust front of the Ruahine Ranges. The basin floor is broken by three major axial-trending anticlinal folds.

Basin development began during early Pliocene times with subsidence continuing into the Nukumaruan. Uplift during Castlecliffian time was accompanied by deposition of the Mangatarata Formation.

Four facies associations are recognised in deposits of the Mangatarata Formation. Facies association one comprises greywacke rubble and gravel deposited in proximal to distal alluvial fan environments. Facies association two is dominated by fluvially deposited, cross-bedded sand and gravelly sand with associated overbank fine deposits. Facies association three is generally a fossiliferous, flaser bedded silt to fine grained sand, deposited in a tidal/estuarine environment. Facies association four is a rarely fossiliferous, fine grained, centimetre bedded silt deposited in a locally subsiding, interfluvial lacustrine environment.

Pumice deposits derived from erosion of unwelded ignimbrite originating in the Taupo Volcanic Zone are significant components of facies association two. They show a range of sedimentary structures associated with rapid deposition. The thickest pumice units, up to 30m, are interpreted to have been deposited in a meandering fluvial environment and display features typical of hyperconcentrated flow and streamflood deposits.

It is possible, using identified pumice units as marker beds, to express the physical and temporal extent of specified sedimentary environments. The boundary between fluvial and tidal/estuarine environments and thus approximate paleoshoreline shows that the overall sea-level trend during the Castlecliffian was one of regression.

Superimposed on this trend are at least ten episodes of transgression related to eustatic sea-level rise. These alternating cycles of tidal/estuarine to terrestrial sediments are interpreted as cyclothems deposited dominantly during 100,000 and 40,000 year long, c. 80-130m magnitude, fifth and sixth order orbitally forced glacio-eustatic sea-level cycles and represent Oxygen Isotope stages 21 to 39.

Thinning of pumice tuffs younger than the Rewa Pumice (c.1.0 Ma) toward anticlinal crests suggests that strata younger than this were deformed contemporaneously with deposition, while strata older than the Rewa Pumice show no evidence of syndepositional deformation. This coincides with the restriction of alluvial fan deposits to the west of the study area due to the growing Dannevirke Anticline, between deposition of the Rewa Pumice (c.1.0 Ma) and the Potaka Pumice (c.0.80 Ma).

ACKNOWLEDGEMENTS

I would like to thank my joint supervisors, Mrs Julie Palmer and Dr Vince Neall for their guidance, advice and support. I would also like to thank Dr Alan Palmer who contributed much in the way of discussion and suggestion. Thanks must also go to Dr Bob Stewart and Dr Clel Wallace for their help with mineralogy.

I am indebted to Dr Margaret Harper, Victoria University for diatom identification and Dr Alan Beu, DSIR for fossil identification and advice.

I am also indebted to Mrs Ann Rouse for help and advice in preparation of this thesis.

Finally, thanks must go to Mum, Dad and especially Claire for their constant encouragement and support throughout the course of this study.

TABLE OF CONTENTS

TITLE PAGE	i
ABSTRACTii
ACKNOWLEDGEMENTS	iv
TABLE OF CONTENTS	v
LIST OF FIGURES	ix

CHAPTER 1 INTRODUCTION

1.1 Objective and scope of study	1
1.2 Location	1
1.3 Methods	3
1.4 Regional setting	3
1.4.1 Physiography	3
1.4.2 Geology and previous work	5
1.5 Dannevirke Basin tectonic history	7
1.6 Structures within the Dannevirke Basin	10

CHAPTER 2 STRATIGRAPHY

2.1 Introduction	12
2.2 Stratigraphy	12
2.2.1 Mangatewainui Stream	13
2.2.2 Mangatewaiiti Stream	14
2.2.3 Whakaruatapu Stream	17
2.2.4 Mangatera Stream	18
2.3 Correlation	20
2.4 Conclusions	23

CHAPTER 3 MINERALOGY

3.1	Introduction	25
3.2	Methods	25
3.3	Mineralogical results	25
3.3.1	Glass	25
3.3.2	Quartz	26
3.3.3	Feldspar	26
3.3.4	Orthopyroxene	27
3.3.5	Clinopyroxene	27
3.3.6	Micas	27
3.3.6.1	Biotite	27
3.3.6.2	Muscovite	28
3.3.7	Glaucouite	28
3.3.7.1	Origin of glaucouite	28
3.3.8	Opaque minerals	29
3.3.9	Rock fragments	29
3.5	Provenance	29

CHAPTER 4 GRAIN SIZE ANALYSIS

4.1	Introduction	30
4.2	Methods	30
4.2.1	Sand	30
4.2.2	Silt and clay	31
4.3	Theory of pipette analysis	31
4.4	Calculation of results	31
4.4.1	Advantages of the grain size analysis programme	32
4.5	Graphically generated parameters versus moment measures	33
4.6	Graphical representation of parameters	33
4.7	Grain size analysis results and discussion	34
4.7.1	Relationship between mean size and sorting	35

4.7.2	Relationship between mean cubed deviation and sorting	39
4.7.3	Relationship between fine and coarse tails and sorting	41
4.7.4	Relationship between skewness and sorting	45
4.8	Environmental interpretation	45
4.9	Conclusion	46

CHAPTER 5 PALEOCURRENT ANALYSIS

5.1	Introduction	48
5.2	Data collection and processing	49
5.3	Reliability of large and small scale cross-stratification as direction indicators	50
5.4	Results and discussion	50
5.4.1	Regional variation	50
5.4.2	Variation in current direction with time	52
5.5	Sediment transport determined from gravel parameters	54
5.5.1	Methods	55
5.5.2	Results and discussion	55
5.6	Conclusions	55

CHAPTER 6 FACIES ANALYSIS AND PALEOENVIRONMENTAL INTERPRETATION

6.1	Introduction	57
6.2	Facies association one	58
6.2.1	Distribution and age	62
6.2.2	Paleoenvironmental interpretation	62
6.2.3	Fan geometry	65
6.3	Facies association two	66
6.3.1	Facies description (Fc)	66
6.3.2	Paleoenvironmental interpretation	68
6.3.3	Facies description (Fb)	74

6.3.4	Paleoenvironmental interpretation	74
6.3.5	Facies description (Fp)	76
6.3.6	Paleoenvironmental interpretation	76
6.3.7	Age	78
6.4	Facies association three (Td)	78
6.4.1	Age	80
6.4.2	Paleoenvironmental interpretation	80
6.5	Facies association four (Lc)	82
6.5.1	Facies description	82
6.5.2	Age	84
6.5.3	Paleoenvironmental interpretation	84
6.6	Pumice deposits	85
6.7	Conclusions	95

CHAPTER 7 SEDIMENTATION HISTORY

7.1	Introduction	98
7.2	Castlecliffian cyclothems	103
7.3	Timing of folding	106
7.4	Concluding remarks	108

REFERENCES		110
------------	--	-----

APPENDIX A	Paleocurrent data	120
APPENDIX B	Diatoms	124
APPENDIX C	Fossil identification	128
APPENDIX D	Grain size analysis data	130

LIST OF FIGURES

Figure 1.1	Location map of study area	2
1.2	Physiography of the Dannevirke area	4
1.3	Tectonic setting of the Dannevirke Basin	6
1.4	Geological map of the Dannevirke Basin	8
Figure 2.1	Mangatewainui Stream stratigraphy	Rear pocket
2.2	Mangatewaiiti Stream stratigraphy	Rear pocket
2.3	Whakaruatapu Stream stratigraphy	Rear pocket
2.4	Mangatera Stream stratigraphy	Rear pocket
2.5	Chronostratigraphy	21
2.6	Pumice distribution	22
Figure 4.1	Textural boundaries and grain size analysis methods	30
4.2	Scatter plot of standard deviation versus mean for silt and sand	36
4.3	Scatter plot of standard deviation versus mean for sand	37
4.4	Scatter plot of standard deviation versus mean for silt	38
4.5	Scatter plot of mean cubed deviation versus standard deviation for sand and silt	40
4.6	Scatter plot of standard deviation versus > 500 micron fraction	42
4.7	Scatter plot of standard deviation versus < 63 micron fraction	43
4.8	Scatter plot of skewness versus standard deviation for sand . . .	44
Figure 5.1	Current rose diagrams	51
5.2	Stratigraphic variability in current direction	53
Figure 6.1	Subfacies Af ₁ , proximal alluvial fan deposits	59
6.2	Subfacies Af ₂ , medial alluvial fan deposits	60
6.3	Subfacies Af ₂ , fining-up cross-bedded gravel	61

6.4	Subfacies Af ₃ , distal alluvial fan deposits	63
6.5	Subfacies Fc ₂ , silt rip-up clasts showing preferred orientation	67
6.6	Subfacies Fc ₁ , random orientation of silt rip-up clasts	67
6.7	Subfacies Fc ₂ , fining-up point bar deposit	69
6.8	Bedform stability fields	71
6.9	Definition diagram for cross-stratification description	71
6.10	Reactivation surfaces	72
6.11	Point bar accretion followed by channel abandonment	73
6.12	Paleo-root channels	75
6.13	Weathered, fractured silt overlain by lignite	77
6.14	Flaser bedding	79
6.15	Herringbone cross-bedding	81
6.16	Shallow dwelling burrow	83
6.17	Pumiceous, hyperconcentrated flow deposit	86
6.18	Water escape structures	88
6.19	Convolute laminated beds	89
6.20	Irregular, convolute laminated beds	90
6.21	Overtuned cross-stratification	90
6.22	Pumice deposits indicative of streamflood processes	92
6.23	Fining-up airfall pumice in gravel	93
6.24	Pumice in contact with lignite	94

Figure 7.1	Paleogeographical changes accompanying deposition of the Mangatarata Formation	101
7.2	Correlation between Wanganui Basin and Dannevirke Basin cyclothems	104
7.3	Correlation between Dannevirke Basin cyclothems and Oxygen Isotope stratigraphy	107

CHAPTER ONE

INTRODUCTION

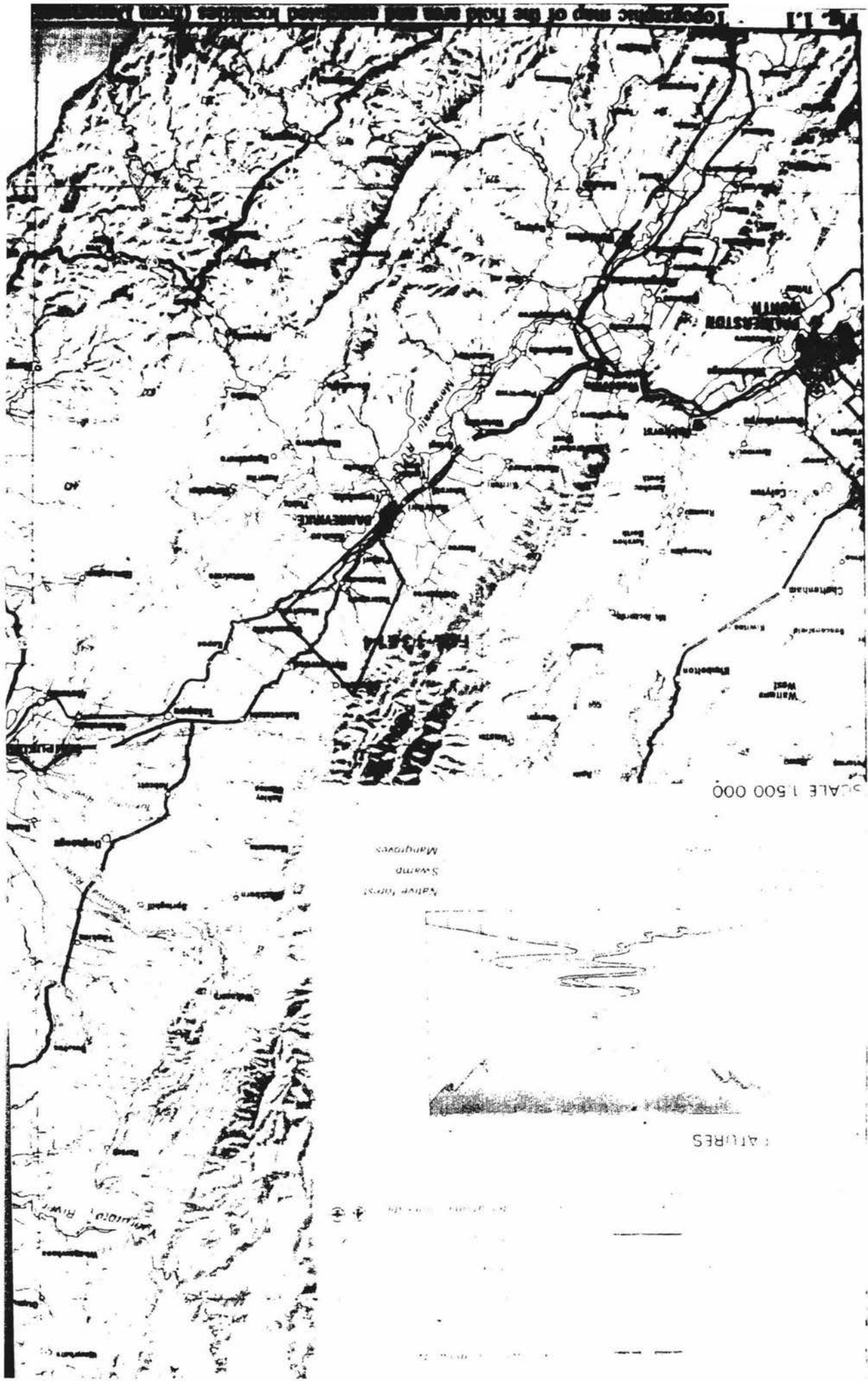
1.1 Objective and scope of study

Castlecliffian strata near Dannevirke were first mapped in detail and described by Lillie in 1953. Of prime importance for correlation, six pumice tuffs were recognised within a sequence of both terrestrial and nearshore marine sediments. Recent work identifying and correlating these tuffs within the Dannevirke Basin (Melhuish, 1990) has now provided the stratigraphic basis for a detailed paleoenvironmental reconstruction of the Basin.

The aim of this study was to make a paleoenvironmental reconstruction of Castlecliffian strata in the Dannevirke Basin by integrating tectonic setting, lithofacies and paleocurrent information into a paleogeographic model and to relate the sedimentation history to relative sea level change during the Castlecliffian.

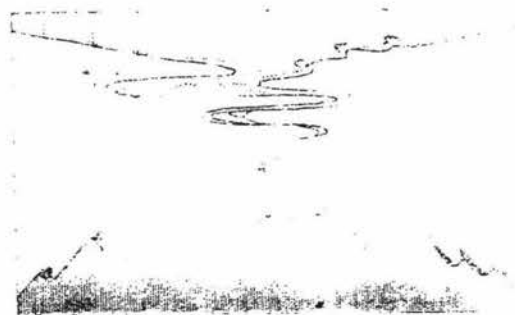
1.2 Location

The study area is located in the Dannevirke district, of southern Hawkes Bay (Fig. 1.1). The area is bounded to the north by the Mangatewainui Stream and to the south by the Mangatera Stream. The western boundary is the Range Front Fault (Melhuish, 1990), where Castlecliffian sediments lie adjacent to upthrust Mesozoic greywacke. To the east the boundary is defined by the confluence of the Mangatewainui and Mangatewaiiti streams and further south by the Napier Highway. The Whakaruatapu Stream is the only other major stream to cross the field area. Dannevirke township (Fig. 1.1), situated at the southeastern boundary of the study area, services the surrounding rural community which is involved predominantly in dairy and sheep farming.



SCALE 1:500 000

Natural forest
Swamp
Mangroves

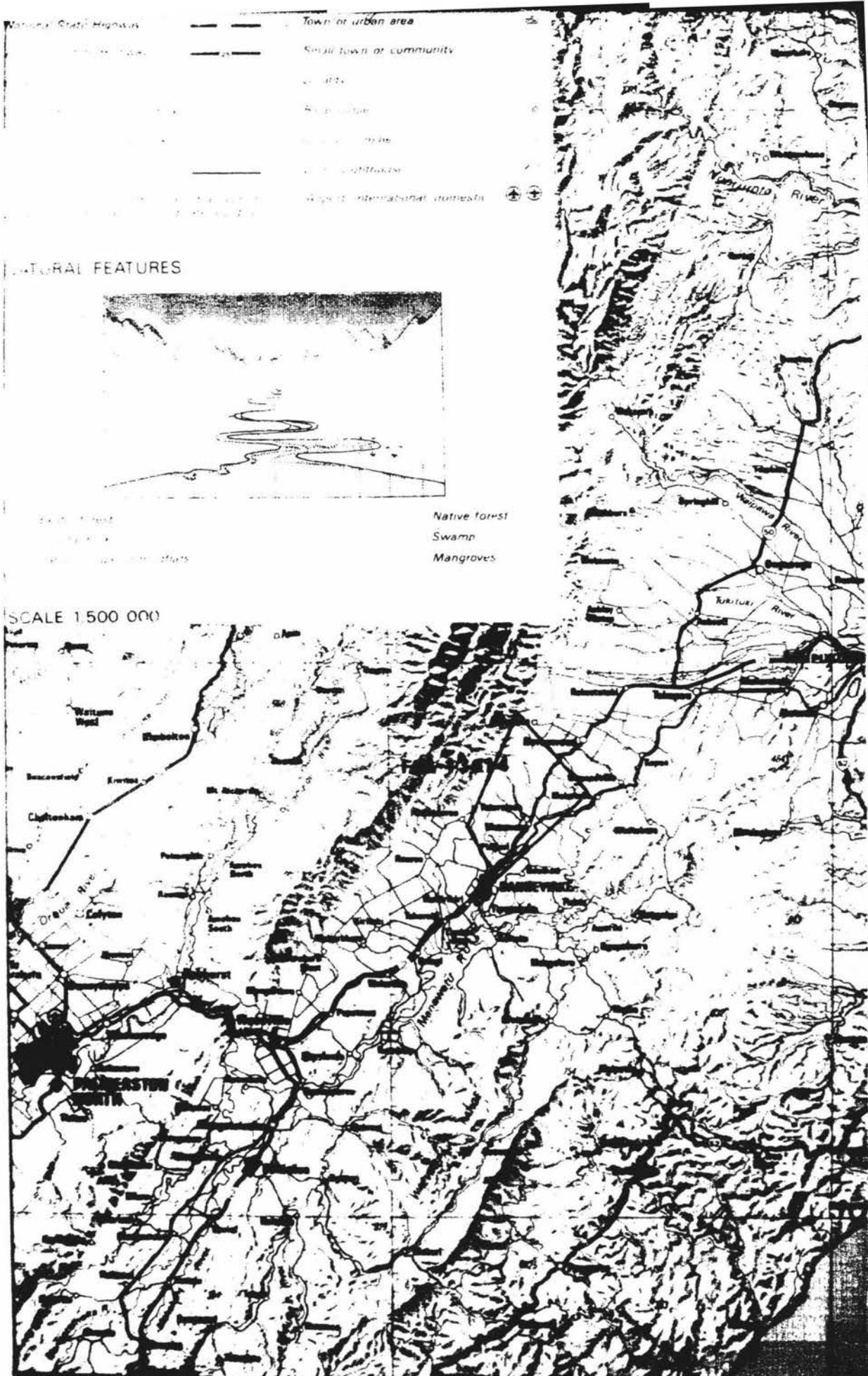


FEATURES



Scale 1:500 000

Map of the ...



The field area comprises a relatively well exposed sequence with a variety of terrestrial and estuarine/tidal facies.

1.3 Methods

The four streams mentioned above were mapped using 1:25000 aerial photos. Wherever good outcrop was exposed sections were logged in detail. All available paleocurrent data (Chapter six) and structural data (dip and dip directions) were collected. Samples for grain size analysis and identification of mineralogy, were collected wherever it appeared this information would be useful *e.g.* where there was a change in lithology, grain size or mineralogy. All data collected were plotted on 1:25000 topographic base map and stratigraphic columns (Fig. 2.1, 2.2, 2.3, and 2.4) were drawn showing the distribution of sediments from which facies associations were recognised.

1.4 Regional setting

1.4.1 Physiography

Two features dominate the physiography of the Dannevirke district. To the east, the NNE-trending Ruahine Range rises to heights of greater than 1500m. Mesozoic rocks comprising complexly deformed, highly indurated, flysch sequences with associated spilite and chert make up the strata of the Range and form the regional basement. The second feature dominating the physiography of the Dannevirke district is the sequence of four main terraces. Of the four main terraces recognised (B,C,D, and E, Fig. 1.2) one (B) is younger than the Aokautere Ash (22.5 ky) and three are older (Rhea, 1968). Minor terraces younger than Terrace B together with the floodplains of the rivers are grouped under Terrace A. The three older terraces are moderately dissected and gently undulating, and are covered by thick loess. The vertical interval between terrace surfaces varies but it is in the order of 10-20m. Except where disturbed by faulting at localities 1 and 2 (Fig. 1.2), post-Aokautere Ash terraces are flat with few

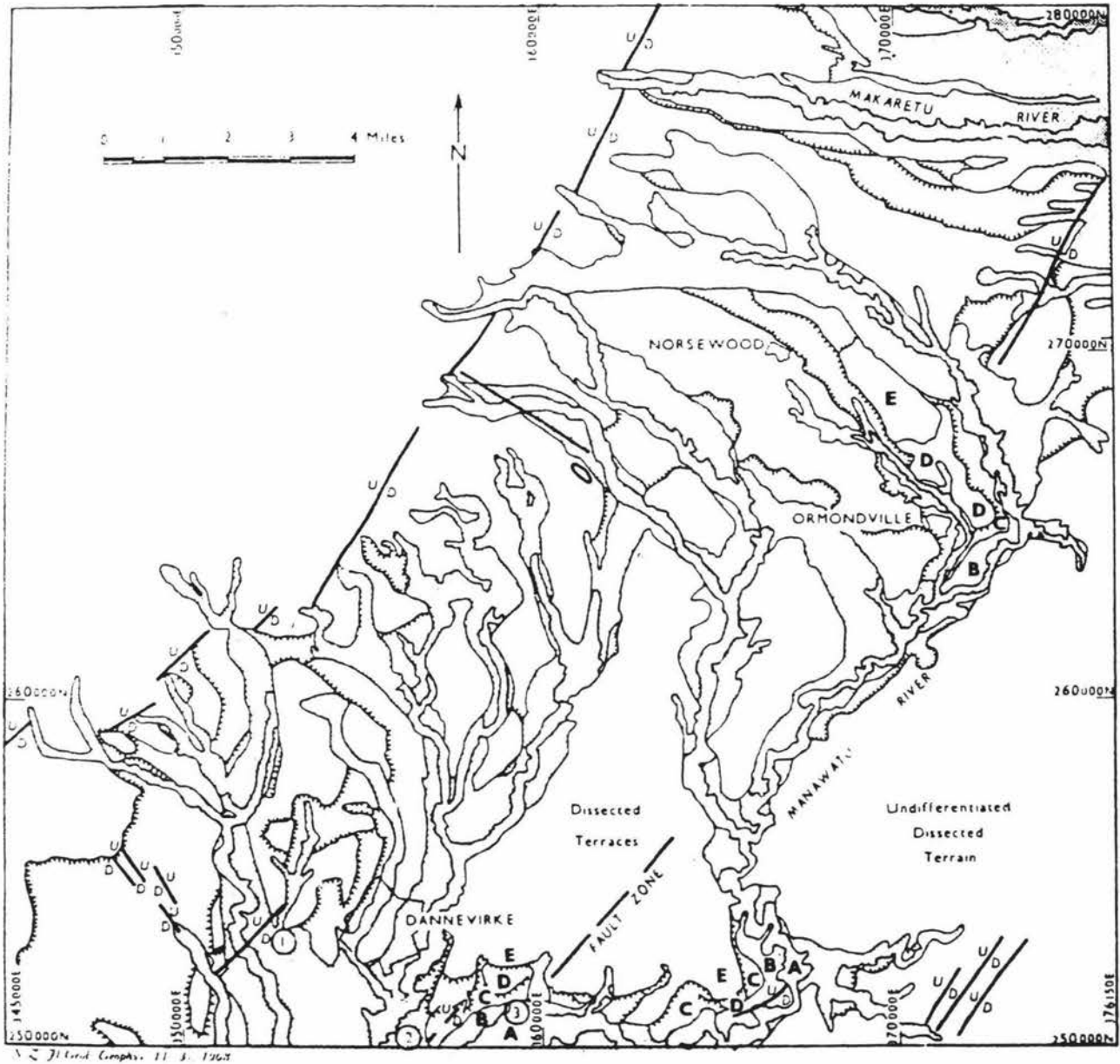


Fig. 1.2 Map of river terraces in Dannevirke district. Young minor terraces and flood plains are finely stippled (A). Terrace B, the oldest post-Aokautere Ash terrace is coarsely stippled. Terraces C, D, and E are pre-ash terraces. Traces of active faults are shown by bold dashes. Numbers in circles mark localities mentioned in text (from Rhea, 1968).

undulations, and are commonly covered by gravelly soil and marked by shallow branching channels that clearly show on aerial photos. They have well defined and steep risers. Terrace B is underlain by as much as 3m of gravel. At locality 3 (Fig. 1.2) these gravels unconformably overlie strongly iron-stained, non-marine, aggradational, pre-Aokautere Ash, terrace gravel. Terrace B, the terrace immediately younger than the Aokautere Ash, is the most extensive terrace in the district, is well defined, and is correlated with the Ohakea terrace in the Manawatu district (Cowie and Wellman, 1962; Cowie, 1964a,b). The base of the Ohakea loess is dated at 25500 yrs B.P. by radiocarbon dating and the top is older than 9450 yrs B.P. The deposition time of the Ohakea loess corresponds to the latest Quaternary cold period (Milne and Smalley, 1979); also the time of Terrace B aggradation. Terraces B,C,D and E represent significant periods of aggradation. By contrast the recent terraces that are grouped together as "A" are not extensive and mark pauses in the period of river downcutting that is still continuing.

1.4.2 Geology and previous work

The Dannevirke Basin (Fig. 1.3), first outlined by McKay (1877), is essentially a fault-angle depression 80kms long and 19-24kms wide. It is formed by a westward tilted block upthrust along the Waewaepa-Oruawharo High to the east (Turner, 1944) (Fig. 1.4). The High is faulted on its eastern margin with a stratigraphic throw of c.2000m (Laing, 1961). A greywacke erosion surface is preserved across the High and on its western boundary. It is covered by Taranaki to Opoitian aged sediment, dipping 20° to the west.

In the west Tertiary aged cover beds are drag folded against the upthrust front of the greywacke basement of the Ruahine Range, giving the Basin a general asymmetrical synclinal structure with a short, steeply east-dipping west limb and a long, gently west-dipping east limb. This east limb makes up most of the Basin floor. It is broken by several axial trending faults which repeat the structure of the block as a whole and cause local accentuation of the general westward tilt. In places asymmetrical anticlinal folds

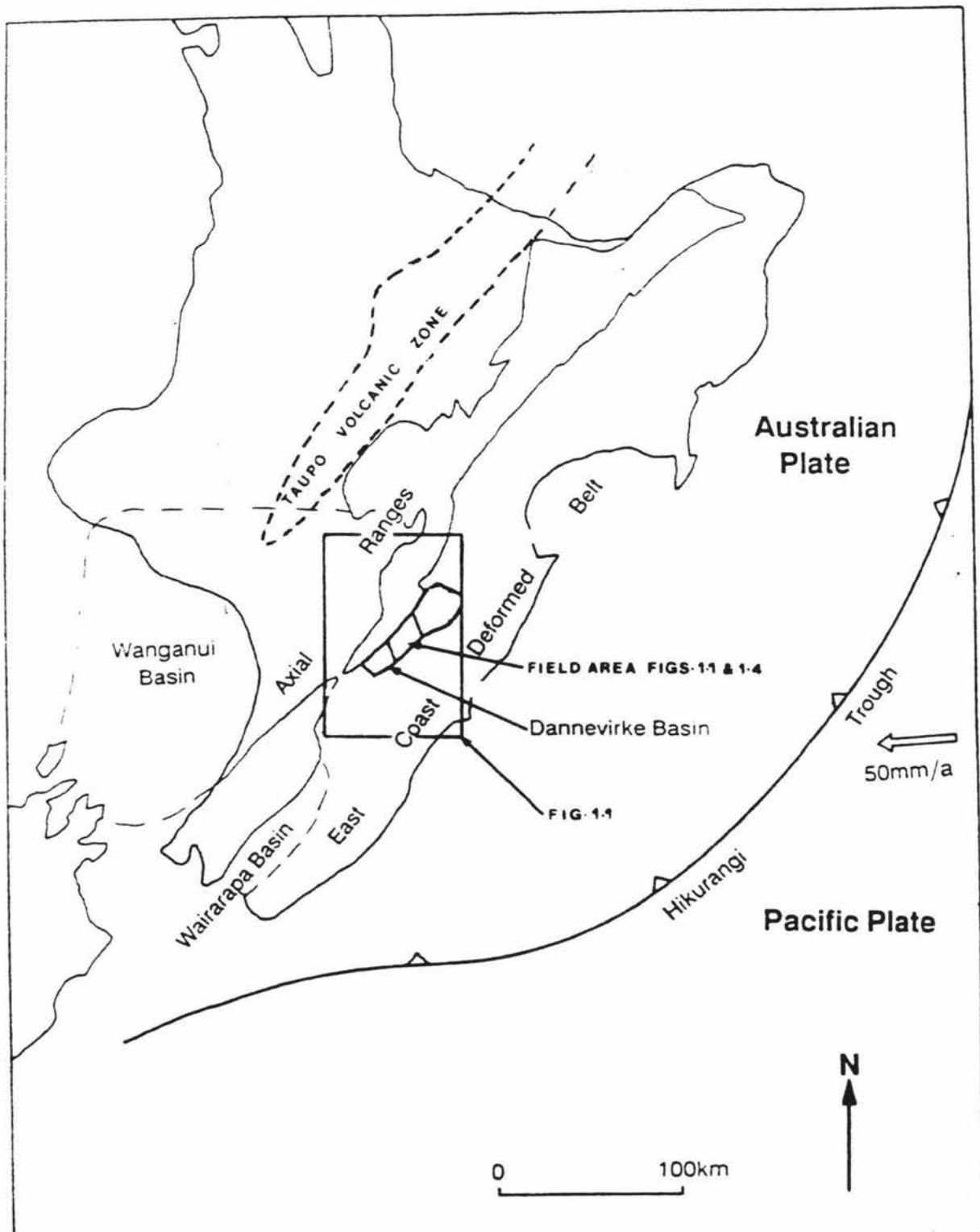


Fig. 1.3 Tectonic setting of the Dannevirke Basin (modified from Melhuish, 1990).

are superimposed which are probably the surface expression of further faulting in the basement (Firth and Feldmeyer, 1943; Melhuish, 1990).

The greywacke basement has been stripped of Tertiary cover beds at several places exposing a line of basement "highs" which form a natural eastern limit to the Basin. A similarly upthrust basement "high" is exposed within the Basin near Kumeroa, northeast of Woodville (Fig. 1.1). This basement high conveniently divides the Basin into a northern or Dannevirke section, and a southern or Pahiatua section (Firth and Feldmeyer, 1943).

The Kumeroa greywacke "high", first mentioned by Thomson (1914) forms the prominent Morgan's Hill and is steeply dipping with an erosion plane on its western edge covered by basal Tertiary conglomerates. At its northern extremity there are several splinter faults considered to run with decreasing throw into the Dannevirke Anticline, and along its eastern edge a prominent scarp overlooking the Manawatu River marks the line of the Kumeroa Fault, which is contiguous with the Dannevirke Anticline.

1.5 Dannevirke Basin tectonic history

During the early Pliocene the sea extended across most of the southern part of the North Island (Lillie, 1953). At this time a basin of sedimentation began to form to the east of the present axial range, with the west flank of the basin extending towards the present range crest. The strike of this basin appears to have been nearly north-south. A number of faults developed at this time and some were active during the whole period of basin development (Lillie, 1953). Development of the basin continued during the Waipipian (3.0-2.5 Ma) with sediments deposited consisting mainly of sands, mud and local gravel. The area of the present range crest was largely still submerged. Basin subsidence associated with faulting continued into the Mangapanian (2.5-2.0 Ma).

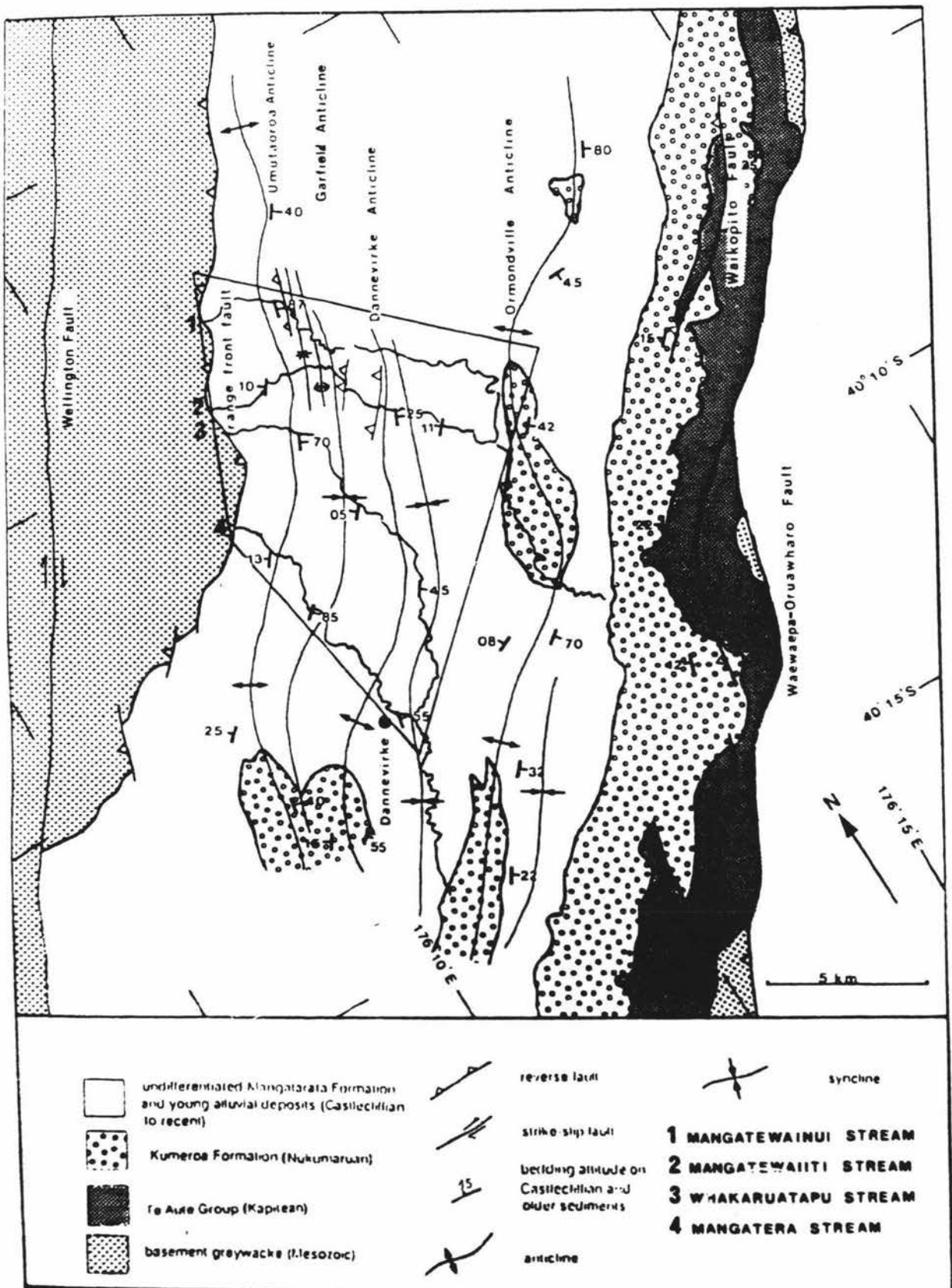


Fig. 1.4

Simplified geological map of the southern part of the Dannevirke Basin (modified from Melhuish, 1990).

During the Hautawan and Nukumaruan (2.0-1.26 Ma) the Dannevirke-Pahiatua Basin continued to deepen, but sedimentation was confined to the area west of the Waewaepu Oruawharo High.

In latest Pliocene - early Pleistocene times the seaway extending from Hawkes Bay to the Wairarapa became constricted in the vicinity of Mt. Bruce and about 1.5 Ma independent drainage basins developed, with the Dannevirke-Pahiatua Basin to the north and the Masterton Basin to the south (Kamp and Vucetich, 1982).

The sudden incoming of floods of pumice, derived chiefly from erosion of unwelded pyroclastic flow deposits originating from the Taupo Volcanic Zone (Kamp, 1981), in the Basin during the Castlecliffian (1.0-0.4 Ma) marked a lithological change from marine mudstone to laminated, interbedded estuarine muds, silts and sands of the Mangatarata Formation (Firth and Feldmeyer, 1943).

The Mangatarata Formation was first used by Quennel (1937), for a group of pumiceous silts with lignites and sands interbedded with gravels which occur in the Mangatarata Valley southeast of Waipukurau (Fig. 1.1). Quennel described these beds as gently tilted to the west and resting on all underlying formations from the Whangai Formation upwards. Quennel (1938) also included in the Formation pumiceous silts, sands and gravels which conformably overlie Nukumaruan beds in the Takapau and Norsewood survey districts. Bands of white pumice sand, cemented gravel, and lignite are unique to the formation, and were assigned Castlecliffian age (Lillie, 1953). In the Mangatewainui Stream the uppermost beds of the Nukumaruan aged Kumeru Formation show the change from offshore marine sedimentation to estuarine and fluvial conditions that characterise the Mangatarata Formation. Thick mudstones containing bands of lignite and shellbeds are indicative of mudflat conditions with swampy vegetation. *Austrovenus stutchburyi* is the dominant species. It is small shelled (suggesting stunting through low salinity), thin shelled (suggesting acid conditions), flat (suggesting lack of wave action) (Lillie, 1953).

Shane (1989) and Melhuish (1990), have distinguished several different rhyolitic tuffs in the Mangatarata Formation of the Dannevirke Basin. It is these tuffs which aid in basin wide correlation by creating stratigraphic marker beds which give time planes across the entire basin allowing approximate rates of sedimentation to be calculated. Tentative correlations can also be made with tuffs in the Rangitikei Valley and in the southern Wairarapa on the basis of mineralogy, glass chemistry and palaeomagnetism (Shane, 1989).

The Mangatarata Formation was tilted and folded by the Kaikoura Orogeny. The beds in general strike N 25 E and dip 6-10 degrees to the NW (Lillie, 1953; Piyasin, 1966). Due to the tilting and folding there is usually marked unconformity between the Mangatarata and younger strata (Lillie, 1953). The thickness of the formation decreases southward from Norsewood (Fig. 1.1), (Leslie and Hollingsworth, 1972). At Norsewood the thickness is at least 600m (Lillie 1953), but thins to less than 100m, 5km south of the Manawatu Gorge (Fig. 1.1) where Piyasin (1966) considered the whole of the Mangatarata Formation was represented. Farther south in the Eketahuna region (Fig. 1.1), Ongley (1935) and Neef (1984) found the Mangahao Formation, the equivalent of the Mangatarata Formation, to be less than 60m thick.

1.6 Structures within the Dannevirke Basin

The general synclinal structure of the Dannevirke Basin is broken by three strongly asymmetrical anticlines, all with steep eastern limbs and gentle western limbs. All three structures have a general plunge to the north, with the result that Castlecliffian strata dominate the surface exposures north of Dannevirke, Nukumaruan strata dominate the area south of Dannevirke, while Waitotoran strata crop out in the south of the basin at Kumeroa (Firth and Feldmeyer, 1943).

The western or Umutaoroa anticline (Fig. 1.4) maintains a northerly plunge and it is clearly defined throughout the field area in Castlecliffian beds. Its strike carries it

closer to the western margin of the basin, until at the Makaretu River north of the field area it is only 1km from the Range Front Fault (Melhuish, 1990).

The central or Dannevirke anticline (Fig. 1.4) is traceable north over a distance of 19km to the Norsewood area. At Dannevirke it converges on the western anticline until their axes are only 1.5km apart. The high dips on the east limbs of both structures in this locality suggest the possibility that both folds may be grading into faults here and to the south.

The eastern or Ormondville anticline (Fig. 1.4) is well defined over a distance of 40km from the Makaretu River west of Takapau (Fig. 1.1) in the north, to Kumeroa in the south (Firth and Feldmeyer, 1943). To the north of the field area a small, north plunging anticline lies between the western and central anticlines. It appears to die out to the south but it is not known whether this is due to closure or whether it grades into a fault.

The only fault apparent at the surface in the field area is a reverse fault with an offset of *c.* 100m. It lies *c.* 2 km west of the Dannevirke anticline in the Mangatewaiiti Stream (Fig. 1.4). Melhuish (1990) has identified other subsurface faults in the field area using seismic profiles and tuff correlation.

CHAPTER TWO

STRATIGRAPHY

2.1 Introduction

In order to reconstruct depositional environments and a paleogeography it is necessary to define a stratigraphic framework for correlation. Lithostratigraphy based on observable lithologic features including composition and grain size, biostratigraphy based on fossil content and chronostratigraphy based on dating of identified pumice units were all used in establishing the stratigraphic sequence of the field area.

Pumiceous tuffs identified by Melhuish (1990) on the western side of the Napier Highway (S.H.2) are used as stratigraphic marker beds throughout the field area. These provide age control and time plane marker beds useful in correlation between streams. Where pumiceous tuff units were not identified by Melhuish (1990) stratigraphic position has been used for identification. Stratigraphic data for the four streams mapped are presented in Figs. 2.1, 2.2, 2.3 and 2.4.

2.2 Stratigraphy

The limit of the stratigraphic sequence of interest in this study is the Nukumaruan (Wn) - Castlecliffian (Wc) boundary. The boundary, as described by Lillie (1953), is only exposed at one locality in the field area *i.e.* in the Mangatewainui Stream, where sandy mudstone with sandstone bands of the upper Kumeroa Formation grades into the fossiliferous siltstones of the Mangatarata Formation. Lillie (1953) used biostratigraphy as the basis for the boundary between the Kumeroa and Mangatarata formations. This change is not readily identifiable in the field so the boundary is accepted in this study as being in the same position as defined by Lillie, (1953). The Wn-Wc boundary is located approximately half way between the confluence of the Mangatewainui and Mangatewaiiti Streams and the Matamau-Ormondville Road at grid reference (G.R.) U23 828147.

2.2.1 Mangatewainui Stream

The lower 100m of the Mangatarata Formation is exposed in the west flank of Ormondville Anticline in the Mangatewainui Stream. It consists of banded siltstone with scattered shellbeds up to 3m thick, composed almost entirely of poorly preserved *Austrovenus stutchburyi* and occasional reworked Nukumaruan fossils (A.G. Beu, pers. comm., 1990). No marine shellbeds were seen at more than 7m above the Wn-Wc boundary or farther to the west in the Mangatewainui Stream. Within the lower 100m of the sequence two pumice tuffs crop out. The first, a 3m thick, centimetre bedded (cmbdd) pumice sand comprising successive fining-upward sequences occurs about 30m above the base of the Mangatarata Formation and is tentatively correlated with the Pakihikura Pumice identified by Shane, (1989) in this area. The second tuff, is a 3m thick pumice silt with a trough cross-bedded base grading up to a massive silt. This unit occurs approximately 70m above the base of the formation. This tuff is correlated on stratigraphic position with 'chemistry F' of Melhuish (1990). The pumice beds and shellbeds occur rarely in comparison to the organic rich, cmbdd to massive silts grading up into lignite (<0.20m) which dominate the lower 100m of the Mangatarata Formation.

Approximately 100m above the base of the Formation the first of a series of organic rich, cmbdd, silt beds crop out. The first of these silt beds is 0.75m thick, contains sparse fossils of the freshwater mussel, *Hyridella menziesi*. The uppermost bed containing *H. menziesi* occurs c.180m higher in the sequence. A second pumice unit is encountered 165m above the base of the Mangatarata Formation. This pumice unit is up to 3m thick and is usually a coarse pumice silt. It has been correlated on stratigraphic position with the Rewa Pumice which has been identified by Melhuish (1990) farther to the west. As with 'chemistry F', the Rewa Pumice is preceded and followed by sequences of organic rich silts up to 10m thick with interbedded lignite up to 0.30m thick. Between the top of these carbonaceous silts and a fourth major pumice unit, at 350m, there is very little exposure. This fourth tuff is again a cmbdd silt and has been corre-

on stratigraphic position with tuff 'chemistry A' of Melhuish (1990), being the youngest tuff identified in the field area.

Strata cropping out in the east and west flanks of the Dannevirke and Umutaoroa anticlines are dominantly terrestrial lithologies but due to increasing structural complexity less of the sediment is represented at the surface. These terrestrial deposits are dominated by greywacke rubble, reaching a maximum thickness of 400m adjacent to the Ruahine Range. The rubble closest to the Range is very poorly sorted, angular, clast supported and contains interbedded silt horizons less than 1m thick. Few lignite beds occur within these rubble sequences. Tuffs 'chemistry C' and the Rewa Pumice are the only two pumice units seen in outcrop. Tuff 'chemistry C' thins to a 0.50m fining-upwards bed at the western margin of the basin. The Rewa Pumice on the other hand is 3-4m thick at the western edge of the basin. Toward the centre of the field area gravels are rounded, slightly weathered and clast supported with interbedded fine sand or silt horizons up to 3m thick. The gravels are generally crudely bedded to massive with rare cross-beds. Tuffs that crop out closer to the centre of the field area are generally thicker, up to 20m, and occur as repetitive fining-upwards sequences. Each fining up bed is up to 0.5m thick and has a pumice clast base.

2.2.2 Mangatewaiiti Stream

The lower 40m of the sequence consists of cmbdd to massive silts and sandy silts containing shellbeds up to 2m thick. These consist almost entirely of *Austrovenus stutchburyii*. This lower 40m of section is similar to the Mangatewainui Stream section. Within it no major tuffs crop out. However, three medium grained, cross-bedded, brown sand beds, up to 5m thick, do contain either interbeds of pumice sand or dispersed pumice sand grains. Overlying the lower 40m of fossiliferous silt beds there is a 1.5m carbonaceous silt and 0.20m lignite. Over the next 60m brown sand, similar to that described above, is exposed almost continuously with occasional interbedded silts generally less than 1m thick. These brown sands usually exhibit some form of cross-bedding (planar or herringbone) and often have an erosive base with silt rip up clasts or well rounded greywacke pebbles.

At 120m above the base the first major pumice unit occurs. It has been correlated on stratigraphic position with tuff 'chemistry F' of Melhuish (1990). This tuff is up to 4m thick and has a crudely cmbdd pumice clast base fining-upwards to a trough cross-bedded pumice silt. Directly above and below this pumice unit carbonaceous silt interbedded with lignite beds up to 4m thick crop out. At 145m a 1m thick, crudely cmbdd diatomaceous silt containing well preserved reed-like vegetation crops out. Above this diatomaceous deposit there are two sequences of interbedded carbonaceous silt and lignite up to 10m thick separated by a 3m brown sand exhibiting undulatory and planar cross-bedding commonly truncated by the overlying beds. Directly above the uppermost of the two carbonaceous silt/lignite beds there is a 2m thick grey sand containing silt flasers. This grey sand gives way to 30m of massive grey silt beds (<4m thick) with interbedded cmbdd brown sand (<1m thick). Near the top of this 30m section of massive grey silt the brown sand becomes more dominant and contains rounded greywacke pebbles, pumice clasts and silt rip up clasts. Sedimentary structures include herringbone cross-bedding, planar cross-bedding and load features. This brown sand is overlain by interbedded carbonaceous silt and lignite (<0.50m thick) at least 5m thick which due to obscured section may be as thick as 40m where a much thicker lignite bed (c.3m) crops out. At this section the lignite is overlain by a 10m thick olive grey, cross-bedded, sandy shellbed containing wood fragments. This in turn is overlain by a 7m thick silt sequence with interbedded lenses of lignite (<1cm).

At 310m a second major pumice unit occurs. At this location it is a 3m thick interbedded pumice sand and pumice silt with associated convolute bedding. This pumice unit has been identified by stratigraphic correlation with tuffs farther to the west, as tuff 'chemistry C' of Melhuish (1990). Twenty meters above tuff 'chemistry C' a 7m fining-upwards, poorly sorted, sub-rounded, clast supported, planar cross-bedded greywacke gravel with interbedded ripple cross-bedded sands less than 0.10m thick, crops out. The gravel grades into a 2m thick, planar cross-bedded, medium grained, grey sand. At the boundary between this sand and the overlying 4m thick cmbdd sand, many feeding trails are exposed. Five meters above this fining-upward sequence a third major tuff occurs as a 3m thick pumice sand containing many pumice clasts. This tuff has been correlated on stratigraphic

position with the Potaka Pumice identified farther to the west (Melhuish 1990). The next 150m is poorly exposed but consists predominantly of cross-bedded sand with some beds displaying convolute bedding and water escape structures. These sand units are commonly overlain by cmbdd silts.

As in the Mangatewainui Stream, the sequence in the west of the basin becomes dominated by organic rich silt and gravel. In the east flank of the Dannevirke Anticline the stratigraphic section is reduced when compared with the west flank due to the greater angle of dip. Only 200m of stratal thickness is exposed below the Potaka Pumice. This 200m is dominated by sand units up to 5m thick, showing a range of sedimentary structures *i.e.* horizontal bedding, cross-bedding and undulatory bedding, overlain by up to 2m of organic rich mm-cmbdd silt and interbedded lignite.

At 106m, a 5m exposure of cross-bedded gravels crops out. This is the most easterly occurrence of non-marine gravels in the Mangatewaiiti Stream. Above this gravel tuff 'chemistry C' crops out as a 2m thick cmbdd pumice exhibiting repetitive fining-upwards sequences. Sixty meters above tuff 'chemistry C' another 2m thick mmbdd, repetitive, fining-upwards pumice unit occurs. This can be correlated on stratigraphic position with the Potaka Pumice identified farther west by Melhuish (1990).

At 45m above the Potaka Pumice a high angle reverse fault occurs. Between this fault and another farther to the west a westward tilted, uplifted block with a vertical offset of 100m occurs (Melhuish, 1990). Within this uplifted fault block the Potaka Pumice crops out as a 1m thick, cross-bedded pumice sand. Tuff 'chemistry C' crops out 10m below the Potaka Pumice as a 10m thick unit with a pumice clast base, fining-upwards to a cross-bedded sand and silt with prominent water escape structures. Approximately 25m above the Potaka Pumice, sequences of gravel up to 6m thick become dominant. At 67m above the Potaka Pumice the sequence ends against the reverse fault forming the western boundary of the uplifted fault block.

In the west flank of the Dannevirke Anticline (Fig. 2.2) a 200m thickness of sediment is represented at the surface, but a large proportion of it is obscured. The Potaka Pumice crops out as a 2m thick cmbdd, pumice sand preceded and followed by interbedded silt and lignite beds. Tuff 'chemistry C' crops out 30m below the Potaka Pumice as a repetitive, fining-upwards pumice sand sequence. Due to the lack of outcrop there is a 100m gap in the stratigraphy below tuff 'chemistry C'. Below this obscured interval a 25m thick section fining-upwards from a decimeter bedded (dmbdd) sand to a millimetre bedded (mmbdd) organic rich silt forms the basal deposit in this sequence. In the east flank of the Garfield Road Anticline (Fig. 2.2) gravels with interbedded silts dominate the upper 135m. Tuff 'chemistry C' crops out as a 0.10m pumice sand and 160m below tuff 'chemistry F' crops out as a repetitive fining-upwards, pumice sand sequence lying with an erosive contact on a 2m thick black lignite. To the west, sediment is dominated by gravels with interbedded silts. Nearing the Ruahine Range gravels become more poorly sorted, more angular and thickness increases.

2.2.3 Whakaruatapu Stream

Towards the south of the field area the geological structure is less complicated and a greater thickness of sediment is represented at the surface. Stratigraphy in the Whakaruatapu Stream is incomplete due to poor exposure and correlation is difficult due to absence of identified pumice units.

In the east flank of the Dannevirke Anticline (Fig. 2.3) the youngest c.300m of sediment is obscured. The 550m sequence mapped, where visible, contains a high proportion of rounded, sandy gravels with common shell fragments. These shelly gravel layers are interbedded with carbonaceous silts and lignites. Two pumice units crop out at 470m and 523m as 2-3m thick, fining-upwards pumice sand sequences. These two pumice units have been tentatively correlated with tuff 'chemistry C' and the Potaka Pumice using stratigraphic position. In the west flank of the Dannevirke Anticline (Fig. 2.3) only the oldest 200m of the sequence is accessible and within it good exposure is rare. Bioturbated and herringbone cross-bedded sand interbedded with carbonaceous silt and lignite dominate this part of the section.

Four pumice units crop out at 44m, 67m, 89m and 194m above the base of the column as 2-3m thick, fining-upward pumice sand sequences. Correlation was not attempted for these tuffs due to a lack of positively identified marker beds. Although lack of exposure prevented further mapping in the Whakaruatapu Stream the stratigraphic column constructed at the western extremity of Mangatewaiiti Stream is in close proximity to the Whakaruatapu Stream. Here the dominant lithology is gravel with interbedded silt. Towards the east these gravels become better sorted and more rounded. Overall gravel thickness decreases to the east. Within these gravels the Potaka Pumice and tuff 'chemistry C' crop out as fining-upwards, 20cm and 23cm thick pumice sands.

2.2.4 Mangatera Stream

The Mangatera Stream forms the southern boundary of the field area and here 700m of stratigraphic section has been measured.

On the east flank of the Dannevirke Anticline (Fig. 2.4) the oldest strata exposed comprise a flaser bedded silt overlain by a 2m thick, cmbdd, fining-upwards pumice sand. This pumice bed lies nearly 600m below a 3m thick, cmbdd, fining-upwards pumice sand with a pumice clast base. This tuff has been correlated, due to its stratigraphic position, with the Potaka Pumice identified by Melhuish (1990) farther north. Between these two pumice units there is a repeated sequence of commonly bioturbated, shell rich, moderately sorted, medium to coarse grained sand, silt and rounded greywacke gravel up to 6m thick with interbedded carbonaceous silts and lignite. A third pumice unit occurs 180m above the basal pumice unit as a 4m thick, cmbdd, fining-upwards pumice sand with a pumice clast base.

In the west flank of the Dannevirke Anticline (Fig. 2.4) the exposed stratigraphic thickness totals 310m due to the lower dip angle. Three major tuffs crop out in this section. The first, 80m above the lowermost strata exposed occurs as a 3m thick, cmbdd, fining-upwards pumice sand correlated stratigraphically with tuff 'chemistry F' of Melhuish (1990). Twenty meters above this tuff a 14m thick, cmbdd, silt with interbedded lignite (<20cm), containing the fresh water mollusc *Hyridella* crops

out. At the base of this silt there is a 2m thick, cross-bedded greywacke gravel with interbedded, mmbdd sand. The second major pumice unit occurs 100m above this gravel as a 6m thick fining-upwards sequence with a pumice clast base and is correlated with tuff 'chemistry C' of Melhuish 1990 due to its stratigraphic relationship with the overlying Potaka Pumice. The third major pumice unit lies 40m above tuff 'chemistry C' and is a 14m thick unit. It comprises a lower 6m thick, cmbdd basal unit comprised of successive sequences of fining-upwards pumice sand, overlain by a fining-upwards 3m thick, mmbdd and trough cross-bedded pumice sand in turn overlain by a 5m thick, cmbdd pumice silt. The pumice unit is then overlain by a 20cm lignite layer with roots penetrating into the pumice. This tuff has been identified as the Potaka Pumice (Melhuish 1990). It lies immediately below a 6m, cmbdd carbonaceous silt that forms the top of the sequence.

To the west good exposure becomes less common and therefore the stratigraphic record is rather poor. In the east flank of the Umutaoroa Anticline (Fig. 2.4) the stratigraphic section is 700m thick and two of the three tuffs that crop out in the west flank of the Anticline also crop out here. The base of the exposed section, approximately 650m below the Potaka Pumice, is a 5m thick, cmbdd silt. Above this basal silt, shelly silts and sands with interbedded lignites occur for at least another 260m. Between the lignites, interbedded carbonaceous silts and sands crop out. These are commonly bioturbated. All outcrop is obscured for 200m above the uppermost shellbed.

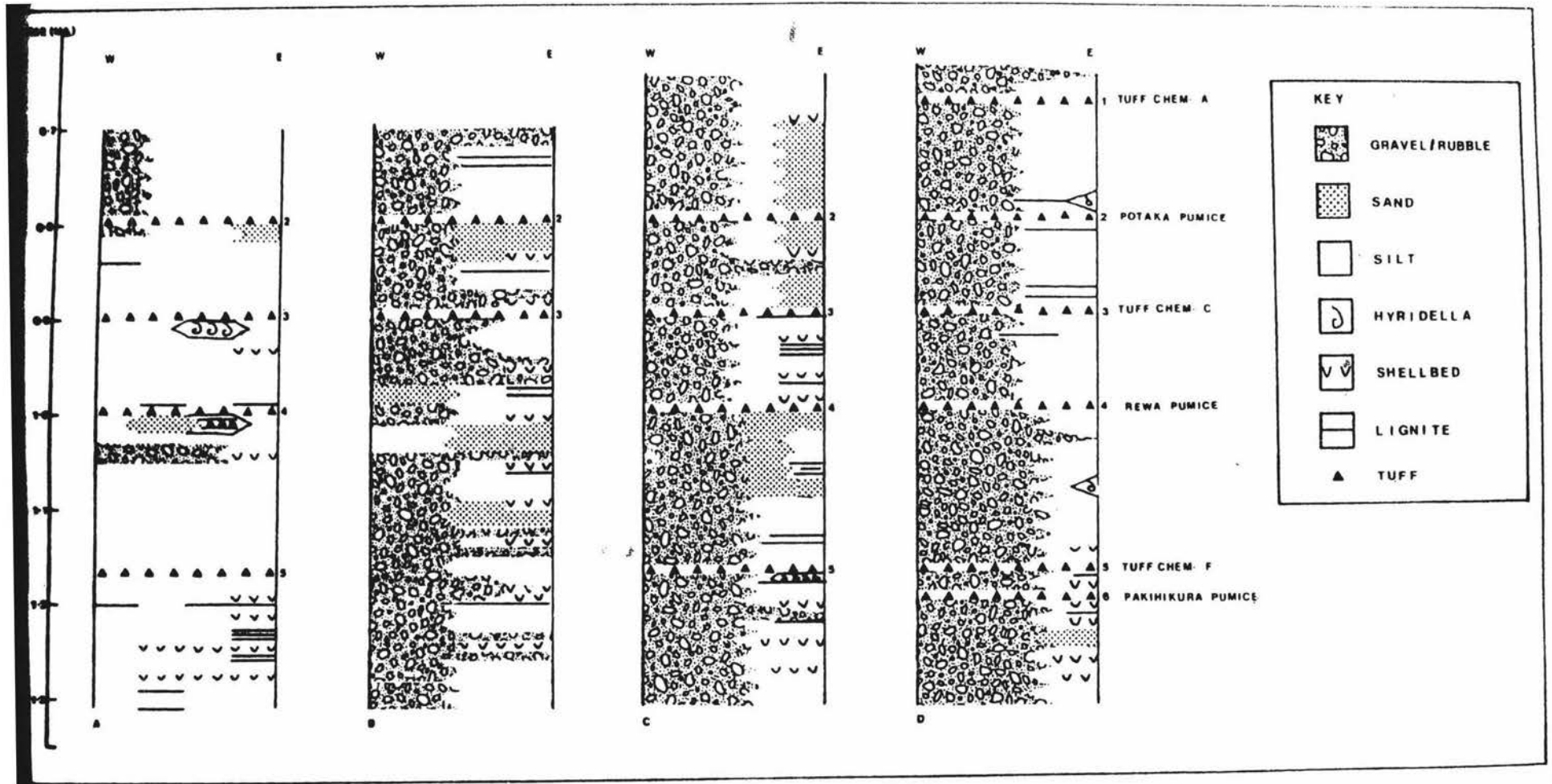
At 460m above the basal silt, tuff 'chemistry F' crops out as a 7m thick, cmbdd, pumice silt overlain by 50cm of lignite and 6m of cmbdd silt. Forty meters further above, the Rewa Pumice crops out as a 4m thick, convolute bedded, pumice sand with a 0.20m thick lens of rounded greywacke pebbles and silt clasts. Above this pumice unit is a 0.10m grey silt bed overlain in turn by a 0.30m thick, matrix supported, poorly sorted, crudely cmbdd greywacke gravel. A 0.10m silt bed overlies the gravel. Above this silt bed there is a 2m thick fining-upwards pumice sand, then a 5 m unexposed section followed by another 10m of fining-upwards pumice, also considered part of the Rewa Pumice (Melhuish 1990). At least 12m of massive grey silt with a 0.20m lignite base lies directly above the Rewa Pumice.

This massive silt contains lenses of angular rubble up to 0.60m thick. One hundred meters above, the Potaka Pumice crops out as a 6m thick, cmbdd, convolute bedded, pumice sand lying with an erosive contact on a 2m thick carbonaceous silt with lenses of angular rubble up to 0.30m thick. The top of the sequence occurs 60m above as a 6m thick massive silt with two interbedded, 0.20m thick, blocky paleosols and a 0.30m platy lignite.

The stratigraphic sequence making up the west flank of the Umutaoroa Anticline (Fig. 2.4) is greater than 650m thick, however exposure is extremely poor. A 2m thick, cmbdd, pumice silt containing wood fragments crops out 550m above the basal cmbdd silt and has been correlated on stratigraphic position with the Potaka Pumice identified farther to the east (Melhuish 1990). This tuff lies with an erosional contact on a 1m thick, interbedded carbonaceous silt and lignite. Three other lignite beds, 1-2m thick, crop out in the sequence at 300m, 520m and 590m above the base. Greywacke gravel is not seen until 20m below the top of the sequence, probably due to the lack of outcrop. The gravel is subangular to subrounded, clast supported, moderately poorly sorted, slightly weathered greywacke with interbedded silt up to 1m thick. The top of the sequence occurs adjacent to Nukumaruan limestone, dragged up along the Range Front Fault.

2.3 Correlation

A composite stratigraphic column was constructed for each stream showing change in lithofacies from east to west (Fig. 2.5). Correlation between streams is possible using pumice tuffs identified by Melhuish (1990) as time planes. Correlation between pumice units was initially by stratigraphic position and as a check the areal distribution of all pumices were plotted (Fig. 2.6) and related to structural axes. No pumice unit was found to crop out more than once on one side of a structural axis indicating a consistent position of the pumice units in relation to the structures. Chronostratigraphic control is provided by the Potaka Pumice (c.0.8 Ma) and the Rewa Pumice (c.1.0 Ma) (Pillans, 1991). Using these radiometric ages sedimentation rates were calculated and ages for undated pumice units estimated. Only four of the six pumice units identified are useful as marker beds across the



2.5 Chronostratigraphic columns for Mangatera (A), Whakaruatapu (B), Mangatewaiiti (C), and Mangatewainui (D) Streams showing lithologic changes from east (E) to west (W) and correlation between streams using identified pumice units as time planes.

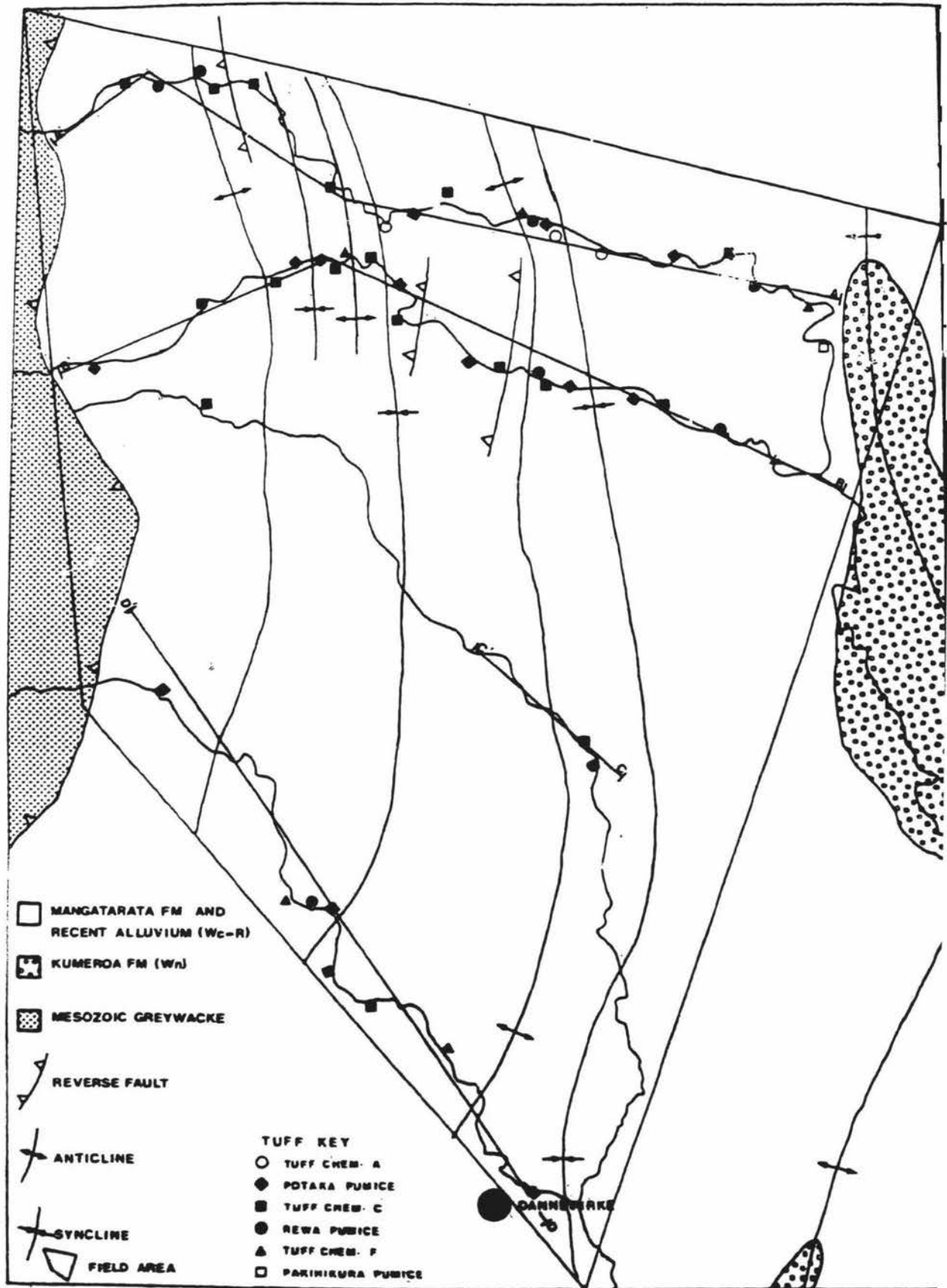


Fig. 2.6

Areal distribution of pumice units in relation to structural axes and cross-sections AA', BB', CC' and DD' for stratigraphic columns, Figs. 2.1, 2.2, 2.3 and 2.4.

field area. They are the Potaka Pumice (c.0.8 Ma), tuff 'chemistry C' (c.0.9 Ma), the Rewa Pumice (c.1.0 Ma) and tuff 'chemistry F' (c.1.17 Ma). The Pakihikura Pumice (c.1.2 Ma) and tuff 'chemistry A' (c.0.67 Ma) were only identified in the Mangatewainui Stream and therefore are not useful for correlation across the field area.

The trend observed in all four composite stratigraphic columns (Fig. 2.5) shows gravel lithofacies wedging out toward the east and interfingering with silt and sand lithofacies. In the north of the field area gravels occur farther east than in the south of the field area. The only means of correlation between streams apart from the use of pumice units is to use the stratigraphic position of shellbeds. The best correlation is between the Whakaruatapu Stream and the Mangatewaiiti Stream where four shellbeds lie in similar stratigraphic positions with respect to the tuff beds. It is the stratigraphic position of these shellbeds in conjunction with the age control provided by pumice tuffs that has been used to identify cyclothems in the field area (Chapter Seven).

2.4 Conclusions

From analysis of field data five groups of sediments can be identified.

1. Bioturbated, commonly cross-bedded and flaser bedded, fossiliferous silts and sands.
2. Centimetre bedded silts containing *Hyridella* and diatomaceous deposits.
3. Cross-bedded sand and horizontally bedded organic rich silts, sands and lignites.
4. Massive to cross-bedded greywacke gravel and rubble.
5. Pumice, with a range of grain sizes from large pumice clasts to fine grained pumice silt occurring within sediments of groups 1,2,3 and 4.

Groups 1,2,3 and 4 form an interfingering series, with group 1 sediments more common to the east *i.e.* in generally younger deposits, and group 4 sediments dominant to the west in younger deposits. Identified pumice units form the

foundation for interstream correlation in an area where facies change is rapid, both laterally and temporally. Pumice units also allow the construction of a chronostratigraphic sequence for the field area which aids in the identification of cyclothem.

CHAPTER THREE

MINERALOGY OF SANDS

3.1 Introduction

Sand mineralogy was studied to ascertain the provenance of the Castlecliffian sediments in the study area.

3.2 Methods

Eleven samples were selected, representing the range of sands in the field area. Due to the significant range in grain size, the samples were split into four size intervals *i.e.* 63-125, 125-250, 250-500 and >500 microns to allow preparation of grain mounts of even grain size and to ascertain whether any specific mineralogy dominated a certain grain size range. An initial analysis using grain mounts was carried out to determine the range of minerals present using the binocular polarizing microscope. Due to the large variation in grain size of the >500 micron grain mount this sample was discarded. Minerals of this grain size also tended to be opaque and were therefore of little use in mineral identification. After the initial study of the range of mineralogy was completed, four samples were selected for thin section preparation and study.

3.3 Mineralogical results

The initial study using grain mounts showed that the dominant feature of the sands is their range in composition from purely volcanic material to non-volcanic detritus.

3.3.1 Glass

About 99% of glass shards within the tuffs are colourless with a silica content in the range of 72-79 wt. % and all have a calcalkaline rhyolitic composition. Most tuffs also contain a small fraction (<1.0%) of highly magnetic brown glasses, some of which have non-rhyolitic compositions (Shane, 1991).

3.3.2 Quartz

Two types of quartz are recognised both occurring in the same samples. Type one quartz grains are subhedral and generally less rounded than type two. They are strain free, monocrystalline and free of inclusions. Occasionally glass shards are visible around the perimeter of these quartz grains.

Type two quartz is far more common, is generally more rounded, is strained and contains dust inclusions, as does the quartz of the Mesozoic greywackes.

3.3.3 Feldspar

In all grain mounts and thin sections examined plagioclase is the dominant feldspar. Again two types are obvious. Type one plagioclase is identified as albite. It is a dusty yellow, slightly altered, subrounded mineral with low relief (< 1.54). The maximum extinction angle of these grains is up to 6 degrees and the interference figure is biaxial positive with a large axial angle. Where grains are sericitised birefringence is strong with upper second order interference colours. There are also very small amounts of other sodic plagioclase present.

Type two plagioclase is identified as labradorite. These more calcic plagioclase grains are less common but more distinctive than type one plagioclase. They are colourless, generally euhedral and usually zoned. Relief is low but always > 1.54 . These often contain glass inclusions and glass around the perimeter. The maximum extinction angles are up to 13 degrees.

Potassic feldspar grains occur, including microcline and orthoclase. Most grains are subrounded and are at least partly sericitised.

3.3.4 Orthopyroxene

The orthopyroxenes are generally pale green in thin section and pleochroic from green to reddish brown. Crystals exhibit euhedral to subhedral form and have high relief i.e. > 1.54 , and are weakly birefringent. Hypersthene is the dominant orthopyroxene with subordinate amounts of non-pleochroic enstatite.

3.3.5 Clinopyroxene

Clinopyroxenes occur as subrounded; euhedral to subhedral crystals with low relief and moderate birefringence with middle second order interference colours. The interference figure is biaxial positive with an axial angle of 55-60 degrees. Clinopyroxenes (generally augite) are rare compared with orthopyroxenes. Many of the hypersthene grains, and more rarely augite, have multiple pyramidal terminations similar to those noted by Hutton, (1959). Fine grained pyroxenes tend to have much sharper needle like pyramids, often two or three times longer than the grain itself, when compared with the coarser grained pyroxenes which have blunter pyramidal terminations. Edelman and Doeglas (1932) in Seward, (1974) suggested that the unusual shape was due to solution along planes of weakness. Due to the highly fragile nature and thus ease of weathering during transport, solution is considered to have occurred after deposition.

3.3.6 Micas

Micas are generally only present in small amounts *i.e.* $< 1\%$.

3.3.6.1 Biotite

Biotite appears as a subhedral to anhedral, platy brown mineral in thin section and is pleochroic from brown to reddish brown. Inclusions surrounded by pleochroic haloes are common and biotite is often at least partly altered to chlorite. Interference figures are biaxial negative with a $2v$ angle of 11-17 degrees.

3.3.6.2 Muscovite

Muscovite is less common than biotite and occurs as long narrow grains that are commonly bent and have tattered ends. It is clear in thin section and has moderate relief (> 1.54) but strong birefringence with upper second order interference colours.

3.3.7 Glaucinite

Glaucinite occurs as a rounded to subrounded, bright green to yellow green pleochroic mineral with no obvious cleavage or extinction. Glaucinite is strongly birefringent with high second order interference colours thus distinguishing it from chlorite which has low birefringence. Each grain appears to be made up of many smaller grains.

3.3.7.1 Origin of glauconite

Glaucinite pellets are formed in the marine environment at the sediment-water interface (Kossovskaya and Drits, 1970). Glaucinite is forming today in the outer shelf and upper continental slope environments (water depths of 50-500 m), but it is unlikely that water depth has any control and pellets may be redeposited (Lewis, 1984). A slow net sediment accumulation rate is essential. Odin and Matter, (1981) in Lewis, (1984) estimate time at the sediment-water interface to be in the order of 1000 to 10,000 years for initial glauconitization. Slightly reducing conditions, but an absence of hydrogen sulphide are necessary. Most pellets are probably perigenic (locally redeposited); some are allogenic (recycled from older sediments) in which case they are few and generally fragmented, and others are authigenic (McConchie and Lewis, 1978). In the study area glauconite occurs in both marine and terrestrial sands therefore it is likely to have been recycled from older sediment. This fits well with its low concentration in samples.

3.3.8 Opaque minerals

The opaque minerals are dominated by those derived from the central volcanic region. Magnetite is most abundant; ilmenite is rare.

3.3.9 Rock fragments

Most rock fragments were difficult to identify positively as they are composed of small and smaller size material. They occur in all samples and are dominated by material from a greywacke source.

3.4 Provenance

Results confirm that at least three classes of sediment with different origins were supplied to the basin. Hypersthene and augite, unstable heavy minerals (Pettijohn 1957) along with type one quartz and type two feldspar were introduced with the immature volcanic detritus. More stable heavy minerals *e.g.* sphene and zircon occur very rarely and along with type two quartz and type one feldspar originate from the axial greywacke ranges or low grade metamorphic rocks. Muscovite crystals are bent and kinked, evidence of a low grade metamorphic or granitic source. There are two possible sources for the muscovite; either the granitic terrain of NW Nelson or the Otago schists. Sediment derived from these areas may have been transported via longshore drift directly into the Dannevirke-Pahiatua Basin into older Tertiary basins which have since been uplifted and thus the muscovite may have been reworked from Tertiary terrain as may be the glauconite.

Although there are three distinct source areas contributing sediment to the basin the mineralogy of sediment is generally a mixture from the three sources. Sediment is dominantly quartz-feldspathic throughout the Castlecliffian reflecting the important contribution the axial greywacke ranges make to overall sediment supply. The amount of volcanic component contributing to overall sediment supply is controlled by proximity to the reworked ignimbrites entering the basin. Generally the volcanic component is < 10 % but during periods of volcanic activity it may be considered more, reaching 100 % in pure pumice beds.

CHAPTER FOUR

GRAIN SIZE ANALYSIS

4.1 Introduction

Any method of grain size analysis is biased by variables of composition, shape and size as well as the efficiency of disaggregation and the specific limitations of the technique being applied. Several different techniques can be used to analyze the full grain size range from gravel to clay (Fig. 5.1). If a sand sample contains less than 20 % mud then sieve analysis alone is sufficient. Conversely if a mud sample contains less than 10 % sand, sieve analysis is not necessary (Lewis, 1981).

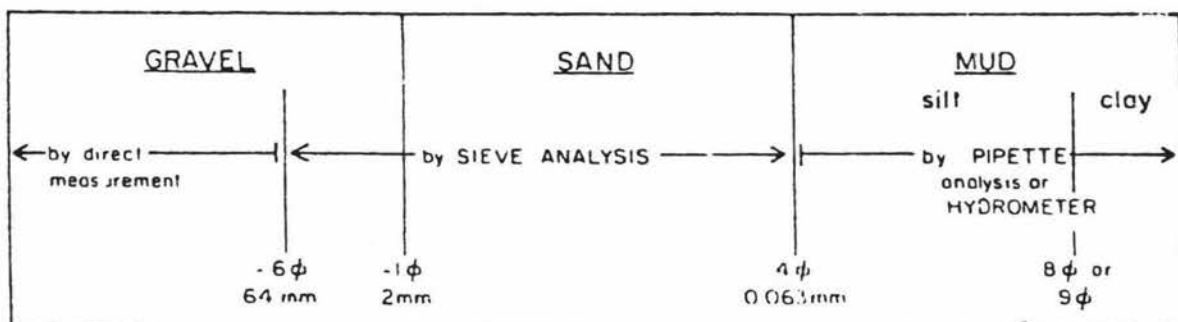


Fig. 4.1 Major textural boundaries and corresponding grain size analysis methods, after Lewis (1981).

4.2 Methods

4.2.1 Sand

Grain size analysis of sand was undertaken using a Ro-Tap shaker following the procedure outlined by Lewis (1981).

4.2.2 Silt and clay

There are a variety of techniques for size analysis of silt and clay. Pipette analysis has been widely used and reproducibility is very good, *i.e.*, better than 0.1 phi unit, but the method is time consuming (Kaddah, 1974). Size analysis by hydrophotometer is faster than the pipette method but reproducibility is not as good (0-3 phi unit). Size analysis by hydrometer gives results which compare well with those of pipette analysis but again reproducibility is not as good (Kaddah, 1974). Grain size analysis using the sedigraph is not accurate where sediment is coarser than coarse silt, so this method was not used as many of the samples in this study were sand sized or contained a significant sand percentage.

For this study, it was decided to use the pipette method for grain size analysis of material finer than 4 phi because of the better reproducibility of results and because the necessary equipment for this method was readily available.

4.3 Theory of pipette analysis

The pipette technique is based on the differing settling velocities of particles of different size (Stokes Law). Samples of a specified volume are extracted from a suspension of silt and clay at specified times and depths. The weights of the dried samples are representative of the proportion of the total silt and clay fraction remaining in suspension above the specified depth at the specified time. Therefore the measure is the proportion of the total finer than the 'size' which will have settled through the specified depth in the specified time (Folk, 1968). A slightly modified outline of Lewis' (1981) procedure for pipette analysis was followed in this study.

4.4 Calculation of results

The calculations required to convert the raw grain size data into a useful form together with statistical characterisation of the grain size distribution, makes computer analysis an accurate and time saving method.

The grain size analysis programme available at Massey University (McArthur, 1970) requires two sets of input data:

- (1) The weight (g) for each phi interval.
- (2) The corresponding phi interval.

The programme calculates the following information:

- (1) Moment measure statistics.
- (2) Inman statistics.
- (3) Folk-Ward statistics.
- (4) Data for drawing frequency curves.
- (5) Data percentiles.

4.4.1 Advantages of the grain size analysis programme

A major advantage of this programme over others *e.g.* Marks, (1975) is the simplicity of the calculation of statistical parameters encountered when the silt and clay fraction is analyzed in larger phi intervals than the coarser sand fractions and the analysis is rapid. Whereas most programmes calculate statistical parameters by either the method of moments (Griffiths, 1967) or the graphic method (Folk, 1968) this programme calculates the parameters by both methods. This allows data in the literature, generated by either method, to be useful. The only disadvantage associated with this programme is that graphic plots are not generated.

4.5 Graphically generated parameters versus moment measures

Moment statistics differ in concept but yield measures analogous to those of graphical techniques. Neither technique is better than the other (McManus, 1988). Graphic techniques are especially appropriate for analysis of open ended distributions whereas the moment method should not be applied unless grain sizes present lie within the defined grain size limits. Although the parameters obtained are analogous to those of graphical statistics their derivation uses the entire grain population and so are more representative than the graphically derived values (McManus, 1988). Distribution of the 'pan residue' fraction from sieving among a specified number of phi classes to permit application of moment methods is not good practice and may lead to misleading results being obtained. This is verified by the results obtained using 6.0 phi as an arbitrary end point for sands. The results obtained from the graphic method were reproducible which was not the case using the method of moments. Due to the open ended size distribution generating unreliable parameters using the method of moments, statistical parameters generated by graphical methods were used in this study.

4.6 Graphical representation of parameters

The range in grain size of a sample must be characterised statistically so that the samples may be compared and interpreted. It is therefore necessary to plot, in some way, frequency of occurrence against a measure of grain size (Leeder, 1982).

The statistical parameters which form the basis of the plots in this study describe the shape of the size-frequency curves. They have been selected because of their environmental significance. The < 62 micron fraction, one of the parameters in the plots, identifies the fraction deposited from suspension. The > 500 micron fraction has been used in preference to the one percentile value adopted by Friedman (1967) due to the ease of calculation. It characterises the maximum grain size which may have been deposited by rolling or sliding, or where a fraction deposited by rolling or sliding is not present distinguishes sands carrying the > 500 micron fraction from those which lack it. Since most sand fractions are deposited by saltation, only the

suspension and rolling or sliding fractions can be used for environmental interpretation (Friedman, 1967).

The standard deviation describes the spread of the distribution, *i.e.* sorting, and is analogous to the angle of slope of log-probability plots (Visher, 1969). The skewness including the mean cubed deviation, reflects the direction of skew of the tails; although in polymodal sands, where several modes are present at the coarse grained end of the distribution, the skewness measures lack significance (Friedman, 1961).

In this study scatter plots are preferred to log-probability plots. The aim of the scatter plots is to show the extent of environmental differentiation and the degree of overlap. Individual log-probability plots may illustrate the shape of individual sand samples from various environments but fail to present a proper image of the total range of variability of the sands. Scatter plots allow a quantitative comparison of the various parameters and therefore are more effective than individual curves for showing the extent of differentiation and the degree of overlap (Friedman, 1967).

4.7 Grain size analysis results and discussion

All statistical data are tabulated in Appendix D.

The sediments examined fall into three textural populations, gravel, sand and silt, with some overlap between the two latter. The gravel is composed almost totally of greywacke clasts, although at a few places in the east and south of the field area sand and shell fragments are components. The sand and silt are mostly greywacke detritus with a subordinate volcanic component.

Mean grain size of gravel was estimated in the field by measurement of the ten largest clasts as suggested by Pelletier (1958), (see Chapter six).

4.7.1 Relationship between mean size and sorting

Mean size is plotted against sorting (standard deviation) for all samples (Fig. 4.2). This scatter plot shows two environmentally distinct but slightly overlapping groups. Group one comprises well sorted sand to coarse silt, deposited in a nearshore environment. Group two comprises more poorly sorted, coarse sand to fine silt deposited by fluvial processes.

The best sorted material is that with a grain size range from 2.5 to 3.0 phi. Inman (1949) explained this relationship using Shields' and Hjulstrom's diagrams which show that fine sand is the most easily removed sediment. At the point where fine sand is deposited a slight increase in velocity leads to erosion and there is a delicate balance between erosion and deposition, leading to good sorting of a sediment that is transported by the lowest velocity currents, and then deposited.

Of the 61 sand samples plotted (Fig. 4.3) 69% fall in the very well to moderately well sorted category i.e. from <0.35 - 0.71 phi fraction (scale after Folk and Ward, 1957). Conversely, of the 83 silt samples plotted (Fig. 4.4) 89% fall in the poorly sorted to very poorly sorted category i.e. 1.0 - 2.5 phi (Folk and Ward, 1957) with the remaining 11% being moderately well sorted to moderately sorted.

Silt (material < 63 microns) transported by true suspension caused by turbulence shows no vertical change in grain size (Lane, 1938). However, matters are complicated by the interchange of suspension and bedload transport in certain grain sizes. This results in a graded suspension, with coarser suspension sediments increasing in concentration toward the sediment-water interface (U.S. Waterways Experiment Station, 1939). The break or truncation point between suspension and bedload transport may be highly variable and reflect physical conditions at the time of deposition. In true suspension no variation in concentration of sediment exists from the surface to the depositional interface. Therefore, some of this material is available for deposition with coarser material at the sediment water interface. A graded suspension increases in grain size downward towards the sediment-water interface allowing an interchange with the bedload. Mixing between these two

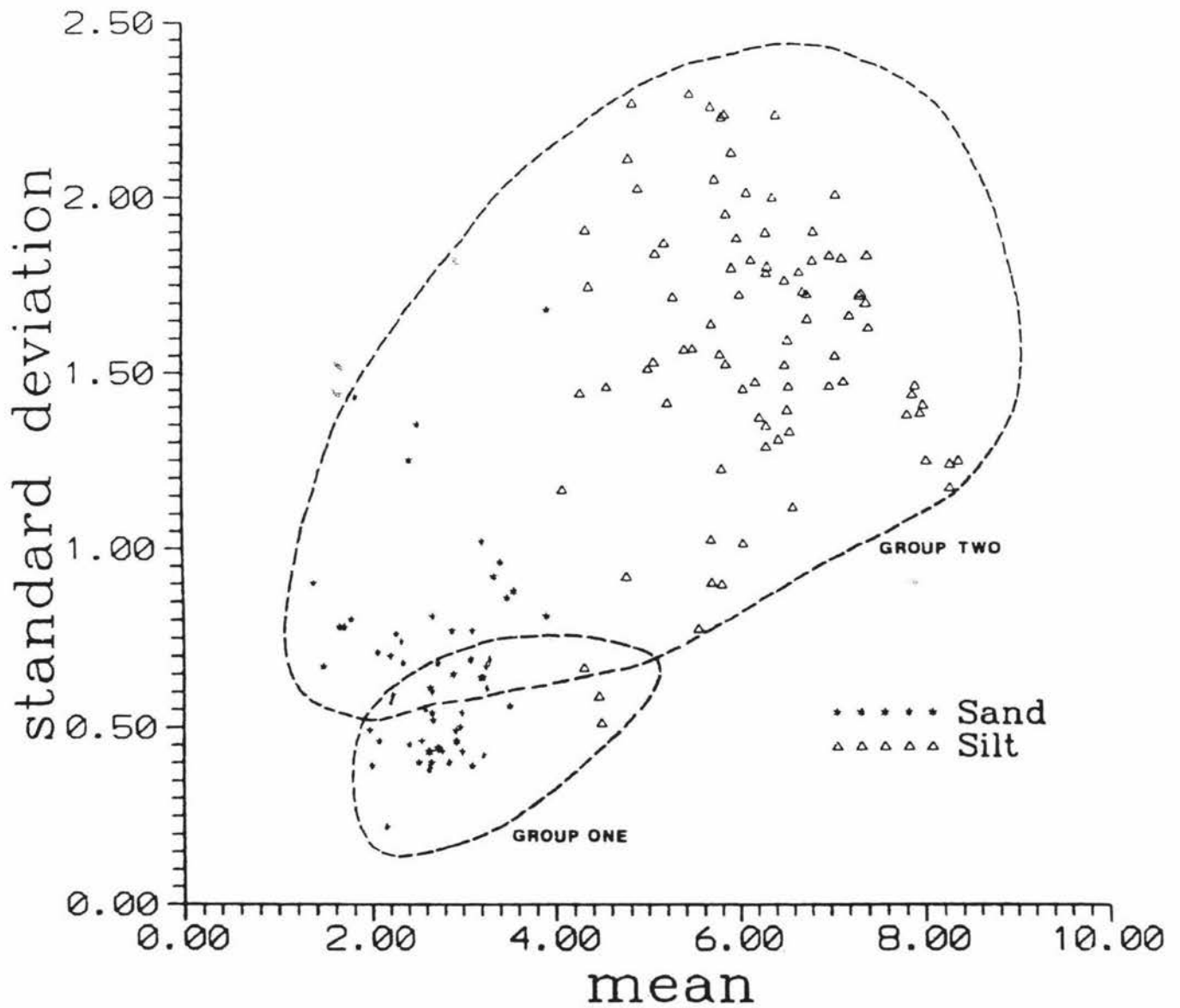


Fig. 4.2

Scatter plot of standard deviation (sorting) versus mean grain size for silt and sand.

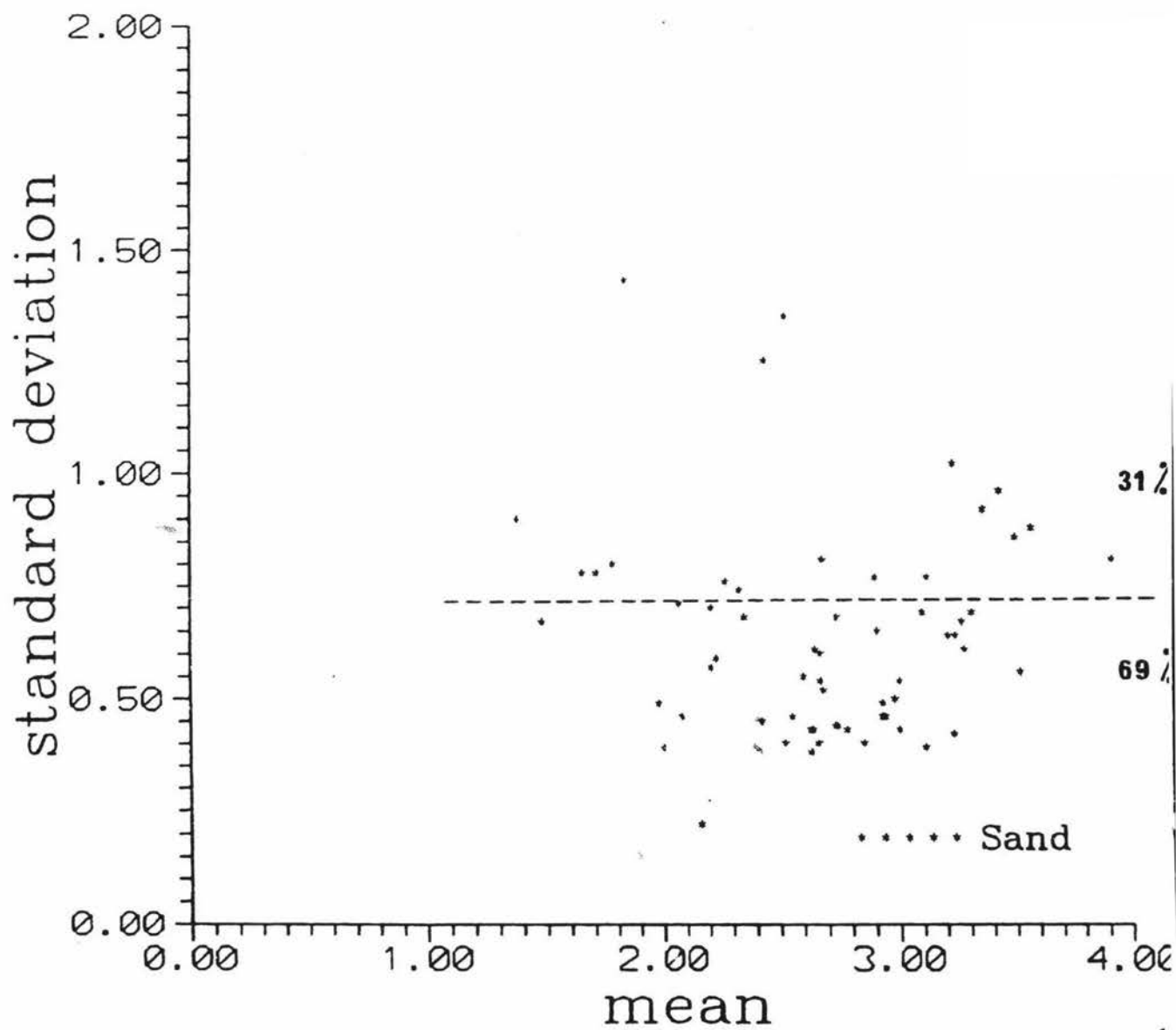


Fig. 4.3 Scatter plot of standard deviation (sorting) versus mean grain size for sand.

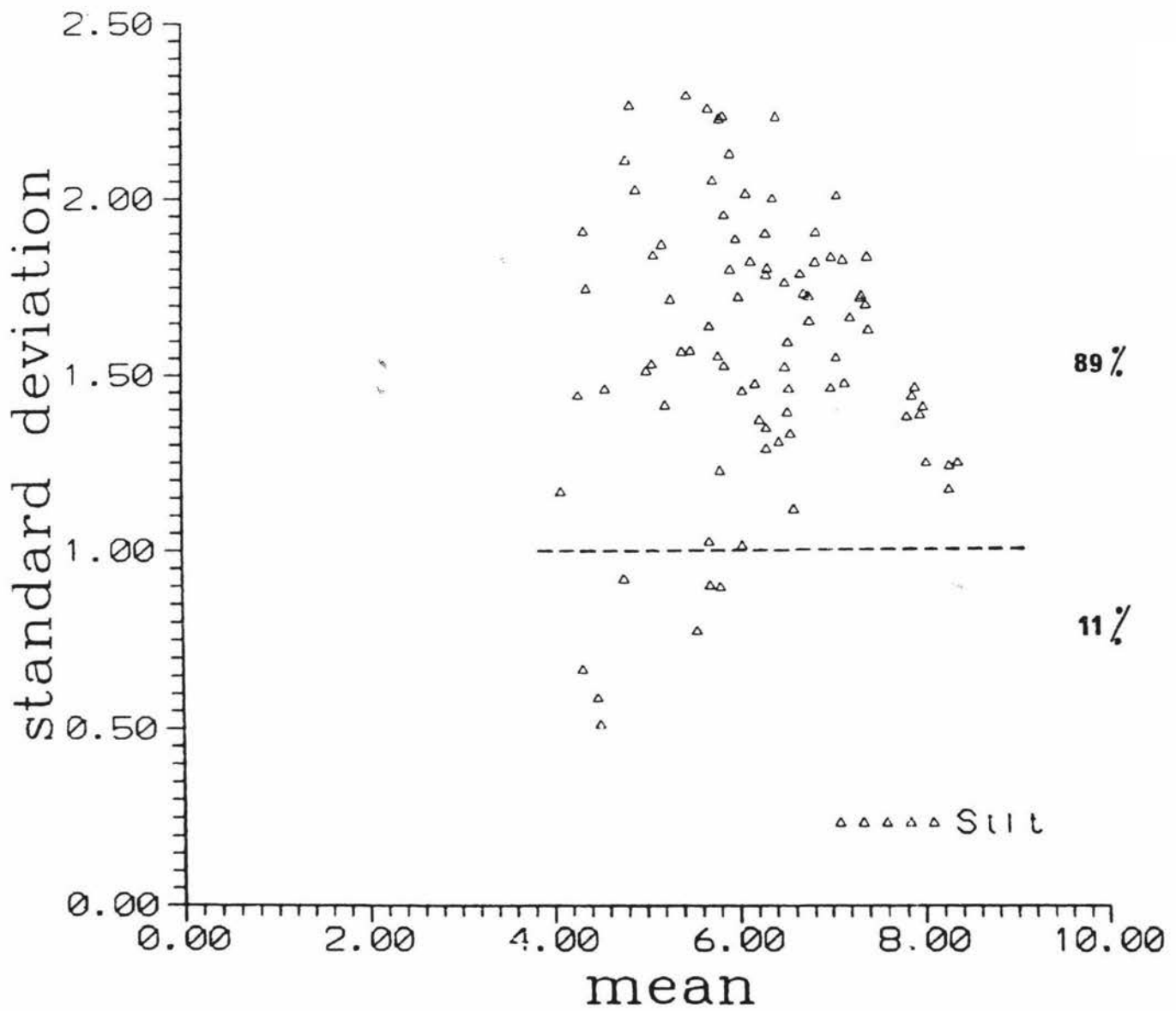


Fig. 4.4

Scatter plot of standard deviation (sorting) versus mean grain size for silt.

populations is common in fine grained sedimentary rocks (Visher, 1967a; 1967b). It is this mixing between populations that is partly responsible for the relatively poor sorting of fine grained samples in this study. Another contributing factor despite the utmost care in sampling is likely to be sampling across more than one depositional episode. This is more likely to occur in massive beds where depositional episodes are not obvious when compared with bedded deposits.

4.7.2 Relationship between mean cubed deviation and sorting

The mean cubed deviation is the third moment about the mean of the distribution. In this study it has been calculated by multiplying skewness and the cubed standard deviation. Friedman (1979) found mean cubed deviation to be less complex and therefore more useful to work with than skewness. Friedman also found mean cubed deviation to be one of the most effective parameters in separating sands of various origin.

The scatter plot generated for mean cubed deviation versus standard deviation (Fig 4.5) shows two distinct groupings. The first group falls in the very well to moderately well sorted category with a mean cubed deviation very close to zero. This well sorted group of tidal/estuarine deposits is almost completely made up of sands and shows a very dense distribution when compared with the scatterplot for the second grouping. The more poorly sorted end of this group (*i.e.* with higher values for standard deviation) tends towards higher positive values for mean cubed deviation. The second grouping comprises fluviially deposited sediment and shows a much greater range in standard deviation, with all samples being more poorly sorted than those in the first group. Mean cubed deviation also shows a great range of values with a general increase in positive value with increasing standard deviation. This observation can be directly related to the poorly sorted nature of silts compared with sands due to mixing of suspension and bedload populations explained previously.

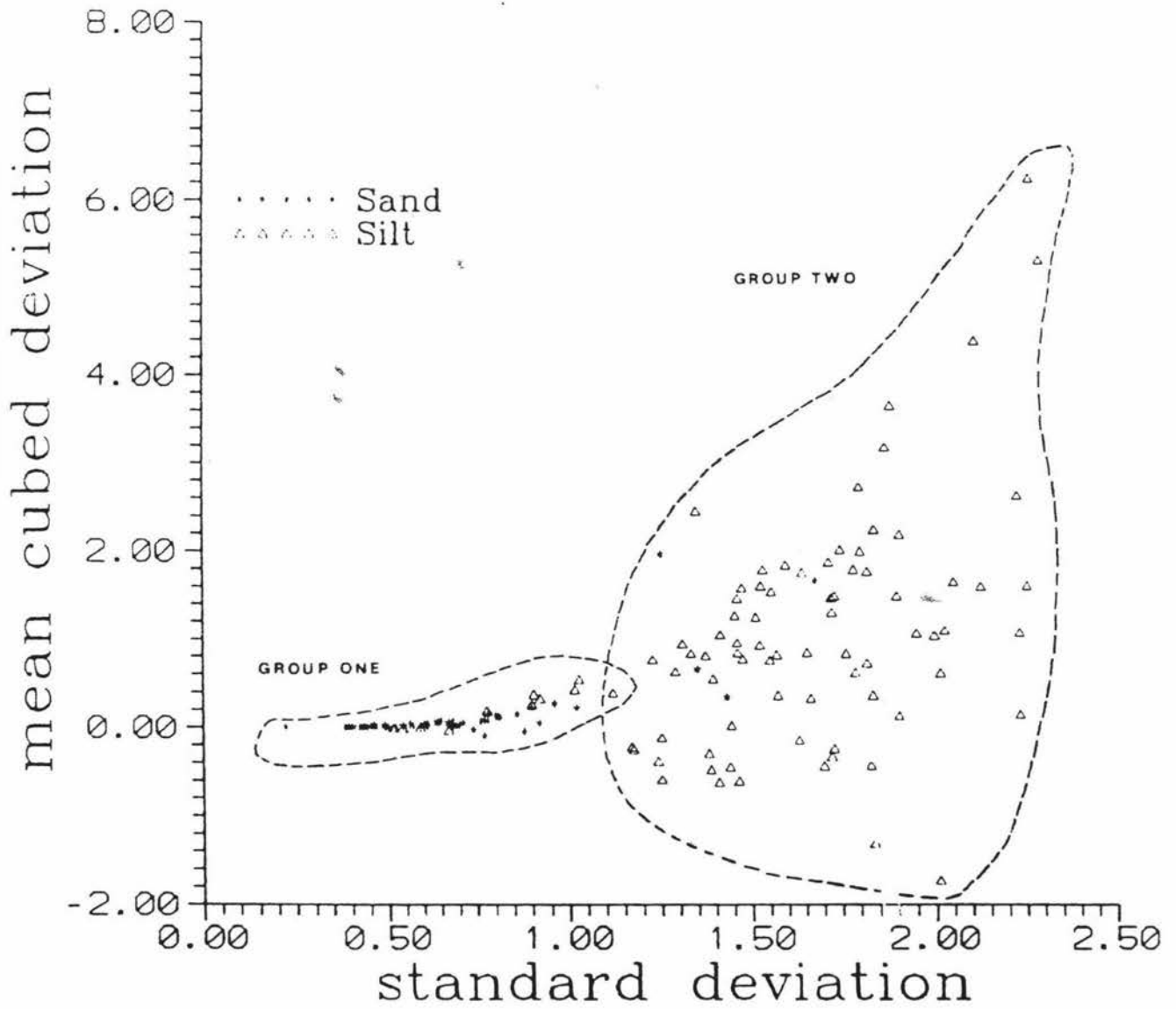


Fig. 4.5 Scatter plot of mean cubed deviation (third moment about the mean) versus standard deviation (sorting) for sand and silt.

4.7.3 Relationship between fine and coarse tails and sorting

Passega (1957) suggested that the first percentile could be used to characterise the depositional agent.

In this study the >500 micron fraction has been used instead of the first percentile due to ease of calculation. The >500 micron fraction is plotted against standard deviation (Fig. 4.6). This graph demonstrates that in the >500 micron range of the size frequency distribution, the more poorly sorted sands generally have a coarser maximum size than the relatively better sorted sands *i.e.* sands with lower standard deviation. Moreover, because the standard deviation is environment sensitive (Friedman, 1967), separation into environmentally designated fields is possible with group one sands representing sediment sorted by tidal/estuarine processes. Other sands are deposited in a fluvial environment.

In Figure 4.7 the standard deviation is plotted against the <63 micron fraction. This figure shows that the poorly sorted fluvially deposited sands generally contain more fine grained material and have a wider distribution than the well sorted nearshore sands and that the two sands fall into separable fields.

4.7.4 Relationship between skewness and sorting

Skewness is a measure of the symmetry of the frequency curve and has been found to be environmentally significant (Friedman and Sanders, 1978).

Skewness is plotted against sorting (standard deviation) (Fig. 4.8) for sands only, as there was no significant pattern apparent for finer grained sediment. The scatter plot generated does not show separate fields but a trend from negative skewed to positive skewed sands with increasing standard deviation, *i.e.* as samples become more poorly sorted. Figure 4.8 demonstrates that the better sorted sands tend to have a more negative skewness and as sands become more poorly sorted they generally have a higher positive value for skewness. This positive skewness is due to relative enrichment in fine grained sediment. Conversely the negative skewness is due to a

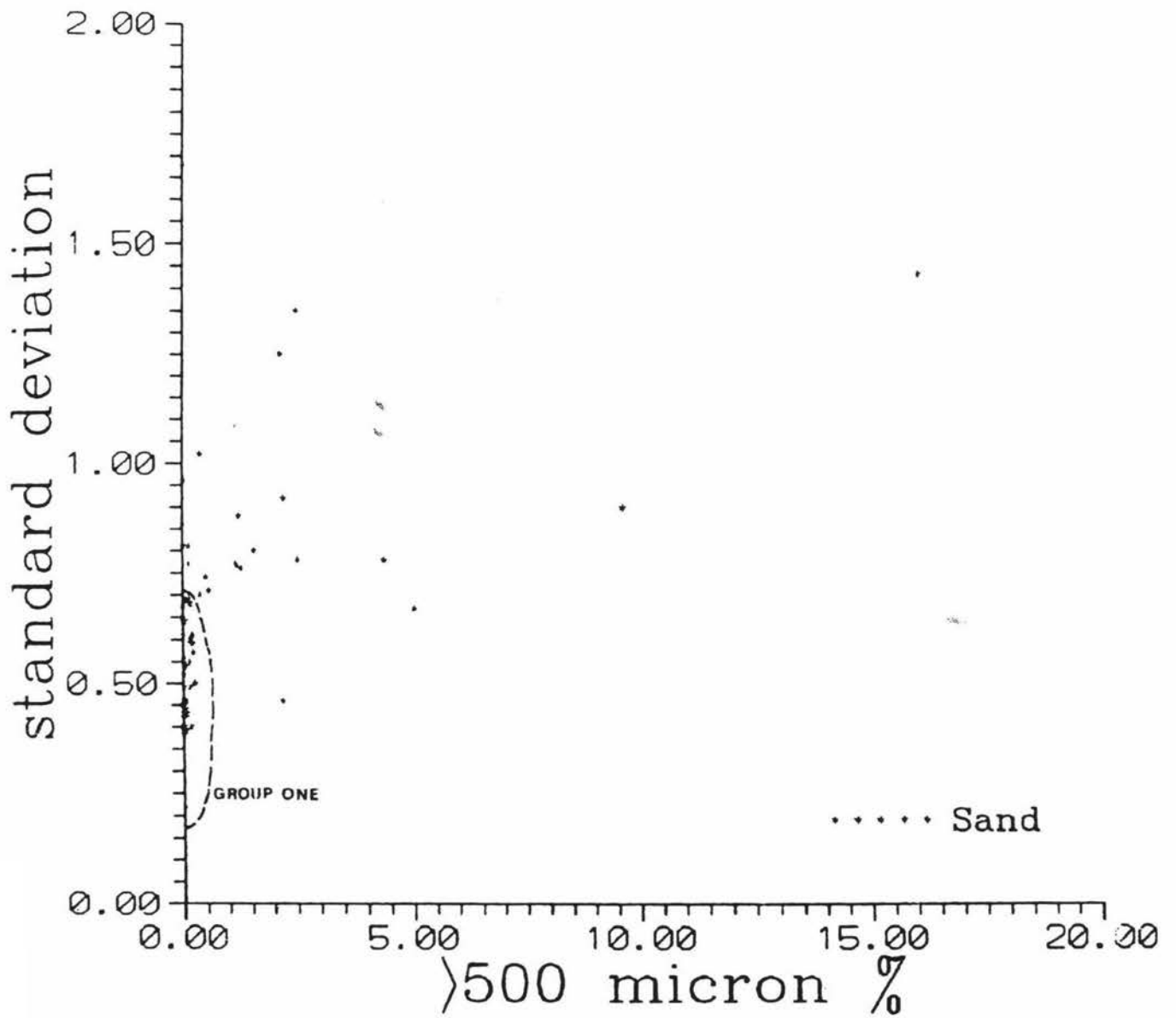


Fig. 4.6 Scatter plot of standard deviation (sorting) versus >500 micron fraction (coarse tail).

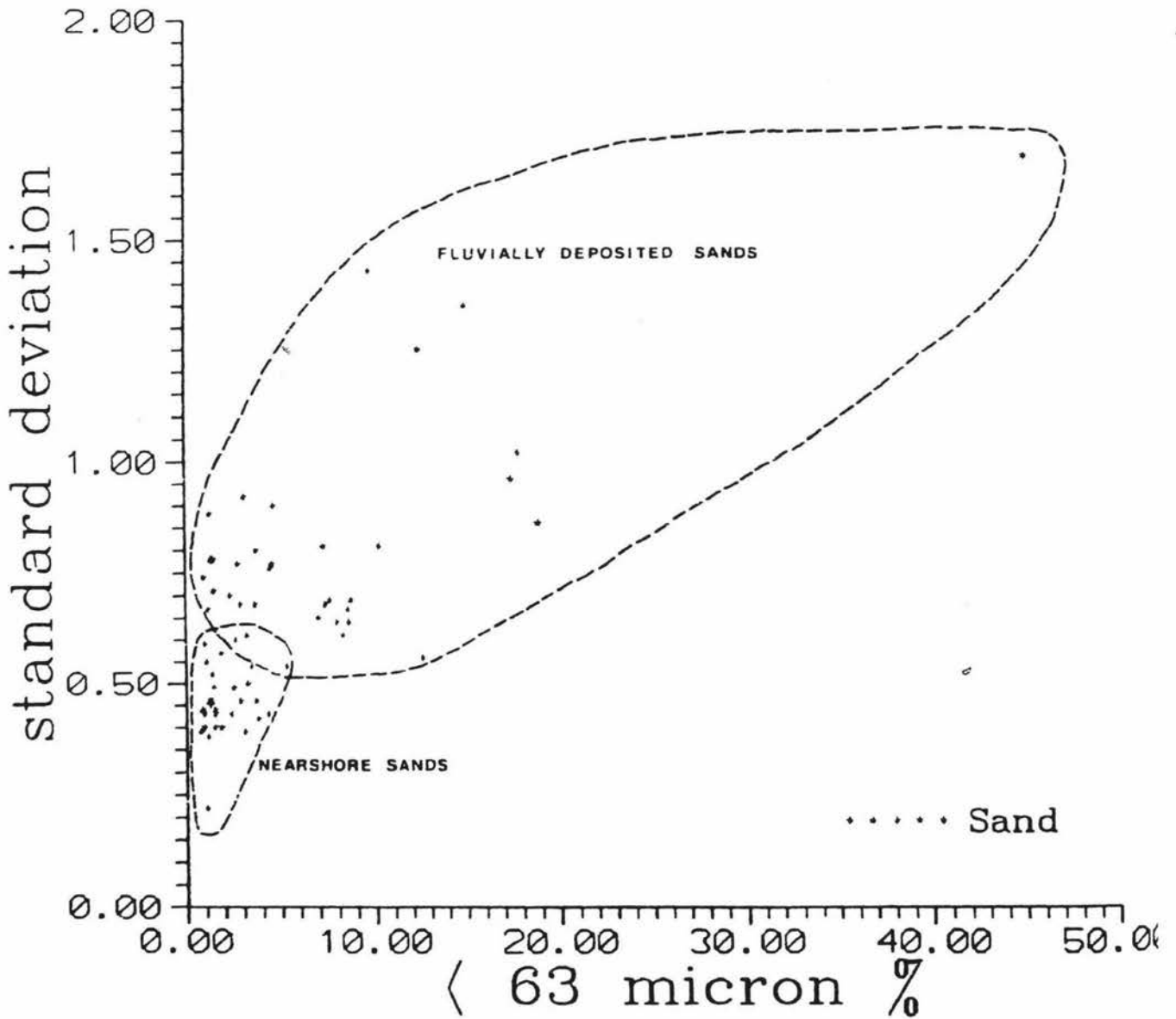


Fig. 4.7 Scatter plot of standard deviation (sorting) versus < 63 micron fraction (fine tail).

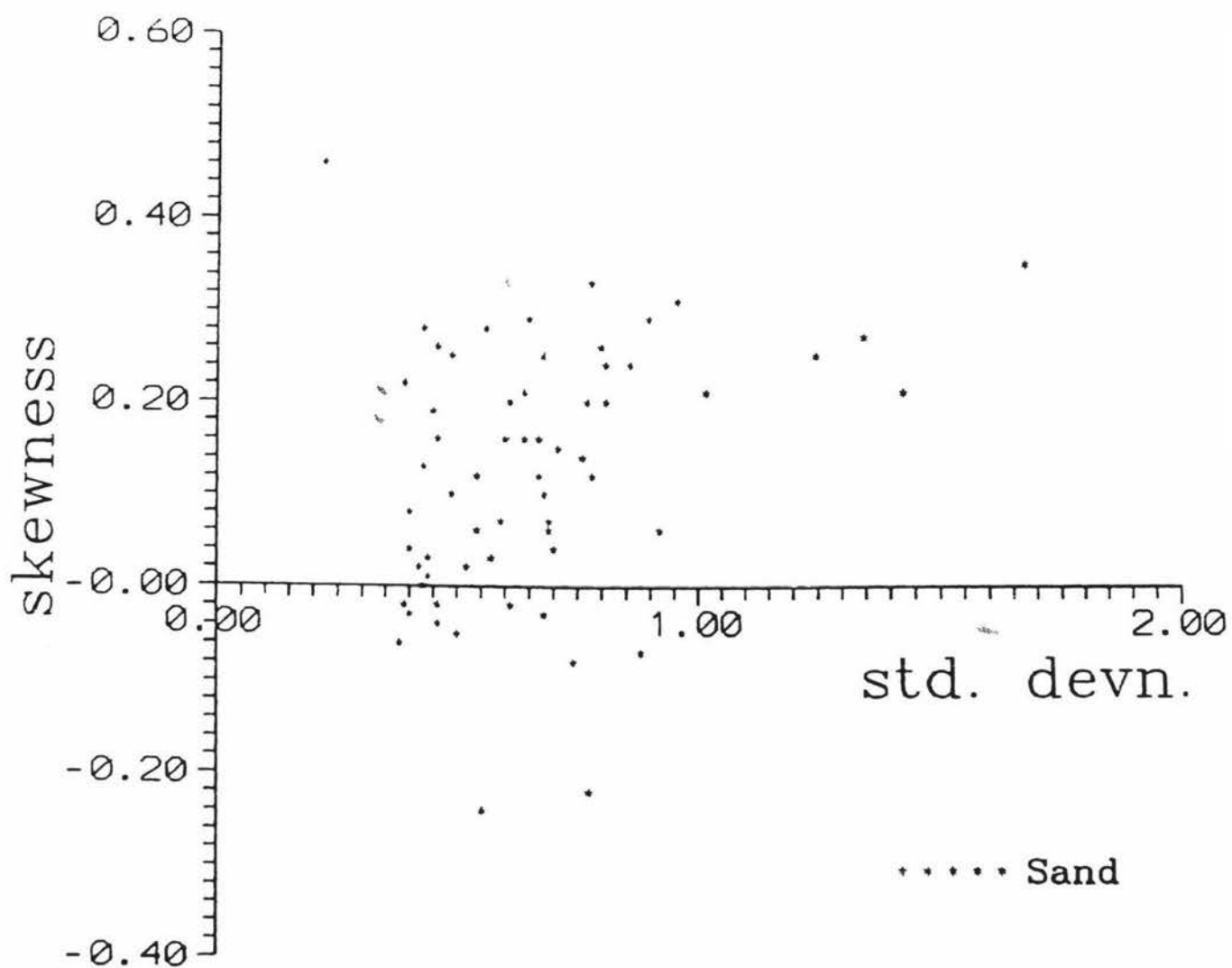


Fig. 4.8 Scatter plot of skewness versus standard deviation (sorting) for sand.

comparative lack of fine grained sediment. It should be noted, however, that although there is an apparent trend with sands generally becoming more poorly sorted as skewness increases in a positive direction, many sands are well sorted and positively skewed.

4.8 Environmental interpretation

To develop a method which will distinguish between sands of different environments, it is necessary to select parameters which reflect the different physical characteristics of the sediments. Parameters found to be useful in this study are:

1. standard deviation
2. mean grain size
3. skewness
4. mean cubed deviation
5. fine and coarse tail fraction

Sediments within the study area fall into two broad groups using these parameters.

Group one

This group is predominantly made up of well sorted, generally positive skewed sand: with a mean cubed deviation close to zero.

Group two

These sediments are composed of relatively poorly sorted silts with a widely varying but generally positive mean cubed deviation.

Within group one sediments a range of properties are obvious *i.e.* from those of classical beach sands (well sorted and negatively skewed) to those that display properties associated with beach and river sands (well sorted and positively skewed)

The positive skewness is due to a tail at the fine grained end of the distribution and may be accounted for by one of two processes:

1. The nearshore environment may not have had sufficient energy to winnow out the fine grained material being introduced, or
2. There may have been so much fine grained material introduced into the environment that not even a high energy system was able to remove all the fines.

It is likely that a combination of these processes is responsible, *i.e.* a low energy environment (possibly estuarine) with a high concentration of fine material being introduced. Friedman (1962) found in a study of ancient nearshore sands of marine origin that most samples were positively skewed. He inferred from this that marine sedimentation was strongly prograding with fines exceeding energy and basin subsidence.

Group two sediments display properties consistent with fluvial deposition *i.e.* they are poorly sorted and have a widely variable mean cubed deviation with a generally fine grained tail. These features are directly attributable to two factors:

- A. In fluvial environments, the fine grained particles that are transported in suspension are not deleted from the sediment. They are an important and essential component of the river load and are trapped between coarse grained particles or deposited in the waning stages of fluvial flow and
- B. A fine grained source rock.

4.9 Conclusion

It was not possible to analyse changing grain size parameters between facies, in the field, due to the lack of continuous outcrop and traceable beds. This is due mainly to the structural complexity in the field area. Because of this there is little evidence

of regional, vertical or lateral trends in grain size, apart from that seen in gravel facies. However, this study does demonstrate that environmental differentiation is possible, with nearshore, estuarine/tidal sands (affected by tidal winnowing processes) more densely crowded in their distribution in the scatter plots than fluviually deposited sands. Due to the overlapping nature of physical processes responsible for sediment deposition there are as expected, areas where grain size populations from different environments overlap.

CHAPTER FIVE

PALEOCURRENT ANALYSIS

5.1 Introduction

Paleocurrent analysis was invented by the nineteenth century English amateur geologist, Henry Clifton Sorby. Sorby (1859) wrote "The examination of modern seas, estuaries and rivers, shows that there is a distinct relation between their physical geography and the currents present in them; currents so impress themselves on the deposits formed under their influence that their characters can be ascertained from those formed in the ancient periods. Therefore their physical geography can be inferred within certain limits."

Paleocurrent analysis is primarily an outcrop study. It emphasizes the interdependence of stratigraphy, sedimentary petrology and structural geology (Potter and Pettijohn, 1977).

The aim of paleocurrent analysis is to provide information on four main aspects of basin development (Selley, 1976).

1. the direction of initial dip or paleoslope
2. the geometry and trend of lithologic units
3. the direction of sediment supply
4. the depositional environment

Paleocurrent analysis depends on the presence in sedimentary rocks of numerous properties from which current direction can be inferred. These properties are of four types. They are, attributes, scalars, directionals and tensors.

Attributes are those properties that are specified only by their presence or absence *e.g.* in the Dannevirke Basin the presence of greywacke gravel outlines the dispersal pattern of that lithology. Scalars are those properties that are specified by magnitude

alone, for examples grain size, mineral proportion, formation thickness, clastic ratio, or other combinations of lithologic proportions. Measurement of a scalar quantity at a point has no directional significance. However, when scalars are mapped across a region they may define the directional derivative of a scalar function. Grain size and formation thickness have proved especially useful in gaining an insight into paleoflow directions in this study. Directionals are those properties that indicate either a line of movement or a direction of movement and are specified by dip and dip direction. Directional data in this study were obtained from small and large scale cross-beds. Other directional indicators such as parting lineation, sole marks and gravel imbrication were not observed. Channels and scours although present were not considered to be large enough to be regionally significant. Tensors describe fabric-dependent properties such as fluid permeability, dielectric coefficient, magnetic susceptibility and others (Potter and Pettijohn, 1977). Description of these properties is beyond the scope of this study.

5.2 Data collection and processing

The Mangatewaiiti Stream was the only one of the four streams in the field area where a significant number of paleocurrent indicators were seen in outcrop. Data from the other three streams have been recorded despite the sparsity of measurable outcrops, to aid in correlation across the field area. The sediments were unconsolidated so it was possible to spade back exposures to determine the true dip and dip direction of each bed. In the case of directional structures dip and dip direction were measured on at least three sets, if present or within reach, of large and small scale cross-stratified beds. In most cases, however, data for only one set of cross beds were collected due to inaccessibility of other suitable bedsets or lack of outcrop. A total of 70 sets of readings were taken and grouped according to the sedimentary structures they were measured on (Appendix A). A vector mean (Curry, 1956) was computed for each set of readings. Magnitude was computed as a percentage and a scale of 1 cm:10% was applied.

Five current rose diagrams were plotted allowing easy assessment of modal direction (Fig. 5.1). They include:

- A. small scale cross-stratification in tidal/estuarine deposits.
- B. large scale cross-stratification in tidal/estuarine deposits.
- C. small scale cross-stratification in terrestrial deposits.
- D. large scale cross-stratification in terrestrial deposits.
- E. large and small scale cross-stratification in pumiceous deposits.

5.3 Reliability of large and small scale cross-stratification as direction indicators

Allen (1967) concluded that large scale structures were truer indicators of flow direction over a large area than small scale structures. The larger structures are the product of higher flow regime conditions where greater bed roughness and more turbulent flow with more cross currents tend to produce a greater variation in direction over a small area, but over a large area are more representative of regional flow. Small scale structures, on the other hand, are formed during more uniform flow conditions, showing little variability over a small area, but great diversity over a large area. Although small scale cross-stratification modal direction parallels that seen in large scale structures, there is a greater overall variability in direction of the large scale structures. This trend is in contrast to that seen by Seward, (1974) and may be due to a real variation or a variation due to sampling.

5.4 Results and discussion

5.4.1 Regional variation

Seward (1974) found that in studying the shallow marine deposited Makiriri Tuff Formation and Kaimatira Pumice Sand in the Wanganui Basin, small scale cross-stratification showed no regional trend. She concluded, therefore that it was controlled by local topography rather than regional structure. In the Dannevirke field area, modal direction of small scale cross-stratification (Fig. 5.1A,C) strongly

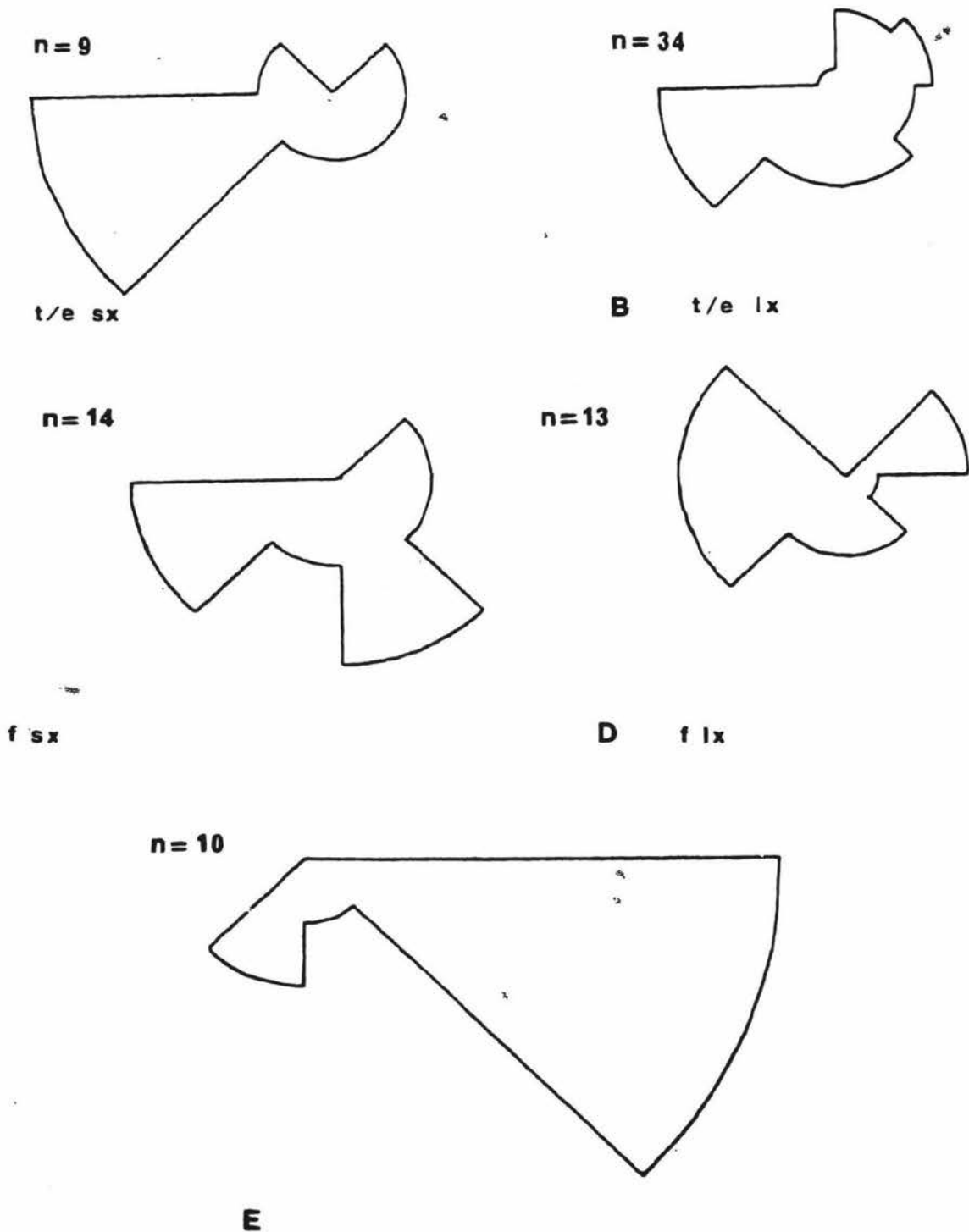


Fig. 5.1

Current rose diagrams of dip azimuths from cross-bedded sandstone and conglomerate in the Mangatarata Formation. A and B represent small (t/e sx) and large (t/e lx) scale cross-bedding in tidal/estuarine sediments, C and D represent small (f sx) and large (f lx) scale cross-bedding in terrestrial sediments and E represents small and large scale cross-bedding in pumiceous sediment.

parallels that of large scale cross beds (Fig. 5.1B,D). This is interpreted to suggest that the regional structure controlled the local topography and the predominant drainage patterns and thereby current direction. This suggests that folding is syndepositional rather than post depositional as suggested by Melhuish (1990). Terrestrial paleocurrent data (collected from predominantly fluviially deposited sediment) shows a trimodal directional pattern (Fig. 5.1C,D) of

1. east-west flow direction.
2. west south west-east north east flow direction.
3. northwest-southeast flow direction.

The east-west and west south west-east north east flow directions are approximately perpendicular to structural trends. The northwest-southeast flow direction of paleocurrent data (collected from fluviially deposited sediment) paralleling the structural trend gives a possible route, for the influx of pumice and associated sediment via a major paleofluvial system, into the area. This modal trend is especially dominant in data generated from small scale cross-stratification. Tidal/estuarine paleocurrent data shows a variation in modal direction in data generated from small scale and large scale cross-stratification. Data generated from small scale structures (Fig. 5.1A) show a dominantly unimodal direction, i.e. northeast-southwest, whereas data generated from large scale structures, (Fig. 5.1B) is polymodal. However, the dominant direction is still northeast-southwest. This variation in modal direction maybe due to tidal influences illustrated by the presence of herringbone cross-bedding and flaser bedding. The dominant paleocurrent direction for shallow marine beds is northeast-southwest which is subparallel to the regional structure.

5.4.2 Variation in current direction with time

Using data collected from the Mangatewaiiti Stream, variations in current direction were plotted in stratigraphic sequence (Fig. 5.2).

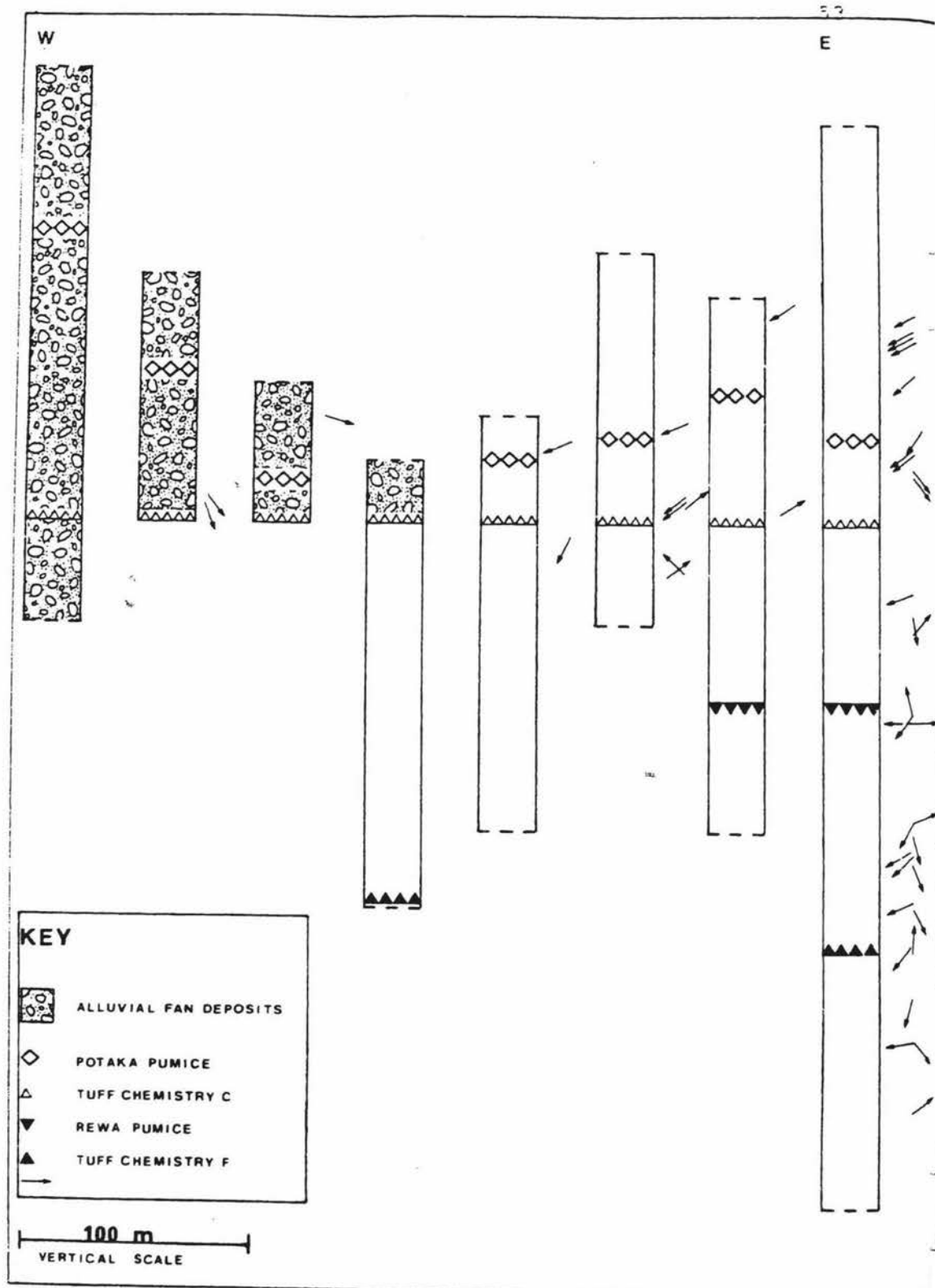


Fig. 5.2 Stratigraphic variability in current direction for Mangatewaiiti Stream sections from west (W) to east (E) and decreasing gravel thickness between the Potaka Pumice and Tuff Chemistry-C, from west to east.

Results indicate that there is little overall stratigraphic variability in current direction. The dominant paleocurrent direction is northeast-southwest. This dominant flow direction can be attributed to the paleogeographic restraints on the tidal/estuarine environment forming a northeast-southwest flowing, shallow marine embayment.

In the lower 250 m of the stratigraphic sequence there is a less dominant east-west, west-east aspect to paleocurrent direction. The east-west flow direction may be caused by uplift along the Ormondville Anticline to the east of the field area. This uplifted anticline is also considered to have formed the eastern boundary to estuarine/tidal conditions during the Castlecliffian *i.e.* there are no Castlecliffian, estuarine/tidal deposits east of this anticline.

The west-east aspect to paleocurrent direction is probably the result of progressive uplift in the Ruahine Ranges, because there are also isolated beds of greywacke gravel cropping out within the sequence.

To the west of the basin, in gravel deposits, paleocurrent analysis shows a dominant west-east flow direction. It should be noted that these deposits are not necessarily younger than sediment to the east but are a western facies of approximately equivalent age.

5.5 Sediment transport determined from gravel parameters

Selective transport from source in a fluvial environment accounts for 75% of the size decrease in gravels, the rest being attributed to abrasion and breakage (Plumley, 1948). Plumley also found that the rate of change of roundness with distance is proportional to some power of the distance. Sphericity increases slightly with distance but is somewhat erratic. As expected, the initial lithological composition of the clasts is directly related to the source area of the gravel. On the basis of these conclusions, mean size, roundness and lithology were determined for each of the major gravels.

5.5.1 Methods

The mean diameter of clasts in gravel is directly proportional to the diameter of the largest clasts (Pettijohn, 1957). Pelletier (1958) argued that the average of the ten largest clasts should be a rapid but reliable way of detecting changes in mean grain size of gravels, and hence indicate transport direction. The mean grain size, lithology and roundness of clasts were noted in the field.

5.5.2 Results and discussion

Mean size of the ten largest clasts is greatest along the western margin of the basin adjacent to the Mesozoic greywacke of the central axial range. Mean size decreases to the east and to the south in an approximately radial pattern while roundness increases. Clast lithology remains constant within the field area. It is concluded that the gravels have a western source. This is supported by a decrease in stratigraphic thickness eastward away from the ranges. The stratigraphic thickness was calculated by measuring the thickness between two identifiable beds, in this case the Potaka Pumice and Tuff 'chemistry C' (Fig. 5.2). Matrix deposited with the gravel ranges in size from coarse sand to silt and commonly contains pumice grains. Matrix pumice content increases away from the ranges.

5.6 Conclusions

There are at least two main sources of sediment for the Dannevirke Basin, one sedimentary and the other volcanoclastic. The high percentage of relatively large, subrounded to subangular greywacke clasts at the western edge of the basin suggests the axial ranges as a source for the gravel. To the east there is an increase in volcanoclastic sediment, a slight increase in roundness, a decrease in size of the greywacke clasts compared to those in the west and a decrease in the gravel facies thickness. The volcanic detritus was sourced from the central North Island (Kamp, 1981) but has been reworked from primary ignimbrites deposited in the north of the Dannevirke Basin by fluvial processes. Paleocurrent data for pumiceous sediment is rare due to mode of deposition (Chapter 6), but confirms pumice was reworked

from the northwest (Fig. 5.1E). A third less dominant source of sediment occurs to the northeast. This is evident from paleocurrent data for tidal\estuarine beds (Fig. 5.1A,B). This paleocurrent evidence agrees with mapping of a marine embayment extending from Hawke Bay to the Dannevirke area (Kamp, 1982).

CHAPTER SIX

FACIES ANALYSIS AND PALEOENVIRONMENTAL INTERPRETATION

6.1 Introduction

The term facies association was defined by Potter (1959) as a collection of commonly associated sedimentary attributes, including thickness and areal extent, continuity and shape of lithologic units, rock types, sedimentary structures, and faunal abundance and type.

Four facies associations are recognised in the Castlecliffian strata in the field area. These facies associations are based on analysis of sedimentary structures and their relationship to lithology, grain size and paleocurrent direction and have been used to develop a paleoenvironmental model for the Dannevirke Basin over Castlecliffian time.

Sediment groups i) to iv) (Chapter 2) are represented by the four facies associations, as outlined below. Group v) sediments (Chapter 2) *i.e.* pumice deposits, are not recognised as a separate facies association due to their widespread distribution throughout facies associations i) to iv). They are considered separately as pumice deposits.

Facies associations

- i) Facies association one (Af), is dominantly comprised of massive greywacke gravel and rubble.
- ii) Facies association two (Fc), (Fb) and (Fp) is dominated by cross-bedded sand with a greywacke pebble base.
- iii) Facies association three (Td) is generally a fossiliferous, flaser bedded silt to fine grained sand deposit.
- iv) Facies association four (Lc) is a rarely fossiliferous, fine grained, centimetre bedded (cmbdd) silt.

6.2 Facies association one (Af)

Facies association one (Af) dominantly composed of greywacke gravel and rubble is comprised of three distinct subfacies. They are:

Af₁ -massive, coarse grained greywacke rubble.

Af₂ -massive to cross-bedded gravel with interbedded silt.

Af₃ -massive to cross-bedded sandy gravel.

Af₁ -massive, coarse grained greywacke rubble

Subfacies Af₁ consists of generally fining-upwards sequences of angular, clast supported greywacke rubble. Two distinct sequence types are apparent,

- (i) sequence one consists of massive beds of extremely poorly sorted, slightly weathered, angular, clast supported, coarse pebble to cobble greywacke rubble with inferred disconformities at erosional contacts between sequences. The beds all lack imbrication.
- (ii) sequence two consists of massive beds of poorly sorted, slightly weathered, angular to subrounded, clast supported, medium pebble to cobble greywacke rubble to gravel, separated by silt beds up to 0.5 m thick. The basal gravel or rubble/silt contact is irregular and the upper contact is generally an erosion surface (Fig. 6.1).

Af₂ -massive to cross-bedded gravel with interbedded silt

Subfacies Af₂ generally consists of massive beds of slightly weathered, subangular to subrounded, poorly to moderately sorted, cobble to fine pebble greywacke gravel. Crudely centimetre to decimetre bedded (cmbdd-dmbdd) silts up to 2m thick are often found interbedded in these gravels and form an association similar to that seen in subfacies Af₁ (Fig. 6.2). Planar cross-bedded gravel is observed in association with subfacies Af₂ deposits but does not commonly occur. Each individual cross-bedded unit forms a fining-upwards sequence, up to 40cm thick, with the total sequence measuring up to 2m thick (Fig. 6.3).

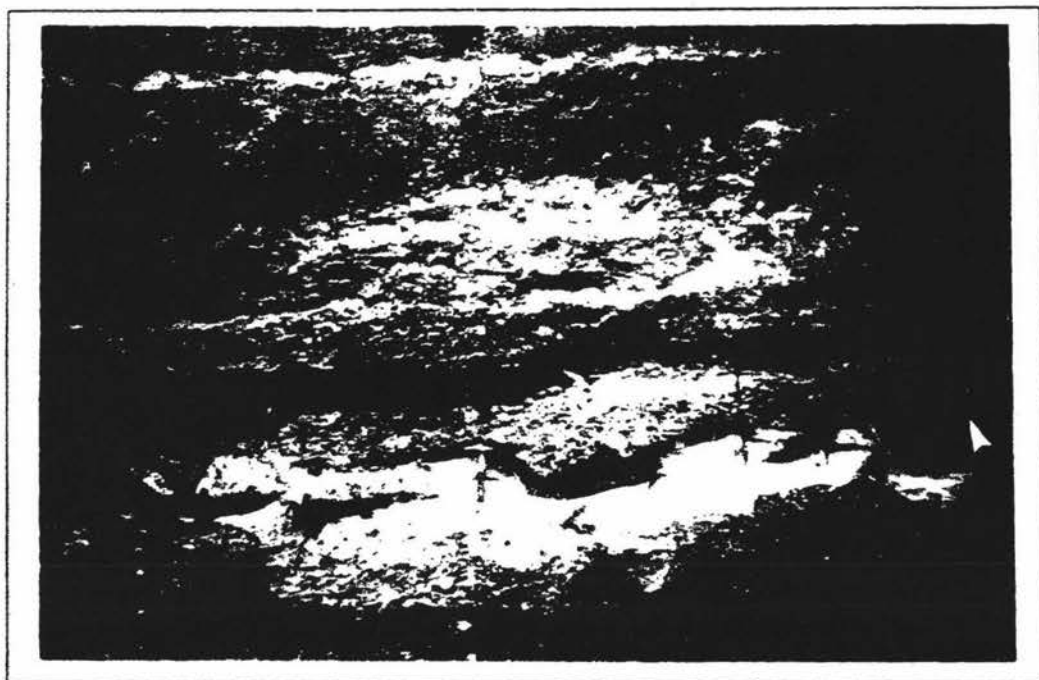


Fig. 6.1 Subfacies Af₁, sequence two. Massive, poorly sorted, angular, clast supported, coarse pebble to cobble greywacke gravel with interbedded silt representative of the proximal alluvial fan environment. Note erosional contact between silt bed and overlying gravel (arrows). Hammer for scale, 0.30m.



Fig. 6.2 Subfacies Af₂. Massive, clast supported, cobble to fine pebble greywacke gravel with interbedded cmbdd-dmbdd silt up to 2m thick representing the medial alluvial fan environment. Note erosional contact at the base of the gravel (arrow). Spade for scale, 0.9m.

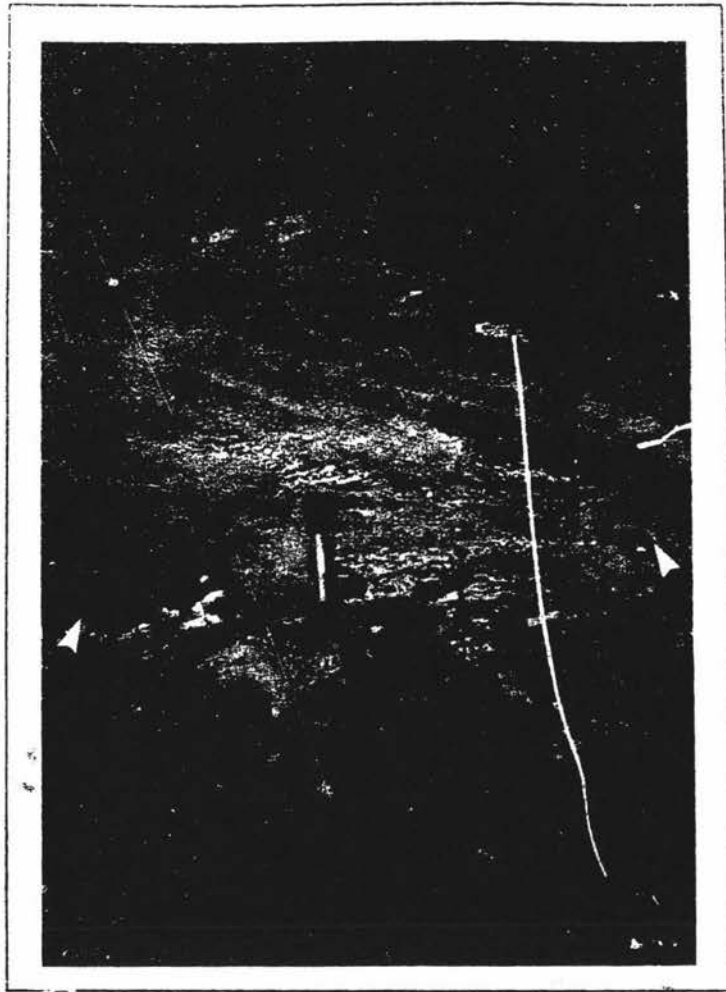


Fig. 6.3 Subfacies Af₂. Planar, cross-bedded, fining-upwards greywacke gravel, representative of the medial alluvial fan environment, overlying carbonaceous silt deposited in a backswamp environment. Arrows at erosional contact. Spade for scale, 0.90m.

Af₁ -massive to cross-bedded sandy gravel

Subfacies Af₃ is characterised by thick sequences of planar, crudely imbedded silt up to 5m thick, with interbedded subrounded to rounded, moderately sorted, very coarse pebble to very fine pebble, generally matrix supported lenses of greywacke gravel. Occasional narrow bands of pebbles form lag deposits at the base of planar and trough cross-bedded sandy gravel sequences. Fossil tree trunks are often preserved within this subfacies (Fig. 6.4).

6.2.1 Distribution and age

Facies association one is a dominantly gravelly facies association. It is most extensive in the west of the basin and wedges out towards the east. The oldest gravel bed seen in the field area crops out in the Mangatewainui Stream. It occurs 105m above the tuff tentatively identified as the Pakihikura Pumice. The gravel is estimated to be about 1.05 Ma, based on a sedimentation rate of 0.45 mm/yr as calculated from other parts of the basin. The youngest Castlecliffian gravels in the area are those exposed near the Ruahine Ranges. They are dated by the presence of a tuff identified as the Potaka Pumice (Melhuish, 1990), with a radiometric age of 0.80 Ma (Pillans, 1991). The presence of the Potaka Pumice within subfacies Af₁ deposits shows that uplift of the Ruahine Ranges was occurring at the time it was deposited.

6.2.2 Paleoenvironmental interpretation

The three gravel/rubble subfacies resemble proximal to distal alluvial fan deposits.

Subfacies Af₁ sequences (i) and (ii), greywacke rubble, occur closest to the ranges and have therefore undergone the least abrasion due to transport. This is reflected in the angularity and extremely poorly sorted nature of the deposit. Subfacies Af₁ is interpreted to represent the proximal alluvial fan environment. The proximal facies in the study area may be attributed to normal streamflow, streamflood and sheetflood processes. Normal streamflow and streamflood processes are responsible



Fig. 6.4 Subfacies Af₃. Trough cross-bedded, matrix supported, sandy greywacke gravel containing fossil tree trunks (arrows) representative of the distal alluvial fan environment. Spade for scale, 0.90m.

for the coarse, extremely poorly sorted rubble, seen adjacent to the Range Front Fault, which form the head of the paleofan.

The poorly sorted rubble deposits interpreted as being deposited by streamflood and sheetflood in the field area are similar to those described by Blissenbach (1954) and Bull (1972) from alluvial fans in the southwestern United States. They interpret streamfloods to be caused by storm events resulting in large amounts of water and debris flowing in alluvial fan channels. Sheetfloods occur when a streamflood overtops or is diverted from its channel so as to cover a substantial part of the alluvial fan surface, depositing sheets of almost structureless gravel. The silt deposits and scoured out pits and gullies up to 0.5m deep, sometimes with a delta of pebbly silt at the downcurrent end as in sequence (ii) (Fig. 6.1), are very similar to deposits described by Harvey (1978) from alluvial fans in southwest Spain. These gravels were deposited by waning flood processes. The fanhead has been characterised as a multi-channel low sinuosity stream with aggradational filling (Ori, 1982).

Subfacies Af₂, massive to cross-bedded gravel and silt interbeds, interfinger with Af₁ deposits but are normally found farther east from the Range Front Fault than Af₁ deposits. The better sorting and finer grain size of the gravel in Af₂ compared with Af₁ reflects the greater distance transported from source. Subfacies Af₂ is interpreted to represent the medial alluvial fan environment. The massive clast supported gravel and associated silts in this subfacies are similar to those deposits described by Harvey (1984) from Spanish Quaternary alluvial fans. These deposits are interpreted to have been deposited by sheetflood and waning sheetflood processes. The thicker silt units (compared with those in subfacies Af₁) are associated with decreasing grain size away from the fan apex and may represent more than one depositional episode. Cross-bedded gravel sequences described by Kostaschuk *et al.*, (1986) in humid region alluvial fan deposits from Peno River, northern Italy are similar to cross-bedding in subfacies Af₂ seen in the field area and are probably formed by longitudinal and point bar evolution as a result of streamflood. This subfacies is attributable to an increase in channel sinuosity and the occurrence of lateral accretion resulting in the existence of a mixed pattern of meandering and braided multi-sinuosity channels (Ori, 1982).

Subfacies Af₃, massive to cross-bedded sandy gravel deposits interfinger with Af₂ deposits. Subfacies Af₃ is deposited farthest from the Range Front Fault of the subfacies in facies association one. These finer grained and better sorted deposits, compared with Af₁ and Af₂, are interpreted to have formed in a dominantly meandering stream environment. The siltstone sequences are interpreted as overbank fines from streamflood deposits while the crude foreset bedding, commonly associated with pebbly sandstones, resemble deposits described by Hein and Walker (1977) in the Kicking Horse River, British Columbia. Hein and Walker interpret these as transverse bars formed under low energy flood conditions. Trough cross-bedded sand and sandy gravel commonly associated with low angle foreset bedded gravel seen in Af₃ are similar to those described by Ori (1982) from the Peno River in Italy. These were probably deposited by migrating megaripples in braided stream channels formed during low flow conditions in what was normally a meandering stream. These deposits differ from sheet gravels seen in Af₁ by their greater clast roundness, better sorting and by the presence of distinct sedimentary structures.

6.2.3 Fan Geometry

In the Mangatewaiiti Stream, facies changes have been traced in fan deposits by following Tuff 'chemistry C' and the Potaka Pumice eastward, away from the Range.

It is possible to demonstrate rapid thinning of the total gravel sequence away from the range front *i.e.* toward the east (Fig. 5.2), and thus infer areal distribution typical of an alluvial fan *i.e.* wedging out away from source. It is not possible to show that distribution of alluvial fan deposits form a radial pattern, as would be expected, due to the lack of exposed sequence in the south of the field area. In westernmost gravels, exposed in the Mangatewaiiti Stream and interpreted to be proximal alluvial fan deposits, there is a thickness of 135m between Tuff 'chemistry C' and the Potaka Pumice. However, this thickness decreases toward the east, to about 25m where the pumice units are again identified, but in association with distal alluvial fan facies.

6.3 Facies association two (Fc, Fb and Fp)

Facies association two can be subdivided into three groups.

- Group one (Fc) -fining up cross-bedded sand with a gravel and silt rip-up clast base.
- Group two (Fb) -interbedded sand and silt grading up into massive, organic matter rich silt.
- Group three (Fp) -fining upwards, organic matter rich, fine sand to silt.

6.3.1 Facies descriptions (Fc)

Facies association two, group one (Fc) is comprised of three distinct subfacies. They are:

Fc₁ -rounded greywacke gravel and silt rip-up clasts in a sand matrix.

Fc₂ -trough cross-bedded sand.

Fc₃ -ripple cross-laminated sand.

Subfacies Fc₁ is represented by lenses (<0.30 m) of rounded, matrix supported, coarse to very fine, pebble, greywacke gravel with occasional silt rip-up clasts. The silt rip-up clasts are generally sub-rectangular with a small degree of rounding, particularly at the ends. Two forms were observed:

- a) a preferred orientation of the blocks which parallel the base of the beds and show some imbrication (Fig. 6.5).
- b) random orientation of blocks (Fig. 6.6).

The coarse grained basal deposits described above are usually covered by medium to coarse grained sand. Subfacies Fc₁ commonly, but not always, forms the base on which other subfacies in this association are deposited.

Subfacies Fc₂ is the most commonly occurring subfacies within this group. The base of Fc₂ is commonly the coarsest part of the sequence and may be up to 0.40m thick. Grain size ranges from cobbles to coarse sand. Rip-up clasts are often present

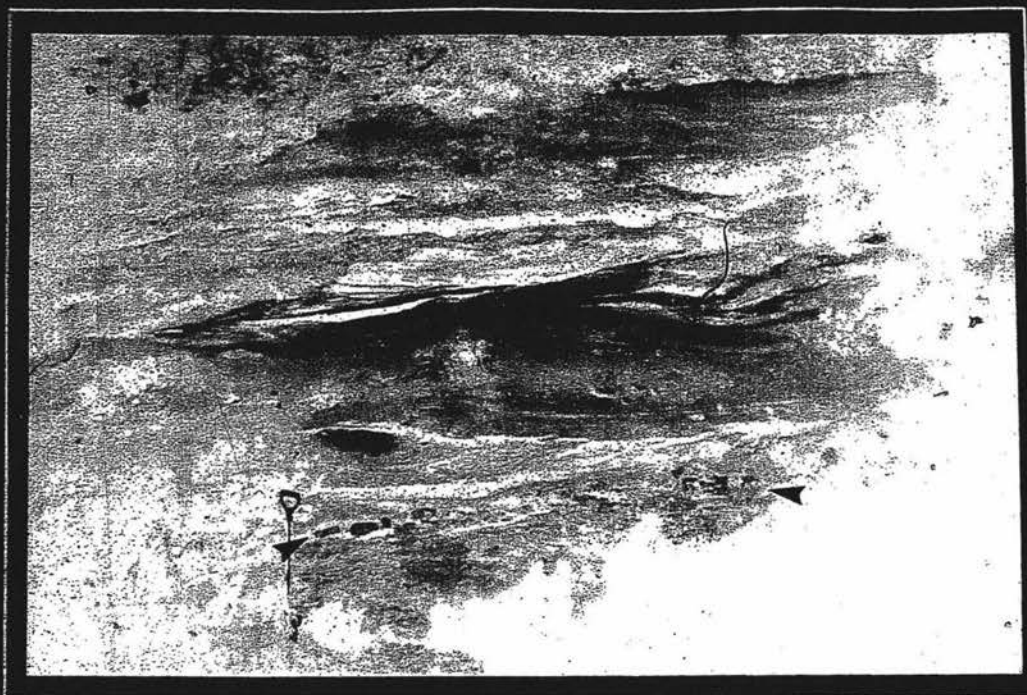


Fig. 6.5 Subfacies Fc_2 . Trough cross-bedded sand interpreted as a point bar deposit overlying an intraformational breccia (arrow) showing preferred orientation paralleling the base of the bed. Spade for scale, 0.95m.



Fig. 6.6 Intraformational breccia (white arrow) showing random orientation of silt clasts in fluvial channel sand. Black arrows point to erosive base of channel. Spade handle for scale, 0.20m.

within this basal part of the sequence. The coarse base fines up into a large scale trough cross-bedded, coarse to medium grained sand unit up to 3m thick. Trough cross-beds typically have a trough-shaped set consisting of an elongate erosional scour filled with curved laminae that dip in a downcurrent direction. These trough cross-bedded sands pass up into smaller scale (<0.5m thick) medium to fine grained, ripple-cross laminated sand units and occasionally the sequence is capped by parallel laminated fine sand or silt (Fig. 6.7).

Subfacies Fc₃ is comprised of two sequences that are similar in content but vary in scale.

Sequence 1 consists of a basal sequence similar to that in Fc₂ but with a much thicker sequence of ripple cross-laminated sand (up to 1.5m thick). This is overlain by a parallel laminated silt with occasionally interbedded fine grained, sometimes ripple cross-bedded sand. The top of the sequence shows an increasing enrichment in organic matter sometimes culminating in the formation of thin platy lignites, less than 0.30m.

Sequence 2 has a basal deposit more like that of Fc₂ *i.e.* the fine grained, ripple cross-laminated sand is less extensive than that in sequence 1 (<0.50m). The sequence is capped by deposits similar to those in sequence 1 although they are generally much thicker (c.3m).

6.3.2 Paleoenvironmental interpretation

The group 1 subfacies (Fc) deposits resemble channel lag, point bar and channel fill deposits formed in a meandering stream environment.

Subfacies Fc₁, greywacke gravel and silt rip-up clasts in a sand matrix, is probably a channel lag deposit representing residual concentration after winnowing of finer sediment and accumulated as discontinuous lenticular deposits. The small degree of rounding of rip-up clasts associated with this deposit suggests at least some abrasion and transport. At some localities erosion of underlying silt beds is evident and the



Fig. 6.7 Subfacies Fc₁. Small-scale cross-bedded, fine-grained sand, overlain by trough cross-bedded, coarse sand fining-upwards to ripple cross-laminated, medium- to fine-grained sand, indicative of point bar deposits. Notebook for scale, 0.20m.

texture and lithology of the blocks are identical to the underlying rock type. This suggests that the rip-up clasts were formed from fragments of the underlying silt beds by currents strong enough to transport the blocks.

Subfacies Fc_2 , trough cross-bedded sand, is interpreted to be a point bar deposit. Lateral migration of the channel produces a tabular sand unit overlying a near horizontal erosion surface commonly with a lag gravel. The sand which forms the bulk of the unit shows a decrease in grain size and a decrease in the size of the trough cross-beds upsection. Dunes (upper, lower flow regime, Fig. 6.8) are the migrating bedforms that deposit trough cross-stratification (Harms, 1975). The erosional surfaces present within sets probably result from erosion of the dune crest and lee side (Fig. 6.9) by falling or low stage flows. The reactivation surfaces (Fig. 6.10) are preserved within the sediment when normal dune formation processes begin again (Leeder, 1982). The decrease in grain size and size of the trough cross-beds upsection is interpreted to be due to a waning flood period or to spiralling flow through the meander loop causing decelerating flow components up the point bar (Walker and Cant, 1984). The parallel laminated fine sand or silt sometimes capping this sequence is probably due to deposition of suspended sediment during receding flood flow (Reineck and Singh, 1980).

Subfacies Fc_3 , ripple cross-laminated, probably represents the initial stages of point bar accretion followed by channel abandonment. Sequence 1 represents chute cut off whereas sequence 2 is indicative of neck cut off (Fig. 6.11). The greater relative thickness of ripple cross-laminated sand and the smaller relative thickness of vertical accretion deposits, compared with sequence 2, capping sequence 1 is probably due to gradual abandonment associated with chute cut off (Walker, 1976). The vertical accretion deposits are probably associated with a swampy environment as the channel is filled with sediment, given the large amount of organic matter often associated with these fine grained sequences (Fig. 6.11.)

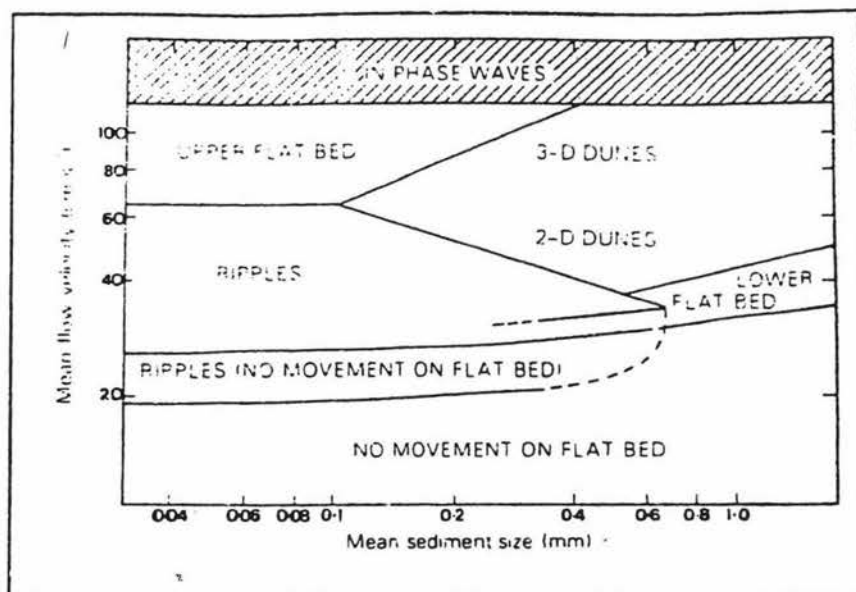


Fig. 6.8 The stability fields of different bedforms in relation to flow velocity and grain size for water depth of 0.20m (Collinson and Thompson, 1989).

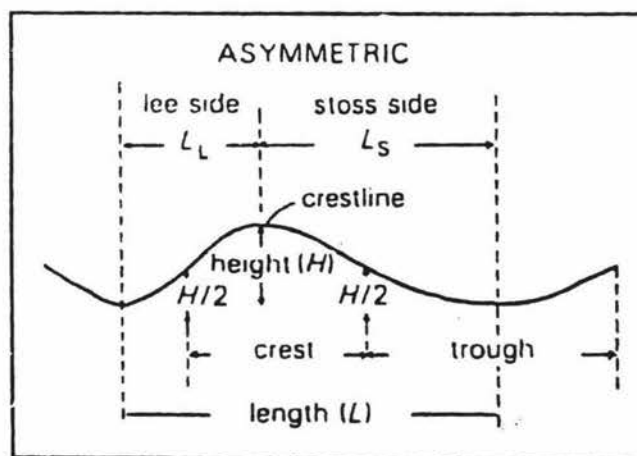


Fig. 6.9 Definition diagram for descriptive terms used in the description of cross-stratification (Collinson and Thompson, 1989).



Fig. 6.10 Reactivation surfaces (arrow) between two sets of cross-beds in medium-grained sand are preserved when normal dune form processes begin after low stage flow.

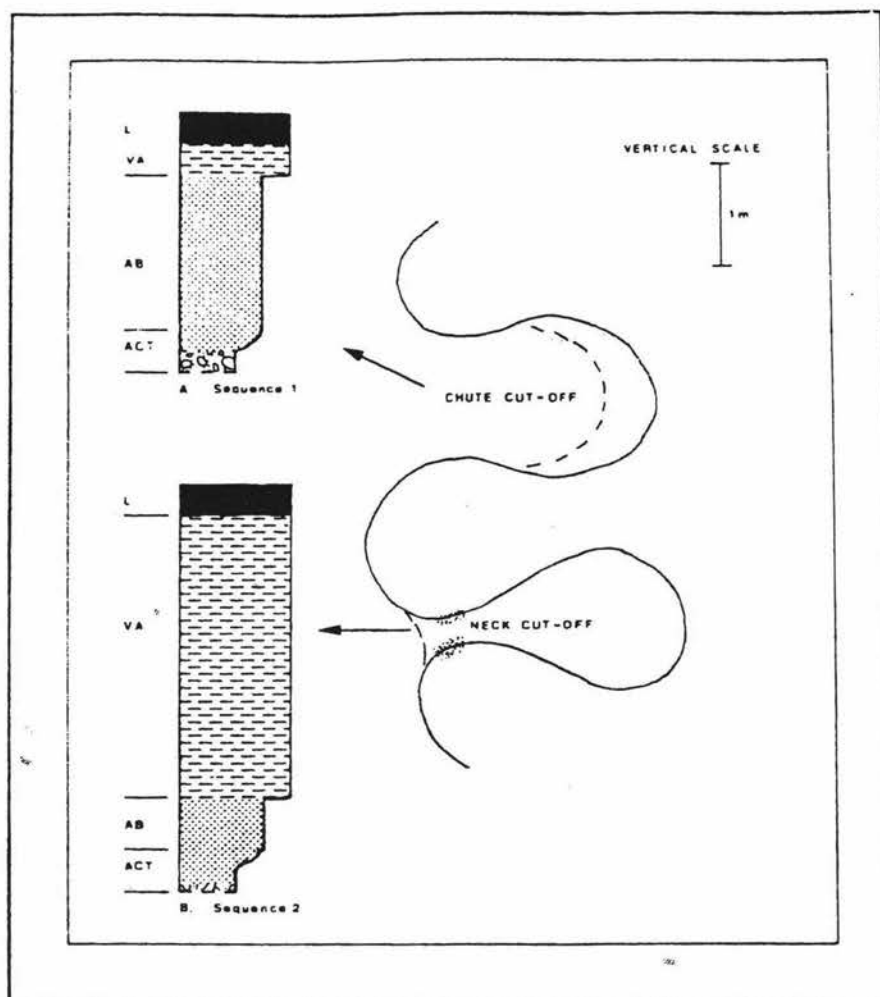


Fig. 6.11 Meander loops can be abandoned by chute or neck cut-off. Old channel shown solid, new channels dashed. Chute cut-off involves gradual channel abandonment. The stratigraphic sequence consists of trough cross-bedded deposits of the active river (ACT) and a thick sequence of ripple cross-laminated fine sands representing gradual abandonment (AB). After cut-off, the sequence is completed by vertical-accretion (V.A.) deposits and peaty swamp deposits (L). By contrast, after neck cut-off the meander loop is suddenly abandoned and sealed off by deposition of sand plugs (stipple). After the active deposits, the ripple cross-laminated fine sands representing low flow during abandonment (AB) are very thin, and most of the sequence consists of vertical accretion deposits washed into the abandoned loop at flood time. Diagram, modified from Walker, 1976.

6.3.3 Facies descriptions (Fb)

The second group (Fb) within facies association two is made up of two subfacies that commonly interfinger and are sometimes difficult to separate.

Fb₁ -interbedded sand and silt.

Fb₂ -massive organic matter rich silt with interbedded fine to coarse grained sand.

Subfacies Fb₁ is commonly associated with subfacies Fc₂ and is made up of interbedded fine to medium grained, moderately well sorted sand and silt up to 5m thick. The sand is commonly ripple cross-bedded or horizontally bedded and up to 4cm thick while the overlying silt is horizontally laminated or massive and is usually less than 2cm thick. These deposits usually contain old root channels (Fig. 6.12). In some cases the sand in Fb₁ is considerably thicker (up to 10cm) than the overlying silt and is quite well sorted. Overall Fb₁ was not very common in the field area.

Subfacies Fb₂ occurs as fine to coarse grained sand, usually only 1-2cm thick, interbedded between beds of organic matter-rich silt up to 5m thick.

6.3.4 Paleoenvironmental interpretation

Subfacies Fb₁, interbedded sand and silt, is interpreted to be a levee deposit due to its association with the relatively coarser grained point bar subfacies (Fc₂). The interbedded nature of the deposit is due to the method of deposition. Natural levees are formed by deposition of sediment when flood waters of a stream overtops its banks. The associated reduction in flow velocity, causes deposition of much of the suspended sediment near the channel. Coarsest sediment is deposited near the channel and grain size decreases away from it as does rate of deposition (Reineck and Singh, 1980). The thicker units of sand associated with this subfacies may be attributable to deposition in a crevasse splay channel. The rare occurrence of Fb₁ in the field area may be accounted for by the low preservation potential due to the levees position on concave banks where erosion commonly occurs.

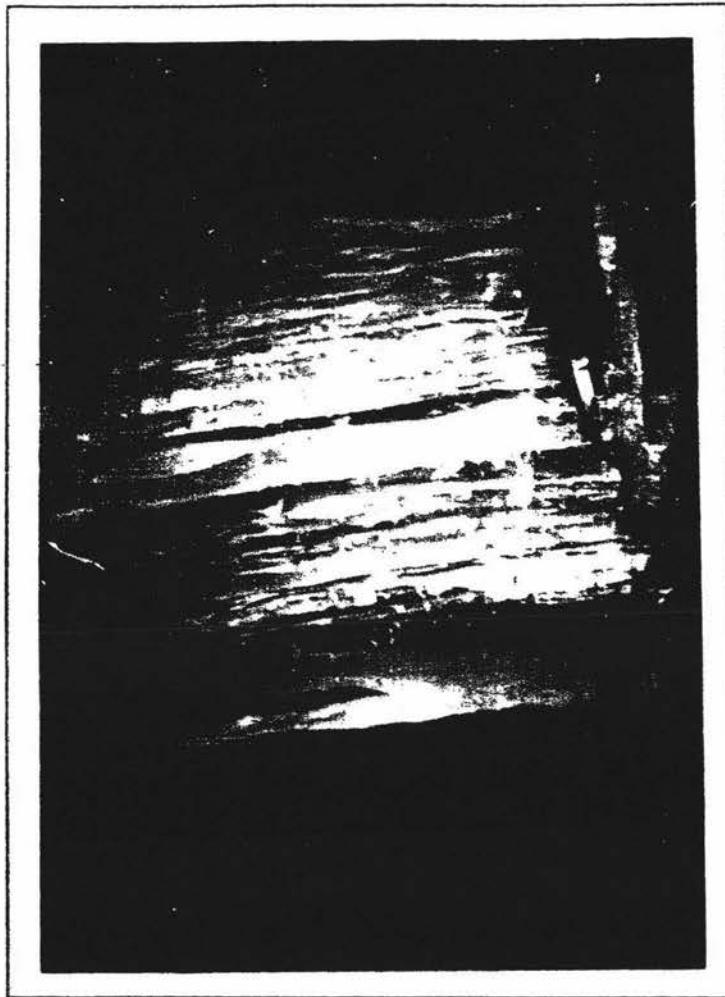


Fig 6.12 Subfacies Fb₁. Root channels in finely interlaminated silt and fine sand levee deposit, representing the onset of pedogenic processes. Knife for scale, 7cm

Subfacies Fb₂, organic rich silt with interbedded sand, probably represents a distal channel splay deposit given its close association with facies Fp. Facies Fp, as is later explained, is a floodplain deposit, and a crevasse splay is the only method envisaged as being able to carry sandy deposits into this environment.

6.3.5 Facies description (Fp)

The third group (Fp) within facies association two contains only one subfacies. Subfacies Fp₁, contains the finest sediment in facies association two. Deposits commonly form a fining upwards sequence of silt to clay sized sediment and usually contain a significant percentage of organic matter. In some cases dark brown to black, platy lignite beds, 0.60-0.70m thick, and weathered and fractured silts are associated with these fine grained sequences (Fig. 6.13).

6.3.6 Paleoenvironmental interpretation

Group Fp is interpreted as flood basin and associated back swamp deposits. Sedimentation is by vertical accretion and the fining up nature of Fp₁ is a result of waning overbank flood flow. The decrease in grain size occurs because coarser sediment is no longer able to remain in suspension. The flood basin is the lowest lying part of the flood plain. It is poorly drained and has little or no relief and is located adjacent to active and abandoned stream channels. Floodplain deposits in the field area are seldom seen to reach thicknesses greater than 30m, due to the actively shifting nature of the channel giving little time for aggradation. Thick vegetation is responsible for the large amount of organic matter seen in these deposits and where this organic matter accumulates in peat layers several meters thick, lignites may be formed.



Fig. 6.13 Subfacies Fp_1 . Massive, fine-grained silt with overlying lignite (arrow) representing overbank fines deposited in a backswamp environment where organic matter accumulates. Spade for scale, 0.90m.

6.3.7 Age

Facies association two is represented by sediments deposited from just above the Castlecliffian-Nukumaruan boundary to at least the end of the Castlecliffian.

6.4 Facies association three (Td)

Facies association three is similar in many respects to facies association two, especially in its range of sedimentary structures. Fossiliferous beds and associated biogenic sedimentary structures along with paleocurrent directions are vital evidence in interpretation of the environment of deposition of facies association three.

Facies association three (Td) is made up of two distinct subfacies. They are:

Subfacies Td₁ -rarely bioturbated, fossiliferous, flaser bedded, interlaminated silt and sand.

Subfacies Td₂ -cross-bedded sand with a coarse pebbly sand base.

Subfacies Td₁ ranges in grain size from silt to medium-grained sand. It is rarely bioturbated with occasional bands (<0.30m) of fragmented, thin shelled, stunted *Austrovenus stutchburyi*. Td₁ is dominated by interlaminated, millimetre to centimetre bedded (mmbdd-cmbdd) silt and sand (<3.0m thick) exhibiting prolific flaser bedding (Fig. 6.14), wavy bedding and lenticular bedding.

Subfacies Td₂, cross-bedded sand with a coarse pebbly sand base, forms two distinct sequences.

Sequence 1 has a basal erosion surface overlain by an intraformational sandy, well rounded gravel (<0.40m) which often contains fossil wood of widely varying size. Trough cross-bedded coarse- to medium-grained sand conformably overlies the pebbly base. Cross-bed foresets are draped by clay laminae less than 2.0cm thick. Finer grained flaser bedded deposits of Td₁ succeed these sands.



Fig. 6.14 Subfacies Td_1 . Flaser bedded, fine-grained sand overlain by wavy and lenticular bedded, very fine-grained sand, indicative of tidal processes. Spade for scale, 0.90m.

Sequence 2 has thick (1-2m) often trough cross-bedded, intraformational shelly gravel containing fossil tree trunks filling large channel-like scours, up to 2m across. Trough cross-bedded medium grained sands grade up into horizontal bedded and herringbone cross-bedded sands (Fig. 6.15), with silt drapes on some of the foresets. Intercalated between these channel like sands are erosive based sheet-like units (1-2m thick) of interlaminated silts and fine grained ripple laminated sands which frequently exhibit flaser bedding and lenticular bedding.

6.4.1 Age

Deposits representing this facies association occur from the Castlecliffian-Nukumaruan boundary to just above the Potaka Pumice (0.80 Ma).

6.4.2 Paleoenvironmental interpretation

Subfacies Td₁ deposits, flaser bedded, interlaminated silt and sand, resemble facies of an estuarine, intertidal flat environment. A.G. Beu (1991 pers. comm.) has identified the *Austrovenus stutchburyi* fossils as estuarine, living in the intertidal environment. All other fossils collected (Appendix C) are thought to be reworked from Nukumaruan strata (A.G. Beu, pers. comm., 1991). Subfacies Td₁ reflects constantly fluctuating but relatively low energy conditions, with brief periods of sand and coarse silt bedload transport by tidal currents and waves alternating with fine sediment deposition from suspension. It is this process that is responsible for the abundant flaser bedding, where ripple troughs in fine to medium grained cross-stratified sand are filled by silt (Reineck and Wunderlich, 1968). The lack of trace fossils associated with what is normally a strongly bioturbated environment may be due to the large amount of pumice being introduced into the basin. This theory was also forwarded by Te Punga (1953) to explain lack of bioturbation and the stunted thin shelled *A. stutchburyi* present in the Castlecliffian aged Rangitikei Valley sequence. All burrows observed in facies association three appear to be dwelling rather than escape features and range in size from 2cm to 7cm in length. The deeper burrows probably represent an environment closer to the high tide mark and thus the need for the organism to burrow more deeply to avoid desiccation. Shallow



Fig. 6.15 Subfacies Td₂. Herringbone cross-bedding consisting of foreset laminae dipping in opposite directions in medium- to coarse-grained sand. Knife for scale, 7cm.

burrows are probably formed by organisms living closer to or below the low tide mark where they are less prone to drying out (Fig. 6.16). Even on the rare occasions when burrows were observed in pumice deposits they were interpreted to be dwelling rather than escape burrows as there was no evidence to suggest that the organism responsible for the burrow had escaped from the bed below the pumice. Only one other type of trace fossil was observed in the field area. A bedding plane in a fine sandy unit was covered in bilobed trails with transverse ornaments. These features are interpreted to be feeding trails (Collinson and Thompson, 1989) deposited by an organism living in a low energy environment with a low sedimentation rate. This conclusion is consistent with other sedimentary structures present that are indicative of an intertidal environment.

Subfacies Td_2 is interpreted to be a tidal/estuarine channel deposit. Clay laminae and interlaminated silt on cross-bedded foresets suggest that bedform migration was intermittent in response to tidal current fluctuations. Paleocurrent data (Fig. 5.2) shows the dominant current direction was from the northeast with subordinate directions from the southwest and west. These bimodal data support the tidal origin of these deposits. The deposits of sequence 2 are interpreted as the relatively deep parts of estuarine/tidal channels whereas the deposits of sequence 1 represent the laterally accreting point bar higher on the inner depositional bank.

6.5 Facies association four (Lc)

Facies association four is generally comprised of very fine grained sand to silt and contains a unique microfossil and macrofossil assemblage reflecting environment of deposition. Facies association four is usually found in close proximity to facies association two.

6.5.1 Facies descriptions

Subfacies Lc_1 is made up of very well sorted fine grained sand to silt. Centimetre to decimetre bedding (cmbdd-dmbdd) within this deposit is prominent but does not appear to be due to a change in grain size. Deposits representing this facies form



Fig. 6.16 Shallow dwelling burrow (arrow) in medium-grained, horizontally bedded sand, fining upwards to cross-bedded and ripple cross-bedded sand and silt. The burrow is probably formed by an organism living near the low tide mark.

sequences up to 15m thick. Within these sequences there are repeated units of 2-5m thick, embdd-dmbdd silt overlain by lignites up to 0.5m thick. The freshwater mollusc, *Hyridella menziesi* is generally present in these beds but is not common. A number of diatom species (Appendix B) have been identified (M. Harper, 1991 pers. comm.) and are important environmental indicators.

Subfacies Lc_2 is a laminated, very fine silt deposit. Large amounts of vegetation are preserved throughout these deposits which are up to 0.75m thick. Diatoms are also common within this subfacies.

6.5.2 Age

Deposits representing this facies association first appear 60m below the Rewa Pumice (1.0 Ma) and last appear at about the time the Potaka Pumice (0.80 Ma) was deposited.

6.5.3 Paleoenvironmental interpretation

Facies association four is interpreted as a repeating evolutionary lacustrine sequence deposited in an interfluvial floodbasin. This facies close association with deposits of facies association two, is considered good evidence for the interfluvial setting of these lacustrine deposits. The fine grained, bedded nature of subfacies Lc_1 is due to intermittent deposition of fine grained fluvial overbank deposits in a locally subsiding interfluvial floodbasin where water has become ponded. Low lying well drained backswamps probably surrounded these lakes. Vegetation in these backswamps, which were partly drowned, formed carbonaceous silt as well as thin lignites. These deposits gradually spread into and filled the lakes, then with renewed subsidence the cycle was able to begin again.

All the diatom species (Appendix B) except the *Navicula* species and *Stephanodiscus sp* are usually found attached to waterweeds. *Stephanodiscus sp* are planktic but small species occur in the open water between emergent waterweeds. All samples have floras which contain a high proportion of benthic diatoms which live in shallow

water, (< 10m depth). These diatoms are freshwater species though most of them prefer slightly hardwater indicating erosion of some calcareous or marine sedimentary rock. There are a few species that will tolerate slightly brackish conditions but they are present in very small numbers and are also tolerant of hardwater so they may merely be incidental. A few diatoms prefer still water and a few flowing water, but the majority are indifferent. This indicates that the flow rate in the water bodies was low but there was some input from streams (M. Harper, 1991 pers. comm.).

Subfacies Lc_2 is interpreted as a well drained backswamp deposit associated with a shallow lacustrine environment due to the presence of a large amount of fossil monocotyledonous leaves typical of *Typha spp* (raupo). This species is typical of nearshore freshwater swampy environments. *Nothofagus solandri var. cliffortioides* (mountain beech) leaves were also found preserved with the raupo leaves. This species is usually found near the tree line and down stream from the tree line (M. Harper, 1991 pers. comm.). The very fine-grained sediment making up these sequences have been deposited by suspension in a low energy environment consistent with nearshore lacustrine processes.

6.6 Pumice deposits

Most of the pumice deposits in the field area can readily be classified as belonging to facies associations one or two. However, because of the unique source and mode of deposition of pumiceous sediment it has been treated as a separate subfacies in facies association two because pumice deposits are most commonly found in association with subfacies included in this group.

The thickest pumice units (10-30m) commonly have a pumice, clast (coarse pebble to cobble) supported base, fine upwards and are horizontally centimetre to decimetre bedded (cmbdd-dmbdd) (Fig. 6.17). I will refer to these deposits as "pulse-bedded" in this study due to the stacking up of the basic fining-up unit. These pulse-bedded pumice units are interpreted to have been deposited in a meandering fluvial environment and are typical of hyperconcentrated flow deposits. The fining up

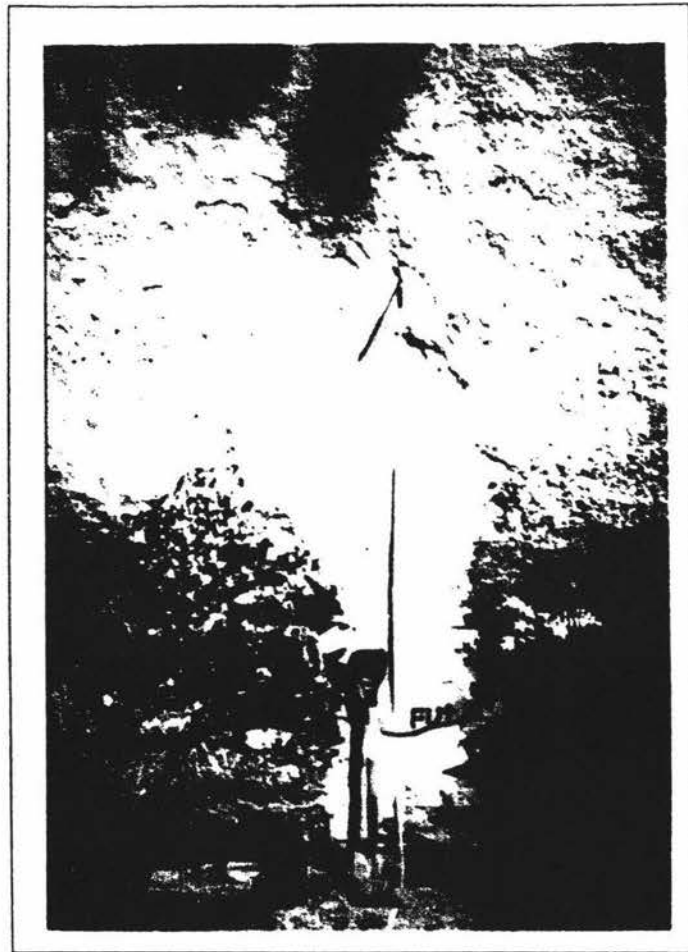


Fig. 6.17 Pumice bed with a clast supported base (arrow), fining upwards (FU) to a horizontally, cmbdd-dmbdd pumice sand, interpreted as a hyperconcentrated flood flow deposit. Spade for scale, 0.90m.

nature of the pulse bedded unit is interpreted to be due to waning hyperconcentrated flow. Hyperconcentrated flow deposits are distinct from normal stream flow deposits because of their lack of cross-stratification or recognisable bar morphologies (Smith, 1987). The thickest of these fluviually reworked pumices are likely to have been deposited in incised channels, thus giving the lateral control necessary to build the thick sequences observed. Planar bedded finer grained pumice units associated with these channelized hyperconcentrated flow deposits are interpreted as overbank deposits.

Water escape structures (Fig. 6.18) and convolute bedding (Fig. 6.19) are commonly observed in pumiceous overbank fines deposits and usually distort any bedding that may be present. The general term water escape structure includes various types of deformation structures (Lowe, 1975). Water escape structures are post-depositional features formed in loose, unconsolidated sediments as a result of pore-water escape leading to consolidation of sediment (Leeder, 1982). They are commonly associated with the pumice-rich beds and either deform the existing laminae or generate new sedimentary structures (Fig. 6.18). The process of their formation is due to fluidization, and it occurs where moving pore fluids exert an upward drag force on the sediment grains, lifting the grains and destroying the grain framework (Lowe, 1976).

Convolute laminated beds display a complex pattern of intraformational folds of variable morphology. Upper and lower surfaces of these beds are generally almost planar. Convolute laminated beds (Fig. 6.19) are generally associated with other features indicating a high sedimentation rate, *e.g.* ripple drift cross-lamination and form by plastic deformation of the bed as a result of loading (Sanders, 1965). As well as the classical forms of convolute laminae, forms with less regular geometric outline were recognised. Some instances of truncation of fold crests were found (Fig. 6.20). It has been shown by Anketell *et al.*, 1969 that these truncations could be produced during liquefaction without erosion, and that in unstable water saturated layers, the sediment extruded with the escaping pore waters settled back on the bed surface to form a thin veneer unconformably overlying the distorted bedding.



Fig. 6.18 Water escape structures in pumice rich beds causing deformation of existing laminae. Spade handle for scale, 0.70m.

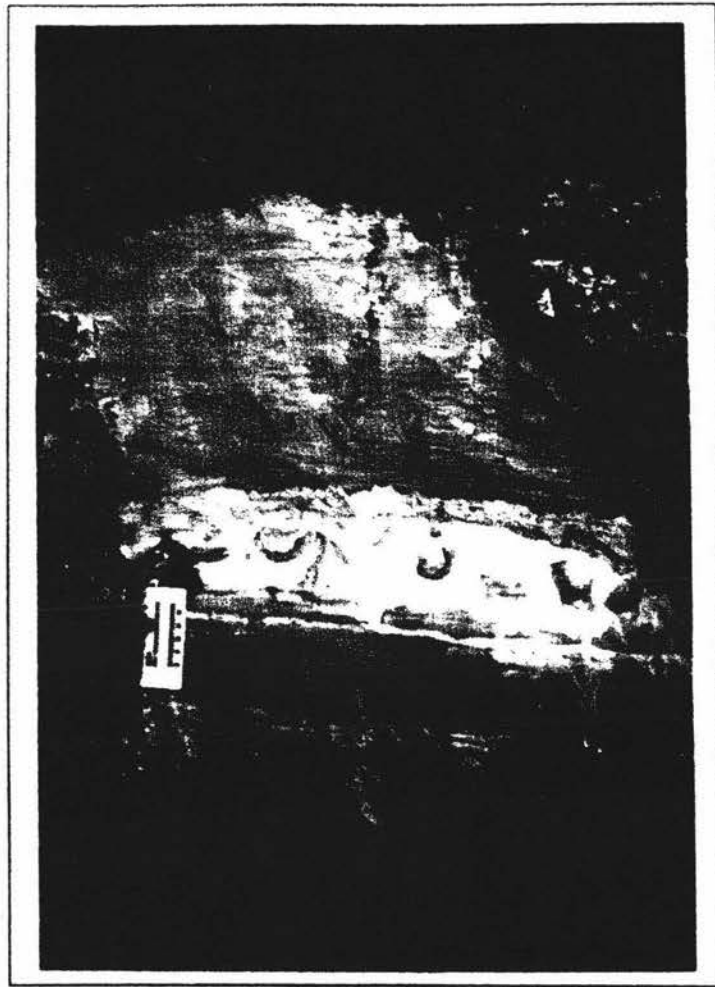


Fig. 6.19 Convolute laminated, fine-grained, pumice rich sand interpreted overbank fines deposits, showing almost planar upper and lower surfaces. Scale 0.10m.

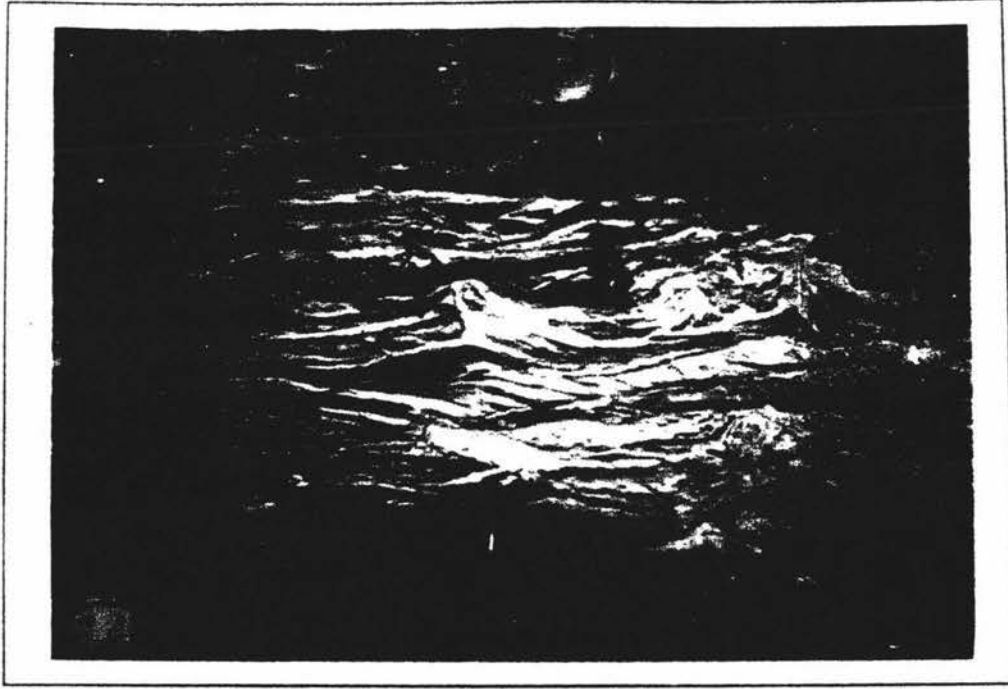


Fig. 6.20 Convolute laminated medium- to coarse-grained pumice rich sand showing a less regular geometric outline (*c.f.* Fig. 6.19) and truncation of fold crests (arrow). Spade for scale, 0.90m.



Fig. 6.21 Coarse- to medium-grained pumice sand to pebbly sand exhibiting overturned cross-stratification (arrow) and cross-bedding. Notebook for scale, 0.17m.

Where sediment close to the sediment-water interface becomes liquified, flowing water may exert a shear stress upon sub-aqueous dune bedforms. Such an effect will lead to progressively less shear being transmitted to the deeper parts of the dune. Since the bed solidifies from the base upwards there will be progressively less time for shear to operate in the lower part of the bed. This can result in a dipping foreset within the dune becoming sheared into a parabolic curve, defining the structure known as overturned cross-stratification (Fig. 6.21) (Allen and Banks, 1972).

Some thick pumiceous sequences (up to 20m) in the study area are generally not as pumice rich or as coarse grained as deposits one might expect from hyperconcentrated flow. Typically these deposits have a pumice clast base fining up into trough cross-bedded pumice sand (containing fossil logs up to 0.35m in diameter and up to 1m long, see Fig. 6.22) and ripple cross-bedded sand, with pumice silt, displaying sedimentary structures associated with rapid deposition *e.g.* water escape structures, capping the sequence. These deposits are indicative of normal streamflood processes. Most pumice beds thin markedly away from this paleofluvial environment, considered to be the major route for pumice entering the field area.

In gravel and rubble (facies association one, Af) to the west of the basin, pumice units form fine grained sand to silt, fining upwards sequences typical of airfall deposits (Fig. 6.23) and do not display the "pulse-bedding" associated with hyperconcentrated flows or the sedimentary structures normally associated with streamflood.

Field work shows little evidence of thick, pure pumice beds associated with estuarine/tidal deposits suggesting that any pumice deposited into this environment became reworked by tidal processes and is therefore preserved in a far less concentrated form than in the fluvial environment.

Many of the pumice units in the field area are in contact with either paleosols or lignites (Fig. 6.24). This common association indicates tuff emplacement events often precede or follow significant hiatuses, which are marked by the establishment



Fig. 6.22 Carbonaceous silt overlain by clast supported pumice, fining-upwards to trough cross-bedded, pumice sand deposited by streamflood processes. Note fossil tree trunk (black arrow) and erosive, silt-pumice contact (white arrows). Spade for scale, 0.90m.

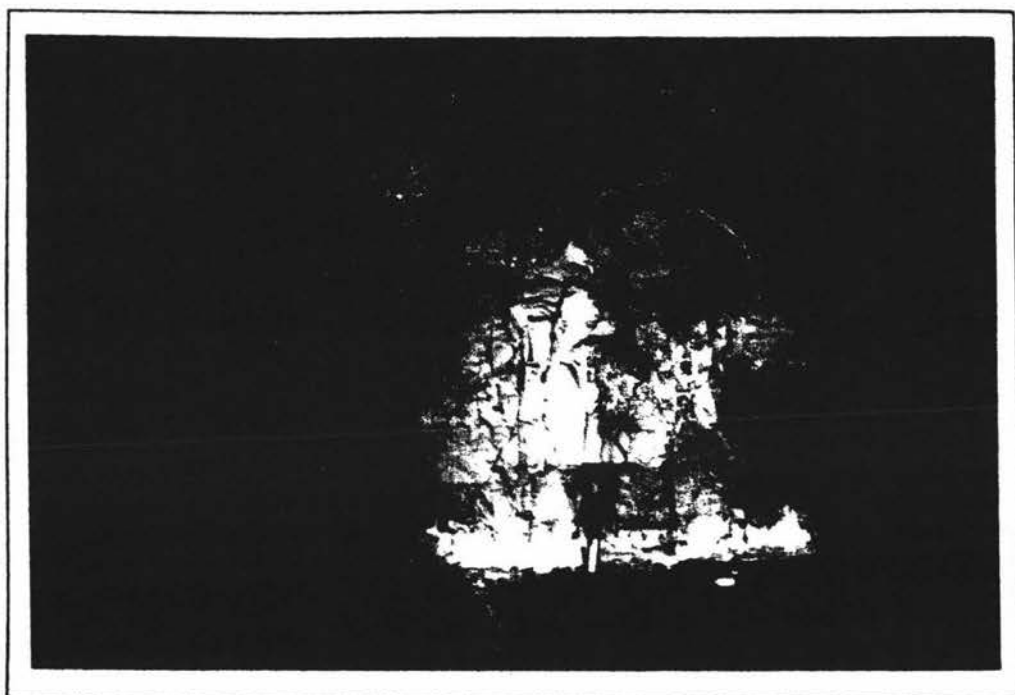


Fig. 6.23 Fine-grained, fining-upward pumice sand typical of airfall deposits in facies association one. Spade for scale, 0.70m.



Fig. 6.24 Lignite overlain by fine-grained pumice silt deposited in a backswamp environment. Lignite-silt contact is non-erosive. Spade for scale, 0.90m.

of vegetation. The close relationship of paleosols and lignites to pumice units points to the strong influence that volcanoclastic sedimentation has had on the fluvial system of the Dannevirke Basin and suggests that rapid aggradation or accretion occurred in a response to input of volcanoclastic sediment.

Vessel and Davies (1981) have shown by using evidence from eruptions at Volcan Fuego (Guatemala) that once a critical volume of volcanogenic material enters a fluvial system a geomorphic threshold is crossed and rivers are transformed from incised, meandering channels to rapidly aggrading, braided streams. Evidence gathered in the Dannevirke Basin suggests that this is also the case in the field area where following deposition of reworked volcanoclastics, broad sheets of sand and gravel-dominated sediment were deposited. Short term aggradation ended when eruption sequences ceased and vegetation stabilized reworked volcanoclastic debris. Streams then attempted to reestablish their former graded profiles, but judging by the extent of well preserved channelized pumice deposits it seems more likely that channel avulsion occurred, causing new channel formation and thus creating a new incised route for subsequent volcanoclastic debris entering the field area.

6.7 Conclusions

Mixed load fluvial facies of the Mangatarata Formation do not correspond to one distinct previously established model. Fluvial facies show evidence of both meandering and braided streams. Jackson (1978) has emphasised the diversity of lithofacies characteristics of modern meandering streams and has drawn attention to the overlap in recognition criteria for meandering and braided streams. Rust (1978) has questioned the distinction between braided and meandering streams. He points out that it is possible for a channel to be highly sinuous and to be divided by bars. Many channels are undivided and sinuous at high discharge, but divide around mid-channel bars at low stream stage (Jackson, 1978; Schwartz, 1978). Furthermore, many channels show marked variation in vertical sequence over short distances. The fluvial system of the Mangatarata Formation may have resembled the Little Wind River of Wyoming, a meandering stream with gravel in riffles and locally on the point bar, grading abruptly into levee-like silt and sand of the upper point bar

(Jackson, 1978). The amount of coarse gravel sediment in the paleofluvial environment of the Mangatarata Formation can be directly attributed to rate of uplift and perhaps climatic affect in and on the Ruahine Range, and therefore increased erosion. The episodic nature of the production of coarse material and therefore in some cases, aggradation has been a dominating factor in controlling the fluvial style of the sedimentary system in the Dannevirke Basin at any one time.

Deposition of massive amounts of reworked pumice has also affected the fluvial style of the sedimentary system. Pumice was introduced via a major northwest-southeast flowing paleofluvial system that transected the west-east fluvial network and caused large-scale aggradation in the Dannevirke Basin.

The boundary between facies associations two and three could best be described as a migrating line whose position is dictated by tidal influences on the lower reaches of a meandering stream. Facies association three ceases where processes and thus deposits associated with tidal currents no longer occur. It is only possible to place the facies association two/three boundary in the field by using structures such as flaser bedding, bidirectional indicators and fossil evidence.

The lacustrine sediments of the Mangatarata Formation were deposited in ephemeral shallow lakes in an interfluvial environment. As the lakes filled they were gradually converted into fluvial plains thus explaining the close relationship between facies associations two and four. The overall history of these lakes was one of marine regression, with nearshore and then fluvial deposits encroaching on and over offshore estuarine muds.

The study of facies associations and related sedimentary structures has shown that sedimentation rates in the field area were episodically high as shown by the abundance of ripple drift cross-lamination and water expulsion structures, especially in the more pumice-rich horizons. The association of flaser bedding, herringbone cross-bedding, bioturbation and the presence of *Austrovenus stutchburyi* indicates a tidal/estuarine environment dominated the eastern margin of the field area for much of the Castlecliffian. In the west of the field area sediments exhibit

characteristics that indicate a fluviially dominated environment. This is suggested by strong erosion surfaces underlying poorly sorted gravel and rubble. The finer sediment is dominantly large scale cross-bedded and has associated lignite beds, that may have formed in back-swamp environments.

CHAPTER SEVEN

HISTORY OF SEDIMENTATION

7.1 Introduction

The Mangatarata Formation preserves the record of changing sea-level in the Dannevirke Basin during Castlecliffian time. The episodic introduction of large volumes of pumiceous debris erupted from the Taupo Volcanic Zone (Kamp, 1981) and reworked from primary ignimbrites, has allowed the establishment of age control for the sea-level changes.

The axial ranges had attained significant relief by early Castlecliffian time. This is demonstrated by extensive gravel deposition, particularly in western Dannevirke Basin (see Chapter 6). The ranges therefore must have provided a barrier to ignimbrite erupted from the Taupo Volcanic Zone, from entering the Hawkes Bay region. Taupo Pumice crops out frequently west of the Mohaka Fault in central Hawkes Bay and at Kuripapango (Fig. 1.1) on the Napier-Taihape Road. It follows therefore, that this or other structural lows across the axial ranges have been major routes for primary ignimbrite transport into the Hawkes Bay region. The fact that the Taupo Pumice (c. 1850 yrs B.P.) crossed the axial ranges demonstrates the ability of a Holocene ignimbrite to reach Hawkes Bay. Thus it is not necessary to invoke uplift of the axial ranges until after deposition of the last Castlecliffian pumice tuff as invoked by Shane, (1989,1991). All the pumiceous sediment examined in the study area has been reworked from primary ignimbrite erupted from the Taupo Volcanic Zone. Primary Castlecliffian ignimbrite occurs at Gwavas (Fig. 1.1) and at Cape Kidnappers on the eastern side of the axial ranges, however, there is no evidence of primary Castlecliffian ignimbrite in the Rangitikei Valley sequence on the western side of the Range. This suggests that ignimbrite crossed the Range into central Hawkes Bay somewhere north of the field area. It follows therefore that the reworked pumice seen in the field area was probably transported via a major northwest-southeast flowing paleofluvial system. For this paleofluvial system to reach the field area there must have been structural control preventing the river

emptying into the marine embayment, that extended from the Hawke Bay bight southwest to the field and thus causing the river to flow south. This paleofluvial system is considered the most likely mechanism, except primary airfall, for transporting large volumes of pumice into an area so far from source. Paleocurrent indicators, although sparse in the pumiceous deposits (see Chapter 5), give a dominantly northwest-southeast flow direction, providing support to the premise the pumice has been reworked from the northwest. This northwestern source is probably the headwaters of the northwest-southeast flowing paleofluvial system, into which primary ignimbrite was deposited and from which pumiceous sediment has subsequently been reworked.

Six major pumice units have been identified in the field area (Melhuish, 1990). They are,

- 1) tuff chemistry A (*c.*0.67 Ma)
- 2) tuff chemistry B = Potaka Pumice (*c.*0.80 Ma)
- 3) tuff chemistry C (*c.*0.90 Ma)
- 4) tuff chemistry E = Rewa Pumice (*c.*1.0 Ma)
- 5) tuff chemistry F (*c.*1.17 Ma)
- 6) tuff chemistry G = Pakihikura Pumice (*c.*1.2 Ma).

Each pumice unit, except the Pakihikura Pumice, crops out several times in each stream due to the repetitive nature of the structure within the field area. It is possible to use the pumice units as time planes to express the physical and temporal extent of a specified sedimentary package. This allows determination of a paleogeography for a specific time interval and also illustrates changes to paleogeography with time.

Five age groups of sediments were delineated in the field area using the four most commonly outcropping pumice units. They are,

- 1) older than tuff chemistry F ($>c.1.17$ Ma) (Fig. 7.1 A)
- 2) Rewa Pumice ($c.1.0$ Ma) - tuff chemistry F ($c.1.17$ Ma)
- 3) tuff chemistry C ($c.0.90$ Ma) - Rewa Pumice ($c.1.0$ Ma) (Fig. 7.1 B)
- 4) Potaka Pumice ($c.0.80$ Ma) - tuff chemistry C ($c.0.90$ Ma) (Fig. 7.1 C)
- 5) younger than the Potaka Pumice ($<c.0.80$ Ma) (Fig. 7.1 D).

By tracing the boundary between fluvial and estuarine/tidal conditions through time, using the five sediment groups above, it is possible to delineate an approximate paleoshoreline position and illustrate migration of that shoreline with time. The overall regressive trend for the Castlecliffian is best developed in the south of the field area. The eastward progradation of fluvio-lacustrine deposits and paleoshoreline from early to late Castlecliffian time are illustrated in Figs. 7.1A,B,C and D.

The boundary between fluvial and estuarine/tidal conditions shows that estuarine/tidal sediments were deposited farther west in the south of the field area, than in the north during early Castlecliffian time *i.e.* >1.17 Ma (Fig. 7.1A). The restricted nature of estuarine/tidal deposits in the north is due to alluvial fan-related, fluvial aggradation. Alluvial fan deposits are shown to have become restricted between sediment age groups 3 (Fig. 7.1 B) and 4 (Fig. 7.1 C) (*i.e.* between deposition of the Rewa Pumice and the Potaka Pumice) in the north of the field area. This restriction appears to be the result of the growing Dannevirke Anticline situated just to the east of alluvial fan deposits. With the restriction of alluvial fan deposits, there was an associated transgression of the estuarine/tidal environment. This transgression was probably due to a rise in eustatic sea level accentuated by the restriction of alluvial fan related fluvial aggradation, imposed by the growing anticline. Eustatic rather than relative sea level rise is considered the cause for transgression due to basin uplift during the Castlecliffian *i.e.* transgression is not due to basin subsidence. By late Castlecliffian time *i.e.* <0.80 Ma (Fig. 7.1D) continued shoreline regression had lead to almost complete withdrawal of the sea from the field area.

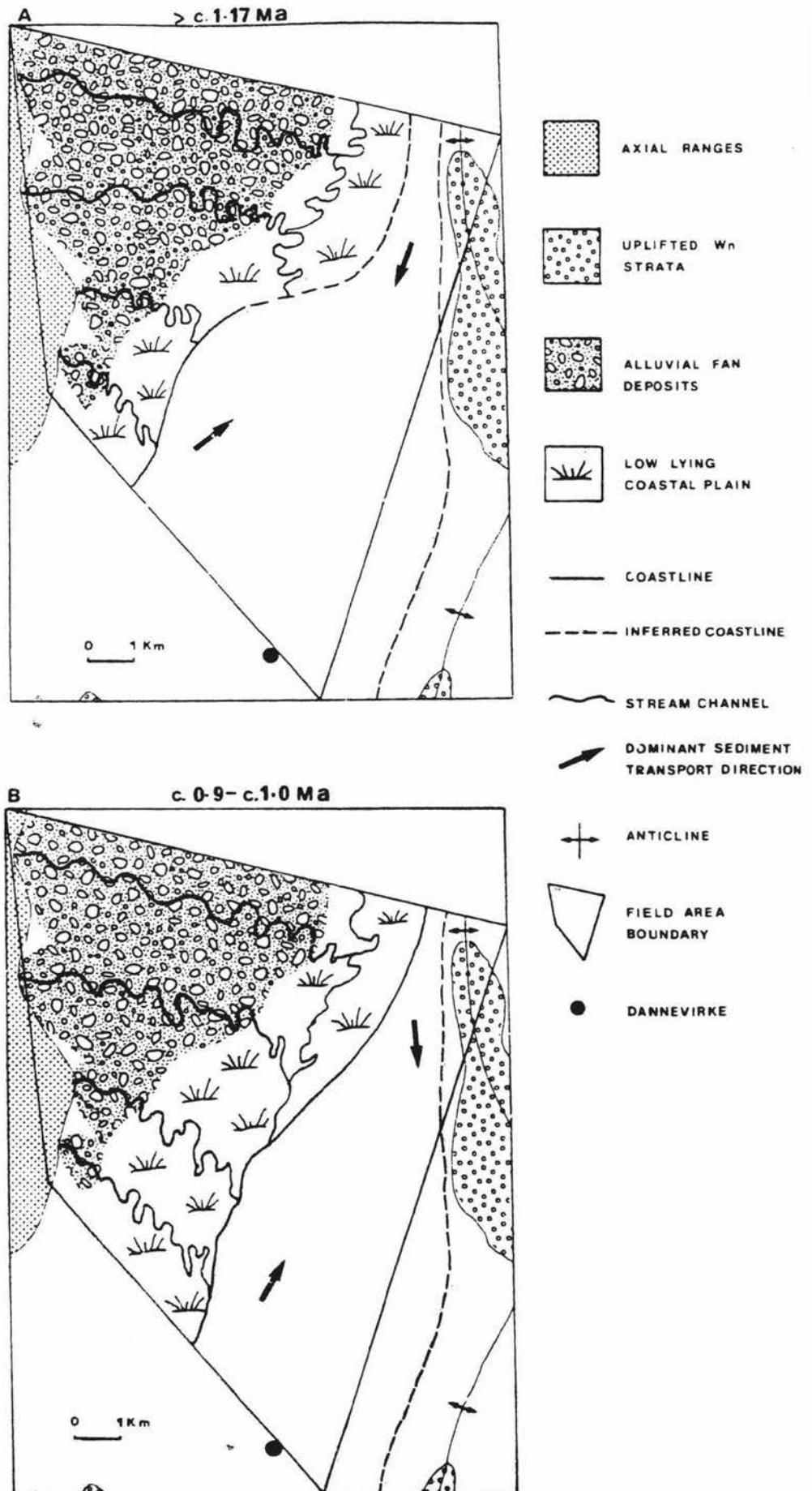
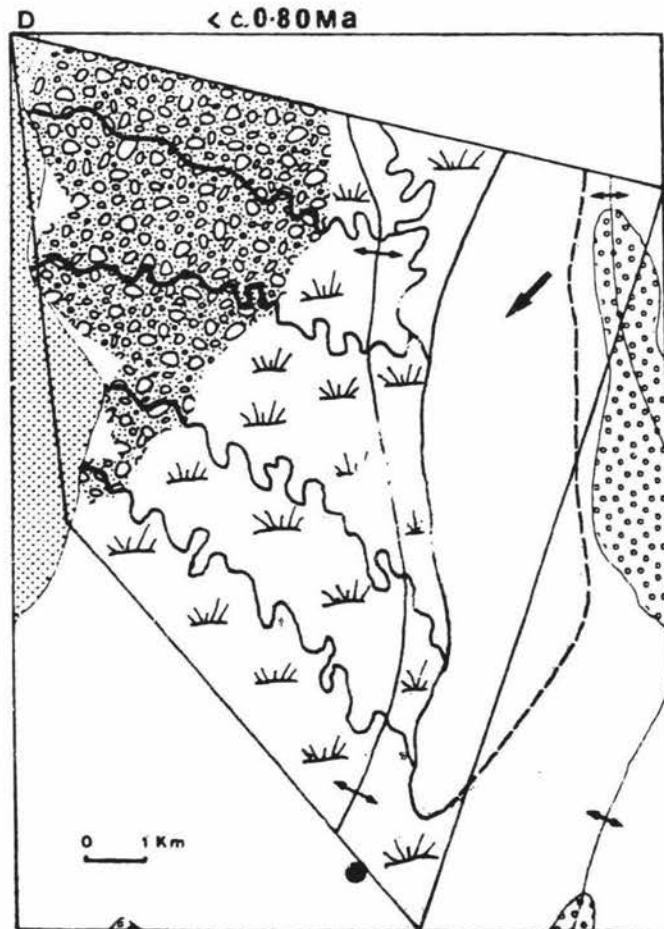
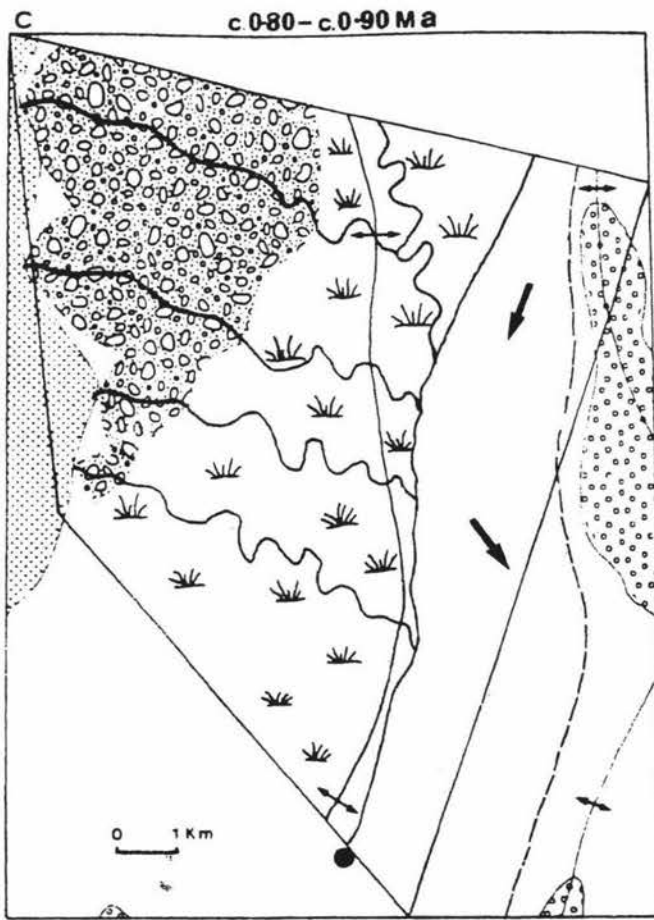


Fig. 7.1 Sequence of diagrams illustrating the inferred paleogeographical changes that accompanied deposition of the Mangatarata Formation.



7.2 Castlecliffian cyclothems

The good age control across the field area using correlation of identifiable pumice tuffs aids in the construction of a stratigraphic framework for the Dannevirke Basin (Fig. 2.5).

This stratigraphic framework has aided in the identification of at least ten Castlecliffian cyclothems consisting of alternating estuarine/tidal to terrestrial deposits in the Dannevirke Basin (Fig. 7.2). Thick and extensive, marine Pleistocene strata now exposed on land in southwestern North Island (Wanganui Basin) display obvious, well documented sedimentary cycles (cyclothems) *e.g.* Carter *et al.* (1991); Beu and Edwards (1984). Though superficially similar to their Wanganui Basin counterparts, the Dannevirke Basin cyclothems differ in several ways. They are significantly thicker overall and are dominated by terrestrially deposited sediments. Whereas the gravel-sand components of the Wanganui cyclothems predominantly belong to the transgressive part of the sequence and were deposited under rising sea level, the coarser grained facies in the Dannevirke Basin represent mostly the regressive part of the sequence and were probably deposited under a static or falling sea level. Sequence boundaries are taken to be at the base of the transgressive part of the sequence. A disconformity is inferred at the base of each transgressive sequence due to the erosive nature of a marine transgression. Time is therefore missing as is the case in the Wanganui sequence where transgressive deposits rest unconformably on a marine planed surface. The Dannevirke Basin's cyclothems represent a nearer shore environment than those exposed at the Wanganui coast.

At least ten episodes of shoreline transgression are recognised in the overall regressive trend for the Castlecliffian in the Dannevirke Basin. The transgressive part of the sequence in the field area is represented by 2-10m thick, fossiliferous, bioturbated and flaser bedded estuarine/tidal deposits (facies association 3). The transgressive part of the sequence is conformably overlain by sediments deposited by the regressive part of the sequence. These sediments are composed of organic rich, fluvio-lacustrine sediments which often contain lignite beds up to 1m thick (facies associations, 1,2 and 4).

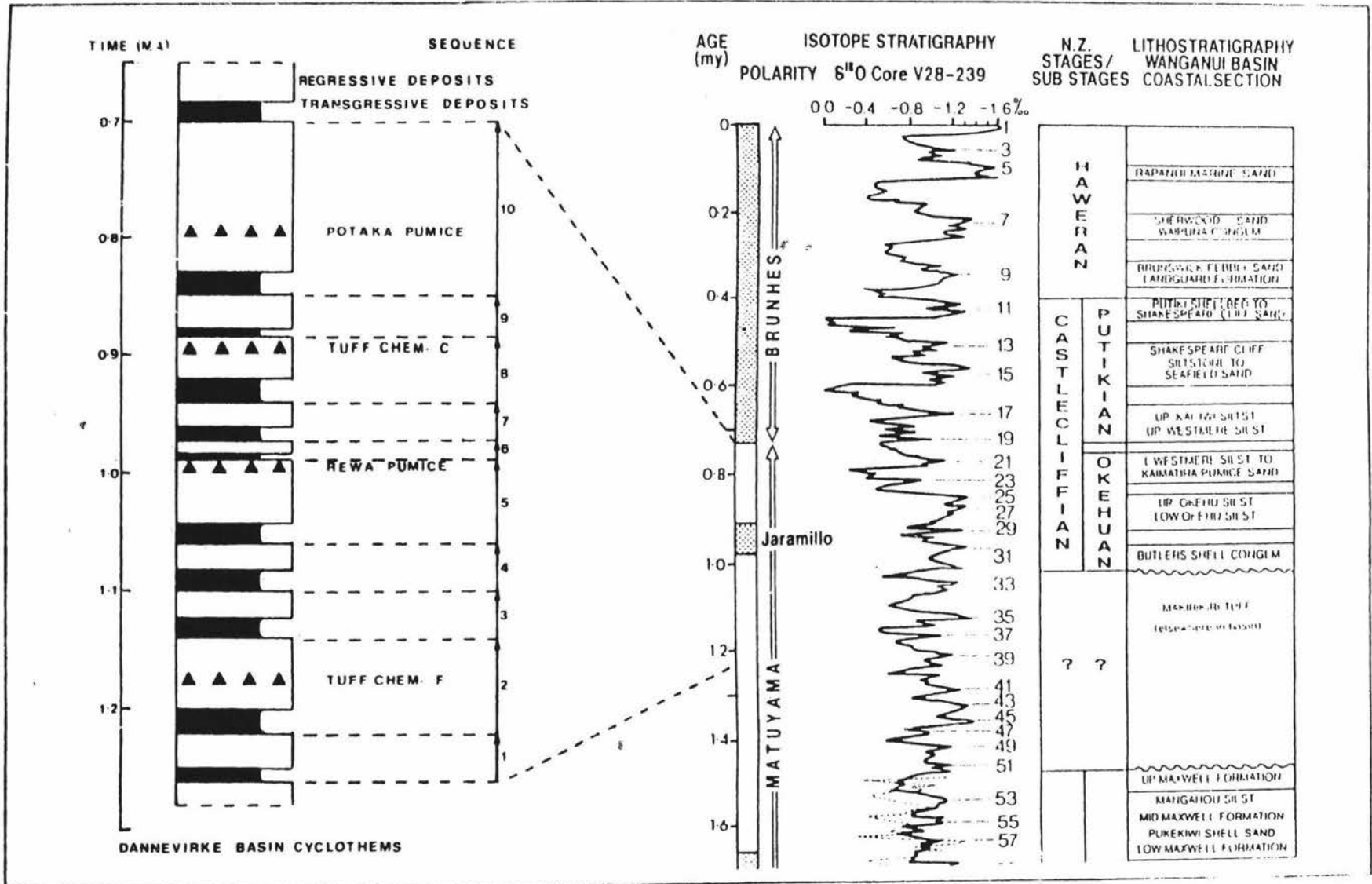


Fig. 7.2 Suggested correlations between Wanganui Basin and Dannevirke Basin cyclothems and Oxygen Isotope stratigraphy of two deep sea cores, modified after Pillans (1991).

Page 105
Missing from microfiche.

The estuarine/tidal deposits in the field area are here considered to represent the maximum rise in eustatic sea level. Even during the maximum eustatic sea level conditions of the Castlecliffian, the area was at most shallow marine but was dominantly estuarine/tidal. These alternating cycles of estuarine/tidal to terrestrial deposition are interpreted as cyclothem, deposited dominantly during the 100,000 and 40,000 year long, *c.* 80-130m magnitude, fifth and sixth-order orbitally forced glacio-eustatic sea-level cycles of the Castlecliffian (Abbott and Carter, 1991). Correlation with the oxygen isotope record for the Castlecliffian has been attempted using control provided by identified pumice units (Fig. 7.2). Cyclothem 1 to 10 (Fig. 7.3) are tentatively correlated to oxygen isotope stages 21 to 39 on the basis of the age control provided by four of the pumice units identified in the field area.

7.3 Timing of folding

The Wairarapa Basin, which lies to the south of the Dannevirke Basin in a similar geological location at the eastern margin of the axial ranges, started to subside in the late Miocene (Wells, 1989; Cape *et al.*, 1989) *i.e.* at about the same time as the Dannevirke Basin. A large increase in the rate of deformation at around 1 Ma has been described from various areas of the Wairarapa (Ghani, 1978; Lamb and Vella, 1987; Cape *et al.*, 1989; Wells, 1989). Considering the close proximity and the similar tectonic setting of the Dannevirke and Wairarapa Basins it seems unlikely that the onset of deformation in the Dannevirke Basin would have begun *c.*0.5 Ma later than in the Wairarapa Basin, as is indicated by Melhuish (1990).

Evidence has been presented of folding in the study area being syndepositional. This is evident by the restricted nature of alluvial fan deposits, which appear to be the result of the Dannevirke Anticline growing adjacent to an alluvial fan. Furthermore fossil assemblages within Castlecliffian strata are dominantly reworked from Nukumaruan strata (A.G. Beu pers. comm., 1991) uplifted along the Ormondville Anticline to the east of the field area (Fig. 7.1). These strata must have been uplifted during, if not before, Castlecliffian times. Nukumaruan strata are considered to have formed the eastern boundary for estuarine/tidal conditions in Castlecliffian time.

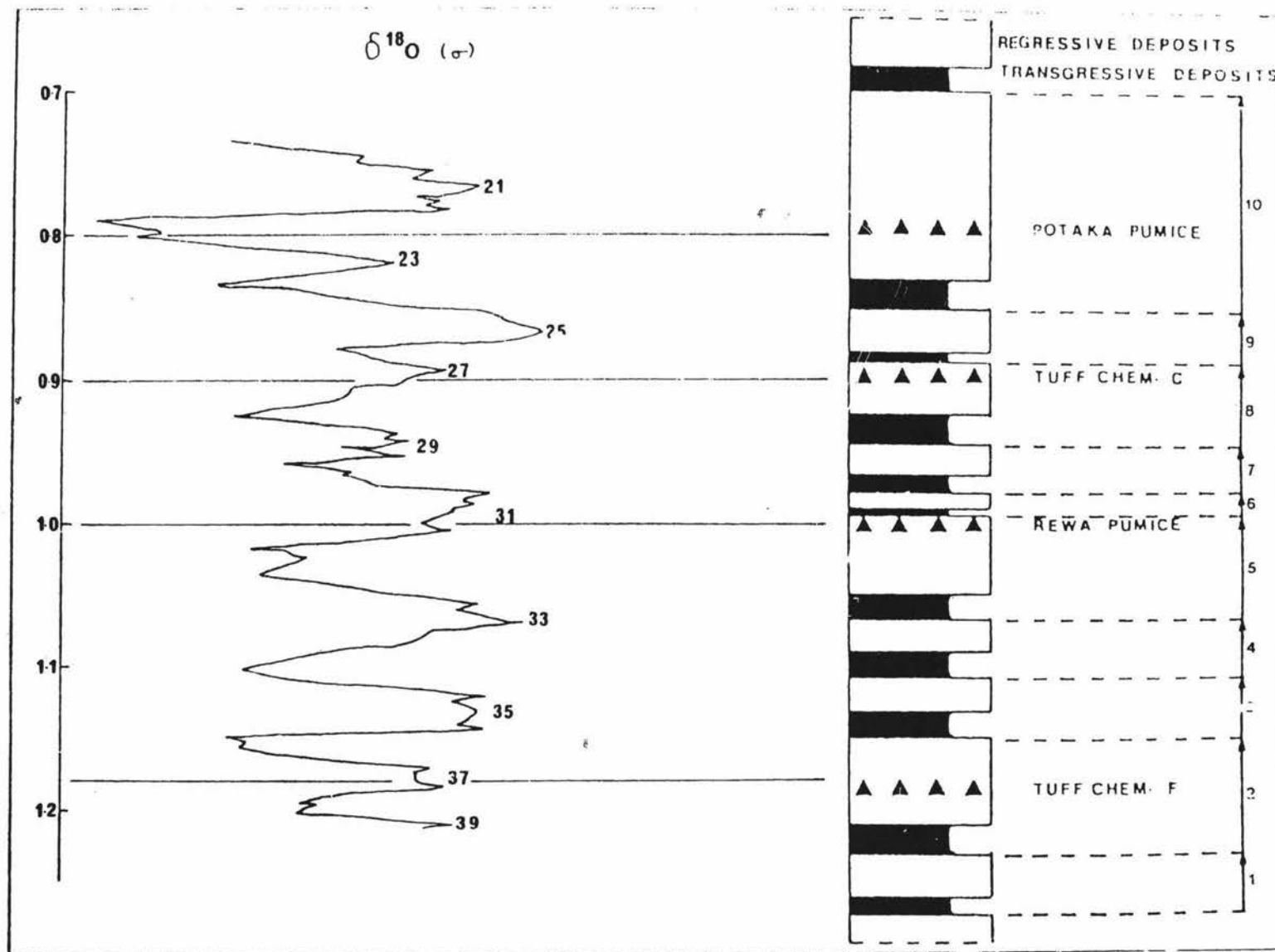


Fig. 7.3 Suggested correlation between Dannevirke Basin cyclothems and Oxygen Isotope stratigraphy of a deep sea core, modified after Carter *et al.* 1991.

Arguments for post-depositional deformation presented by Melhuish (1990) are not supported by field evidence gathered in this study. Melhuish claims that strata in the steep limbs of folds are sub-parallel. However, nowhere in the field area are there any sufficiently large exposures where good dip angle readings can be taken in the steep limbs of folds to prove whether strata are sub-parallel or whether they show a decreasing dip, as would be expected if deformation was syndepositional.

Melhuish also explains how strata would be expected to thicken in synclines and thin over anticlines if structure was syndepositional. Field evidence collected during this study and presented in Figs. 2.1, 2.2, 2.3 and 2.4 shows that only in pumice tuffs deposited after the Rewa Pumice (*c.*1.0 Ma) is there notable thinning toward anticlinal crests. This indicates folding has been occurring in post-Rewa Pumice time *i.e.* < *c.*1.0 million years ago. This is in agreement with the Castlecliffian alluvial fan deposits being restricted to the west of the study area due to the growing Dannevirke Anticline *i.e.* between deposition of the Rewa Pumice (*c.*1.0 Ma) and the Potaka Pumice (*c.*0.80 Ma). This is in direct contrast to Melhuish (1990) who considered structure to be post-depositional.

Field evidence, and that inferred from the related Wairarapa Basin, as well as a lack of evidence to support post-depositional deformation, suggests syndepositional deformation of Castlecliffian strata. This deformation probably began between deposition of the Rewa Pumice (*c.*1.0 Ma) and tuff 'chemistry C' (*c.*0.90 Ma).

7.4 Concluding remarks

The middle Pleistocene Mangatarata Formation of the Dannevirke Basin comprises a relatively well exposed sequence recording at least ten episodes of shoreline transgression, due to eustatic sea level rise, that are part of an overall regressive trend for the Castlecliffian.

Evolution of the middle Pleistocene Dannevirke Basin has been controlled by five major factors:

- i) the introduction of large amounts of greywacke gravel and finer sediment due to erosion and uplift of the Ruahine Ranges.
- ii) cyclothem sedimentation related to fifth and sixth order orbitally forced glacio-eustatic sea-level cycles.
- iii) overall basin uplift during the Castlecliffian.
- iv) syndepositional deformation and
- v) the introduction of massive amounts of reworked pumiceous ignimbrite from the Taupo Volcanic Zone.

REFERENCES

- Abbott, S.T. and Carter, R.M., 1991, *in press*, The sequence architecture of mid-Pleistocene (c. 1.1-0.4 Ma) cyclothems from New Zealand: Facies development during a period of orbital control on sea-level cyclicity, *in de Boer, P.L. and Smith, D.G. (eds.), "Orbital Forcing and Cyclic Sequences"*, IAS Special Publication 1.
- Allen, J.R.L., 1967, Notes on some fundamentals of paleocurrent analysis, with reference to preservation potential and sources of variance, *Sedimentology*, v.9, p. 75-88.
- Allen, J.R.L., 1982, *Sedimentary Structures, their character and physical basis*, vol.1, Elsevier scientific publishing company, 593p.
- Allen, J.R.L., and Banks, N.L., 1972, An interpretation and analysis of recumbent-folded deformed cross-bedding, *Sedimentology*, v.19, p. 257-83.
- Anketell, J.M., Cegla, J., and D^ualunski, S., 1969, Uncomformable surfaces formed in the absence of curent erosion, *Geol. Rom.*, v. 8, p. 41-46.
- Blissenbach, Erich, 1954, Geology of alluvial fans in semi-arid regions, *Geological Society of America Bulletin*, v. 65, p. 175-189.
- Bull, W.B., 1972, Recognition of alluvial fan deposits in the stratigraphic record *in* Recognition of ancient sedimentary environments, Editor, Rigby, J.B., and Hamblin, K.K., Special Publications of the Society of Economic Paleontologists and Mineralogists, Tulsa, v. 16, p. 63-83.
- Cape, C.D., Lamb, S.H., Vella, P., and Woodward, D., 1989, Geological structure of Wairarapa Valley, New Zealand, from seismic reflection profiles, *Journal of the Royal Society of New Zealand*, v. 20,(1) p. 85-105.

Carter, R.M., Abbott, S.T., Faltherpe, C.S., Haywick, D.W., and Henderson, R.A., 1991, Application of global sea-level and sequence-stratigraphic models in Southern Hemisphere Neogene strata from New Zealand, Special Publication International Association of Sedimentologists, v. 12, p. 41-65.

Collinson, J.D. and Thompson, D.B., 1989, Sedimentary Structures, 2nd Edition, Unwin Hyman Inc., 207p.

Cowie, J.D., 1964a, Aokautere Ash in the Manawatu district, New Zealand, New Zealand Journal of Geology and Geophysics, v. 7,(1) p. 67-77.

Cowie, J.D., 1964b, Loess in the Manawatu district, New Zealand, New Zealand Journal of Geology and Geophysics, v. 7,(2) p. 389-396.

Cowie, J.D. and Wellman, H.W., 1961, Age of Ohakea terrace, Rangitikei River, New Zealand Journal of Geology and Geophysics, v. 5,(4) p. 617-619.

Curry, J.R., 1956, The analysis of two dimensional orientation data, Journal of Geology, v. 64, p. 117-131.

Edelman, C.H., and Doeglas, D.J., 1932, Reliktstrukturen Detritischer Pyroxene and Amphibole: Tschermaks mineralogische und petrographische Mitteilungen, v. 42, p. 482-490 in Seward, 1974, Some aspects of sedimentology of the Wanganui Basin, North Island, New Zealand.

Firth, G.W., and Feldmeyer, A.E., 1943, The geology of the Pahiatua-Dannevirke Basin, "east side" North Island, New Zealand, New Zealand Geological Survey unpublished open file, petroleum report 166.

Folk, R.L., 1968, Petrology of sedimentary rocks, Hemphill's Austin, Texas, p. 170.

Folk, R.L., and Ward, W.C., 1957, Brazos River bar: a study in the significance of grain size parameters, *Journal of Sedimentary Petrology*, v. 27, 3-26 p.

Friedman, G.M., 1961, Distinction between dune, beach and river sands from their textural characteristics, *Journal of Sedimentary Petrology*, v. 31, p. 514-529.

Friedman, G.M., 1962, On sorting, sorting coefficients, and the lognormality of the grain-size distribution of sandstones, *Journal of Geology*, v. 70, p. 737-753.

Friedman, G.M., 1967, Dynamic processes and statistical parameters compared for size frequency of beach and river sands, *Journal of Sedimentary Petrology*, v. 37(2), p. 327-354.

Friedman, G.M., 1979, Address of the retiring President of the International Association of Sedimentologists: Differences in size distributions of populations of particles among sands of various origins, *Sedimentology*, v. 26(1), p. 3-32.

Friedman, G.M., and Sanders, J.E., 1978, *Principles of Sedimentology*, John Wiley and Sons, 792p.

Jhani, M.A., 1978, Late Cenozoic vertical crustal movements in the southern North Island, New Zealand, *Journal of Geology and Geophysics*, v. 21(1) p. 117-125.

Griffiths, J.C., 1967, *Scientific method in analysis of sediments*, McGraw-Hill, 507p.

Harms, J.C., 1975, Stratification produced by migrating bedforms, *in* *Depositional environments as interpreted from primary sedimentary structures and stratification sequences*, Chapter 3, p. 45-61, Society of Economic Paleontologists and Mineralogists, Short course No. 2, Dallas 1975.

Harvey, A.M., 1978, Dissected alluvial fans in Southwest Spain, *Catena*, v. 5, p.177-211.

- Harvey, A.M., 1984, Debris flows and fluvial deposits in Spanish Quaternary alluvial fans; implications for fan morphology, p. 123-132 *in* Koster, E.H., Steel, R.J. (Eds), *Sedimentology of gravels and conglomerates*, Canadian Society of Petroleum Geologists, Memoir 10.
- Hein, F.J., and Walker, R.G., 1977, Bar evolution and development of stratification in the gravelly, braided Kicking Horse River, British Columbia: *Canadian Journal of Earth Science*, v. 14, p. 562-570.
- Hutton, C.O., 1959, Mineralogy of beach sands between Halfmoon and Monterey Bays, California, California Division of Mines, Special Report, v, 59, 32p.
- Inman, D.L., 1949, Sorting of sediments in the light of fluid mechanics, *Journal of Sedimentary Petrology*, v. 19, p. 51-70.
- Jackson, R.G., II, 1978, Preliminary evaluation of lithofacies models for meandering alluvial streams, *in* Miall, A.D. (ed), *Fluvial sedimentology*: Canadian Society of Petroleum Geologists, Memoir 5, p. 543-576.
- Kaddah, M.T., 1974, The hydrometer method for detailed particle-size analysis: 1. Graphical interpretation of hydrometer readings and test of method, *Soil Science*, v. 118, p. 102-108.
- Kamp, P.J.J., 1981, Pleistocene tephtras in Hawkes Bay and their potential for dating geologic events, *Proceedings of tephra workshop 1980*, Department of geology publication no. 20 Victoria University of Wellington, Wellington.
- Kamp, P.J.J., 1982, Landforms of Hawke's Bay and their origin: A plate tectonic interpretation, *in* *Landforms of New Zealand*, Chapter 12, Ed. Soons, J.M. and Selby, M.J., Longman Paul, 392p.

- Kamp, P.J.J., and Vucetich, C.G., 1982, Landforms of Wairarapa in a geological context, *in* Landforms of New Zealand, Chapter 13, Ed. Soons, J.M. and Selby, M.J., Longman Paul, 392p.
- Kossovskaya, A.G. and Drits, V.R., 1970, Micaceous minerals in sedimentary rocks, *Sedimentology*, v.15, p. 83-101.
- Kostaschuk, R.A., Macdonald, G.M., Putnam, P.E., 1986, Depositional processes and alluvial fan-drainage basin morphometric relationships near Banff, Alberta, Canada, *Earth Surface Processes and Landforms* 11, p. 471-484.
- Laing, A.C.M., 1961, The geology and petroleum prospects of the Dannevirke area: BP Shell and Todd Petroleum Development Ltd, (unpublished, confidential).
- Lamb, S.H. and Vella, P., 1987, The last million years of deformation in part of the New Zealand plate boundary zone, *Journal of structural geology*, v. 9(7), p. 877-891.
- Lane, E.W., 1938, Notes on the formation of sand, *American Geophysics Union Transactions*, v. 19, p.505-508.
- Leeder, M.R., 1982, *Sedimentology: Process and Product*, George, Allen and Unwin, 344p.
- Leslie, W.C. and Hollingsworth, R.J.S., 1972, Exploration in the East Coast Basin, New Zealand, *The Australian petroleum exploration association journal*, v. 12,(1), p. 36-44.
- Lewis, D.W., 1981, *Practical Sedimentology*, Apteryx, Christchurch.
- Lewis, D.W., 1984, *Practical Sedimentology*, Apteryx, Christchurch, 229p.

- Lillie, A.R., 1953, The geology of the Dannevirke Subdivision, New Zealand Geological Survey, bulletin 46.
- Lowe, D.R., 1975, Water escape structures in coarse-grained sediments, *Sedimentology*, v.22, p. 157-204.
- Lowe, D.R., 1976, Subaqueous liquified and fluidized sediment flows and their deposits, *Sedimentology*, v. 23, p. 285-308.
- Marks, G.P., 1975, Sedimentology of Omaro Barrier Spit, Whangaparoa Harbour, Coromandel Peninsula, Unpublished M.Sc. thesis, lodged in the library, University of Waikato.
- McArthur, D.S., 1970, Size Stats; Programme to compute Folk and Ward, Inman, and moment-measure statistics.
- McConchie, D.M., and Lewis, D.M., 1978, Authigenic, perigenic, and allōgenic glauconites from the Castle Hill Basin, North Canterbury, New Zealand, *New Zealand Journal of Geology and Geophysics*, v. 21, p. 199-214.
- McKay, A., 1877, Report on country between Masterton and Napier, New Zealand Geological Survey Report on Geological Exploration during 1876-1877, p. 67-94.
- McManus, J., 1988, Grain size determination and interpretation, *in* *Techniques in sedimentology* Ed. Tucker, M. Chapter 3, Blackwell Scientific Publications, 394p.
- Melhuish, A., 1990, Late Cenozoic deformation along the Pacific-Australian plate margin, Dannevirke region, New Zealand, Unpublished MSc thesis, lodged in the library, Victoria University of Wellington.
- Miall, A.D., 1977, A review of the braided-river depositional environment, *Earth Science Reviews*, v. 13, p. 1-62.

- Milne, J.D.G., and Smalley, I.J., 1979, Loess deposits in the southern part of the North Island of New Zealand: An outline of stratigraphy, *Acta Geologica Academiae Scientiarum Hungaricae*, v. 22, p. 197-204.
- Neef, Gerrit, 1984, Late Cenozoic and early Quaternary stratigraphy of the Eketahuna district (N153), New Zealand Geological Survey, bulletin 96.
- Odir, G.S., and Matter, A., 1981, De glauconiarum origine, *Sedimentology*, V. 28, p. 611-641.
- Ongley, M., 1935, Eketahuna subdivision, New Zealand Geological Survey, 29th annual report, p. 1-6.
- Ori, G.G., 1982, Braided to meandering channel patterns in humid-region alluvial fan deposits, River Peno, Po Plain, Northern Italy, *Sedimentary Geology*, v. 31, p. 231-248.
- Passega, Renato, 1957, Texture as characteristic of clastic deposition, *American Association of Petroleum Geologists, Bulletin* 41, p. 1952-1984.
- Pelletier, B.R., 1958, Pocono paleocurrents in Pennsylvania and Maryland, *Geological Society of America, Bulletin* 69, p. 1033-1064.
- Pettijohn, F.J., 1957, *Sedimentary rocks*, Harper's Geoscience Series, 718p.
- Pillans, B., 1991, New Zealand Quaternary Stratigraphy: An Overview, *Quaternary Science Reviews*, v. 10.
- Piyasin, Sanguat, 1966, The geology of the Woodville district, Unpublished MSc thesis, lodged in the library, Victoria University of Wellington.
- Plumley, W.J., 1948, Black Hills terrace gravels: a study in sediment transport, *Journal of Geology*, v. 56, p. 562-577.

Potter, P.E., 1959, Facies models conference, *Science*, v. 129, p. 1292-1294.

Potter, P.E., and Pettijohn, F.J., 1977, *Paleocurrents and basin analysis*, 2nd edition, Springer-Verlag, New York, 425p.

Quennel, A.M., 1937, Dannevirke Subdivision, New Zealand Geological Survey, 31st Annual Report, p. 2-3.

Quennel, A.M., 1938, Dannevirke subdivision, New Zealand Geological Survey, 32nd annual report, p. 2-3.

Reineck, H.E., and Singh, I.B., 1980, *Depositional sedimentary environments*, Springer-Verlag, 549p.

Reineck, H.E., and Wunderlich, F., 1968, Classification and origin of flaser and lenticular bedding, *Sedimentology*, v.11, p. 99-104.

Rhea, K.P., 1968, Aokautere ash, loess, and the river terraces in the Dannevirke district, New Zealand, *New Zealand journal of Geology and Geophysics*, v. 11, p. 685-692.

Rust, B.R., 1978, A classification of alluvial channel systems, *in* Miall, A.D. (ed), *Fluvial sedimentology*, Canadian Society of Petroleum Geologists, Memoir 5, p. 187-198.

Sanders, J.E., 1965, Primary sedimentary structures formed by turbidity currents and related resedimentation mechanisms, *in* Middleton, G.V. ed., *Primary sedimentary structures and their hydrodynamic interpretation*, Society of Economic Paleontologists and Mineralogists Special Publication, Number 12, p. 192-219.

Schwartz, D.W., 1978, Hydrology and current orientation analysis of a braided-to-meandering transition: the Red River in Oklahoma and Texas, United States of America, *in* Miall, A.D. (ed.), *Fluvial Sedimentology*: Canadian Society of Petroleum Geologists, Memoir 5, p. 231-255.

Selley, R.C., 1976, *Introduction to sedimentology*, Academic Press, London, 408p.

Seward, D., 1974, Some aspects of sedimentology of the Wanganui Basin, North Island, New Zealand. Unpublished Ph.D. thesis, lodged in the library, Victoria University of Wellington.

Shane, P.A.R., 1989, The characterisation and correlation of late Cenozoic tuffs in south eastern, North Island, New Zealand. Unpublished MSc thesis, lodged in the library, Victoria University of Wellington.

Shane, P.A.R., 1991, Glass chemistry paleomagnetism, and correlation of middle Pleistocene tuffs in southern North Island, New Zealand and Western Pacific, *New Zealand Journal of Geology and Geophysics*, 1991, v. 34, p. 203-211.

Sorby, H.C., 1859, On the structures produced by the currents present during the deposition of stratified rocks, *Geologist*, v. 2, p. 137-147.

Te Punga, M., 1953, *The Geology of the Rangitikei Valley*, New Zealand Geological Survey, Memoir Number 8, 46p.

Thomson, J.A., 1914, Mineral prospects of the Maharahara District, Hawkes Bay, *New Zealand Geological Survey, 8th Annual Report*, p. 162-170.

Turner, R.E., 1944, *Geology of northern Wellington and southern Hawkes Bay provinces*, Petroleum report series no. 1225, Superior Oil Company of New Zealand.

United States Waterways Experimentation Station, 1939, Study of materials in suspension, Mississippi River, Technical Memorandum, 122-1, Vicksburg, La, 27p

Vessell, R.K., and Davies, D.K., 1981, Non-marine sedimentation in an active forearc basin, Society of Economic Paleontologists and Mineralogists, Special Publication Number 31, p. 31-45.

Visher, G.S., 1967a, Grain size distributions and depositional processes, Pre-print VII International Sedimentologic Congress, Reading and ^dErinburg, England, 4p.

Visher, G.S., 1967b, The relation of grain size to sedimentary processes (Abst.) American Association of Petroleum Geologists Bulletin, v.51, p. 484.

Visher, G.S., 1969, Grain size distributions and depositional processes, Journal of Sedimentary Petrology, v. 39(3), p. 1074-1106.

Walker, R.G., 1976, Facies Models, Sandy fluvial systems, Geoscience Canada, v. 3, p. 101-109.

Walker, R.G., and Cant, D.J., 1984, Sandy fluvial deposits *in* Walker, R.G., Facies models.

Wells, P.E., 1989, Late Neogene vertical tectonic movements in western Wairarapa, New Zealand, unpublished PhD thesis, lodged in the library, Victoria University of Wellington.

APPENDIX A

PALEOCURRENT DATA

Location	Structure type	Current direction
Mangatewainui stream		
U23/225793	FP-lx	106
U23/203798	G-lx	086
U23/183819	FP-lx	098
U23/179825	FP-lx	115
U23/175828	F-lx	203
U23/173832	FP-sx	198
U23/171834	F-sx	088
U23/160834	F-sx	117
U23/160834	FP-lx	130
U23/160834	F-lx	123
U23/168835	FP-lx	120
U23/168836	E/T-lx	261
U23/168836	E/T-sx	285
U23/166839	E/T-lx	286
U23/157833	E/T-lx	047
Mangatewaiiti stream		
U23/199785	FP-sx	170
U23/199785	FP-sx	130
U23/199790	G-lx	115
U23/180797	F-sx	249
U23/187796	F-sx	205
U23/186801	E/T-lx	249
U23/179800	F-lx	251

U23/178801	F-lx	231
U23/178801	F-lx	225
U23/178802	F-lx	061
U23/176804	F-lx	31
U23/176804	F-lx	229
U23/172809	FP-lx	112
U23/171811	E/T-lx	245
U23/168814	E/T-sx	252
U23/168815	E/T-sx	243
U23/168815	E/T-sx	245
U23/168815	E/T-sx	252
U23/166815	E/T-sx	227
U23/166816	E/T-lx	217
U23/166816	E/T-sx	229
U23/166816	E/T-lx	232
U23/167817	F-sx	137
U23/167817	F-lx	139
U23/162816	E/T-lx	251
U23/161816	E/T-lx	174
U23/161816	E/T-lx	040
U23/159820	E/T-hbx	270
		093
U23/159820	E/T-lx	345
U23/159820	E/T-lx	221
U23/156822	F-sx	077
U23/156822	F-lx	210
U23/155822	F-lx	165
U23/155822	F-lx	245
U23/155822	F-lx	228
U23/155823	F-lx	160
U23/155824	E/T-sx	153
U23/153823	E/T-lx	249
U23/152824	E/T-sx	214

U23/151823	E/T-lx	009
U23/151824	E/T-lx	197
U23/151825	E/T-hbx	139
		310
U23/149827	E/T-sx	061

Whakaruatapu stream

U23/146785	E/T-hbx	231
		015
U23/145785	E/T-lx	028
U23/143785	E/T-lx	165
U23/142785	E/T-lx	051
U23/138787	E/T-lx	223
U23/134788	E/T-lx	104
U23/132788	PE/T-lx	222
U23/132788	GE/T-lx	059
U23/131788	E/T-lx	117
U23/129785	E/T-lx	157
U23/128784	E/T-lx	135
U23/126785	E/T-lx	058

Mangatera stream

U23/146754	F-lx	148
U23/140752	E/T-sx	242
U23/115753	F-lx	229
U23/114752	F-lx	287
U23/114753	F-lx	287
U23/112754	F-sx	158
U23/111753	F-sx	160
U23/090753	E/T-lx	113

KEY

l - large-scale
s - small-scale
x - cross-bed
hbx - herringbone cross-bed

E/T - estuarine/tidal
F - fluvial
P - pumice
G - gravel

Locations - Grid Refs. from NZMS 260 series

APPENDIX D

Diatoms identified by Dr Harper, Victoria University, Wellington.

SPECIES NAME	SAMPLES			pH	SALT	HABITAT	CURRENT
	A	B	D				
<i>Achnanthes clevei</i>		B		+	i	e	l
<i>A. lanceolata</i>	A			+	i	b	r
<i>Amphora aequalis</i>		B		i	i	e	i
<i>A. ovalis</i> var. <i>libyca</i>			D	+	i	b	i
<i>A. ovalis</i> var. <i>pediculus</i>		B		+	i	b	i
<i>Aulacoseira crenulata</i> as <i>Melosira italica</i>			D	+	i	p?	i
<i>A. granulata</i>	A			+	i	p?	
<i>Cocconeis disculus</i>	A			+	i	b	i
<i>C. placentula</i> var. <i>lineata</i>	A	B	D	+	i	e	i
<i>Cymatopleura solea</i>		B		+			
<i>Cymbella</i> aff. <i>aequalis</i> ?	A						
<i>C. aspera</i>			D	+	i	a	i
<i>C. cistula</i>	A	B	D	i	i	b	l
<i>C. sumatrensis</i>	A			+	i	b	
<i>Cyclotella meneghiniana</i>	A			+	+	p	i

SPECIES NAME	SAMPLES			pH	SALT	HABITAT	CURRENT
	A	B	D				
<i>Cyclotella</i> spp.			D				
<i>Epithemia sorex</i>		B		++	i	b	i
<i>E. zebra</i> var. <i>porcellus</i>	A			++	i	b	i
<i>Eunotia bilunaris</i>			D	i	i	b	
<i>E. formica</i>	A	B				b	
<i>E. implicata</i>			D			b	
<i>E. serpentina</i>		B	D	i	i	b	
<i>Fragilaria brevistriata</i>	A			+	i	e	i
<i>F. brevistriata</i> var. <i>elliptica</i>	A	B		+	i	e	i
<i>F. capucina</i>			D	+	i	p?	l
<i>F. construens</i>	A		D	+	i	b	i
<i>F. construens</i> var. <i>venter</i>			D	+	i	b	i
<i>F. exiqua</i>			D	i	-	b	i
<i>F. pinnata</i>	A	B		+	i	b	i
<i>F. ulna</i> var. <i>acus</i>	A	B		+	i	b?	
<i>F. zelleri</i> var. <i>elliptica</i>			D				
<i>Gomphonema augustum</i> var. <i>producta</i>			D	+	i	e	i
<i>G. gracile</i>			D	+	i	b	l

SPECIES NAME	SAMPLES			pH	SALT	HABITAT	CURRENT
	A	B	D				
<i>G. parvulum</i>	A	B		+	i	b	r
<i>Gyrosigma acuminatum</i>		B	D	++	i	b	r
<i>Hyalodiscus lentigenosus</i>			D	i	+	p	r
<i>Melosira sp.</i>		B					
<i>Navicula atomus</i>	A			+	i	a	i
<i>N. minima</i>	A			+	i	b	
<i>N. placentula</i>		B		+	i	b	
<i>N. radiosa var. parva</i>	A			-	i	b	
<i>N. radiosa var. tenella</i>	A			i	i	b	i
<i>Nitzschia amphibia</i>	A			+	i	e	i
<i>N. debilis</i>			D	i	i	a	
<i>N. frustulum</i>	A			+	+	b	l
<i>N. vitrea</i>			D	+	+	a	
<i>Nitzschia spp.</i>	A	B	D			b/p	
<i>Pinnularia obscura</i>			D	i	i	b	
<i>P. viridis</i>	A						
<i>Rhopalodia gibberula var. van Heuckii</i>		B	D	+	i	b	
<i>R. novae-zealandiae</i>		B		+	i	b	
<i>Selophora pupula</i>	A			i	i	b	
<i>Stephanodiscus astraea var. minutata</i>		B		++	i	p/e	

SPECIES NAME	SAMPLES			pH	SALT	HABITAT	CURRENT
	A	B	D				
<i>Surirella bohémica</i>			D				
<i>S. gracilis</i>		B					
<i>S. tenera</i>	A	B		+	i	b	
<i>Surirella spp.</i>			D			b/p	
<i>Tabellaria fenestrata</i>		B	D	-	i	p	i

KEY

Samples A = Mangatewainui Stream sample, site A99, G.D. U23 82831754.
 B = Mangatewaiiti Stream sample, site B67, G.D. U23 82301525.
 D = Mangatera Stream sample, site D37, G.D. U23 75201142.

pH ++ = alkalibiontic, requires pH >7.5.
 + = alkaliphil, prefers pH >7.5.
 i = indifferent, prefers circumneutral pH 6.5-7.5.
 - = acidophil, prefers acidic water pH <6.5.

Salt + = halophil, prefers some salt (freshwater, brackish).
 i = oligotrophic, tolerates a little salt.
 - = halophobic, salt intolerant.

Habitat a = aerophil, terrestrial found on damp soils.
 b = benthic, lives on surface in photic zone.
 e = epiphytic, lives attached to waterweeds, specialist benthic.
 p = planktonic, lives in open water, some species are p/b that is live either free floating or attached.

Current l = limnophil, prefers still water.
 i = indifferent.
 r = rheophil, prefers running water.

APPENDIX C

Grid Reference (NZMS 270)	Fossil record no.	Name and age
Mangatera Stream		
U23 75401070	f180	<i>Hyridella menziesi</i> (R)
U23 75280910	f178	Ostreidae <i>Purpurocardia purpurata</i> (Wo?; Wp-R) <i>Ziracolpus blacki</i> (Wc?-R)
U23 75351078	f182	<i>Purpurocardia purpurata</i> (Wo?; Wp-R) <i>Zeacolpus vittatus</i> (Wo?-R) <i>Crepidula radiata</i> (Ld?-Wn) <i>Penion sulcatus</i> (Wm-R) <i>Lamprodomina neozelanica</i> (Sl-Wn)
U23 75031413	f179	<i>Purpurocardia purpurata</i> (Wo?; Wp-R)
U23 75491004	f181	<i>Hyridella menziesi</i> (R)
U23 75401188	f183	<i>Pellicaria convexa</i> (Wn) <i>Alcithoe brevis</i> (Win-Wn)
Mangatewaiiti Stream		
U23 81611783	f175	<i>Austrofuscus glans</i> (Wn?; Wc-R) <i>Zeacolpus vittatus</i> (Wo?-R) <i>Patro undatus</i> (Tk?-Wn) <i>Pleuromeris zelandica</i> (Wm?-R) <i>Zeacumantus lutulentus</i> (Wm-R)

Xymene expansus (Wn-Wc)

Alcithoe fusus fusus (Wn?-R)

Mangatewainui Stream

U23 83701737 f176 *Austrovenus stutchburyi* (Wo?-R)

Whakaruatapu Stream

U23 78431324 f177 *Tucetona laticostata* (Tt?-R)

Zeacolpus vittatus (Wo?-R)

APPENDIX D GRAIN SIZE STATISTICAL DATA

GRID REFERENCE NZMS 270 U23	MEAN (PHI)	STANDARD DEVIATION	SKEWNESS	KURTOSIS	MEAN CUBED DEVIATION	ST-DEVIATION CUBED	< 62 MICRON %	> 500 MICRON %
82661466	3.11	0.39	-0.02	1.06	-0.001	0.06	3.05	0.03
83001513	3.52	0.56	0.28	1.54	0.05	0.18	12.56	0.01
83201560	2.53	1.35	0.27	1.19	0.65	2.46	14.95	2.52
83301570	2.93	0.46	0.26	1.22	0.03	0.10	3.68	0.004
83401635	2.90	0.77	-0.22	1.22	-0.10	0.46	4.58	1.17
83851662	2.44	1.25	0.25	1.35	1.96	1.95	12.44	2.17
83551672	2.07	0.71	0.15	1.01	0.05	0.36	1.48	0.56
83401699	2.21	0.70	0.04	1.10	0.02	0.34	2.31	0.38
83401699	2.35	0.68	0.10	1.14	0.03	0.31	2.85	0.16
83291710	2.63	0.43	-0.002	1.02	0.0	0.08	1.51	0.053
83281723	2.66	0.40	-0.03	1.23	-0.002	0.06	1.48	0.003
83341739	2.42	0.45	0.19	1.15	0.02	0.09	1.26	0.02
82831754	2.67	0.60	0.16	1.04	0.04	0.22	2.59	0.16
82461790	3.23	1.02	0.21	1.33	0.22	1.06	17.83	0.39
81951828	2.67	0.54	0.06	1.25	0.01	0.16	3.43	0.06
81501910	2.94	0.46	0.16	1.14	0.02	0.10	2.84	0.004
82551502	2.08	0.46	-0.04	1.14	-0.004	0.10	1.19	2.19

82351520	3.24	0.64	0.21	1.40	0.06	0.26	8.62	0.004
82421549	2.74	0.68	0.25	1.86	0.08	0.31	7.35	0.003
82251543	1.84	1.43	0.21	1.06	0.34	2.92	9.76	16.11
82101578	2.74	0.44	0.01	1.20	0.0	0.09	0.82	0.03
81621610	2.91	0.65	0.29	1.43	0.08	0.28	7.01	0.02
81621610	2.23	0.59	0.07	0.92	0.01	0.21	0.97	0.20
81601622	2.52	0.40	0.04	0.96	0.003	0.06	0.93	0.01
81601622	2.16	0.22	0.46	0.99	0.005	0.10	1.03	0.024
81421655	3.10	0.69	0.07	1.52	0.02	0.33	7.61	0.13
81421655	1.78	0.80	0.26	1.35	0.13	0.51	3.72	1.57
81351682	3.31	0.69	0.06	1.59	0.02	0.33	8.73	0.08
81061709	2.33	0.74	-0.08	0.85	-0.03	0.41	0.93	0.49
8061174i	3.43	0.96	0.31	2.19	0.27	0.88	17.45	0.04
80611741	1.65	0.78	0.33	1.25	0.15	0.48	1.34	2.53
80611741	3.27	0.67	0.12	1.40	0.04	0.30	8.57	0.003
80611741	2.74	0.68	-0.03	1.14	-0.01	0.31	3.63	0.15
80591743	2.99	0.43	0.28	0.99	0.02	0.08	4.34	0.003
80581749	2.73	0.44	0.03	1.18	0.003	0.09	1.52	0.01

80081858	2.60	0.55	-0.24	1.25	-0.04	0.17	1.06	0.14
80081858	2.85	0.40	0.08	1.27	0.01	0.06	1.84	0.16
78122003	3.23	0.42	0.02	1.24	0.001	0.07	3.77	0.003
81601662	3.12	0.77	0.20	1.17	0.09	0.46	2.74	0.12
80591743	3.92	0.81	0.24	1.32	0.13	0.53	10.26	0.002
80581749	3.36	0.92	0.06	1.20	0.05	0.78	3.08	2.23
78481265	2.68	0.52	0.02	1.05	0.003	0.14	1.38	0.003
78531291	2.63	0.38	-0.06	1.13	-0.003	0.06	1.14	0.003
78811340	2.93	0.49	0.10	1.16	0.01	0.12	2.49	0.15
78811340	3.95	1.68	0.35	1.03	1.66	4.74	45.15	0.01
78751325	2.0	0.39	0.22	0.95	0.01	0.06	0.74	0.003
78751347	2.78	0.43	0.13	1.46	0.01	0.08	2.35	0.042
78661375	2.64	0.43	0.004	1.02	0.0	0.08	0.94	0.003
78351440	3.50	0.86	0.24	1.46	0.15	0.64	18.89	0.02
75300878	2.65	0.61	-0.02	1.34	-0.003	0.23	3.19	0.20
75300878	1.38	0.90	0.29	1.58	0.22	0.73	4.65	9.65
75150953	2.98	0.50	-0.05	1.07	-0.006	0.13	3.23	0.26
75311135	1.48	0.67	0.16	1.29	0.05	0.30	1.17	5.03

75311135	3.57	0.88	-0.07	1.04	-0.05	0.71	1.29	1.24
74851240	2.55	0.46	-0.02	1.07	-0.002	0.10	1.33	0.05
74861245	3.21	0.64	0.16	1.49	0.04	0.26	7.95	0.03
74991312	3.28	0.61	0.20	1.47	0.05	0.23	8.32	0.003
74861310	1.71	0.78	0.12	1.04	0.07	0.48	1.45	4.39
75021384	1.98	0.49	0.25	1.17	0.03	0.12	1.47	0.003
75231440	2.21	0.57	0.03	1.23	0.01	0.19	1.84	0.23
75231440	3.0	0.54	0.12	1.17	0.02	0.16	5.32	0.05
75361462	2.27	0.76	0.14	1.25	0.06	0.44	4.46	1.28
75071498	2.68	0.81	0.20	1.45	0.10	0.53	7.27	0.14
82831485	7.36	1.72	-0.07	0.73	-0.33	5.09		
82661466	6.79	1.73	0.25	0.72	1.30	5.18		
83001513	6.46	1.31	0.42	1.10	0.95	2.24		
83251549	6.06	1.02	0.41	1.28	0.43	1.37		
83201156	6.21	1.47	0.50	1.10	1.59	3.18		
83301570	7.84	1.38	-0.06	0.85	-0.29	2.63		
83571595	6.57	1.60	0.45	0.84	1.84	4.10		
83651620	8.29	1.18	-0.15	0.86	-0.25	1.64		

83401635	7.04	1.83	0.06	0.71	0.36	6.13		
83771658	7.03	1.46	0.27	0.86	0.84	3.11		
83651682	7.98	1.39	-0.18	0.80	-0.47	2.69		
83401699	6.33	1.35	0.48	1.12	2.45	2.46		
83261740	6.56	1.39	0.20	1.03	0.55	2.69		
83151744	8.02	1.41	-0.22	0.82	-0.62	2.80		
83071750	5.77	2.05	0.19	0.94	1.65	8.62		
82691799	4.59	1.46	0.47	1.42	1.47	3.11		
82461790	4.36	1.91	0.32	1.28	2.19	6.97		
81951828	6.34	1.78	0.32	0.87	1.79	5.64		
81841850	6.71	1.79	0.11	0.88	0.62	5.74		
81651881	7.12	2.01	-0.21	0.77	-1.73	8.12		
81501910	5.21	1.87	0.49	0.98	3.17	6.54		
81101931	5.85	2.23	0.24	0.79	2.62	11.09		
81101931	7.42	1.70	-0.09	0.74	-0.43	4.91		
80621982	7.17	1.83	-0.07	0.85	-0.43	6.13		
80421990	8.04	1.25	-0.06	0.80	-0.12	1.95		
79802017	5.96	2.13	0.17	0.88	1.60	9.66		

79692018	4.30	1.44	0.01	1.71	0.02	2.99		
79321980	6.33	1.90	0.22	0.83	1.50	6.86		
83481638	4.51	0.52	-0.03	1.12	0.0	0.14		
82891498	8.38	1.25	-0.30	1.03	-0.59	1.95		
82681495	6.58	1.46	0.31	1.01	0.96	3.11		
82681495	5.50	2.29	0.44	0.77	5.30	12.0		
82581479	6.75	1.73	0.29	0.71	1.49	5.18		
82551502	5.72	1.64	0.40	1.00	1.76	4.41		
82351520	5.56	0.78	0.41	1.67	0.19	0.48		
82301525	5.70	1.03	0.50	1.67	0.54	1.09		
82421549	5.82	0.90	0.36	1.21	0.26	0.73		
82301550	7.93	1.46	-0.19	0.83	-0.60	3.11		
82101562	6.62	1.12	0.28	1.26	0.39	1.41		
81621610	4.93	2.03	0.13	0.87	1.10	8.37		
81621650	4.78	0.92	0.42	2.27	0.33	0.78		
81621650	5.70	0.91	0.51	1.71	0.38	0.75		
81461679	5.89	1.95	0.14	0.96	1.07	7.41		
81461679	6.04	1.72	0.29	1.12	1.47	5.09		

81351682	5.52	1.57	0.09	1.05	0.36	3.87		
81121710	5.24	1.41	0.37	1.24	1.05	2.80		
81061709	5.04	1.51	0.36	1.13	1.25	3.44		
80721740	4.39	1.75	0.38	1.23	2.01	5.36		
80591743	8.29	1.24	-0.20	0.65	-0.38	1.91		
79951810	6.25	1.37	0.31	1.14	0.81	2.57		
80081858	5.83	1.23	0.41	1.33	0.77	1.86		
80081858	6.80	1.66	0.19	0.84	0.85	4.57		
79651870	5.42	1.57	0.21	0.97	0.82	3.87		
79801898	4.83	2.11	0.46	0.93	4.37	9.39		
79801898	7.90	1.44	-0.15	0.87	-0.44	2.99		
79691951	5.88	1.53	0.45	1.09	1.61	3.58		
79521970	6.46	2.23	0.01	0.85	0.15	11.09		
79381965	6.32	1.29	0.29	1.19	0.63	2.15		
78881999	5.73	2.26	0.14	0.86	1.61	11.54		
78291997	6.86	1.82	0.12	0.76	0.72	6.03		
78122003	6.07	1.45	0.41	1.24	1.27	3.05		
82891498	4.48	0.59	-0.02	1.38	0.0	0.21		

79701900	4.32	0.67	-0.04	1.12	-0.03	0.30		
78132013	4.10	1.17	-0.14	1.12	-0.22	1.60		
78501257	6.01	1.88	0.55	0.77	3.65	6.64		
78501257	7.45	1.63	-0.03	0.73	-0.14	4.33		
78471258	7.18	1.48	0.24	0.84	0.77	3.24		
78471267	6.54	1.54	0.23	0.91	0.93	3.51		
78531291	5.10	1.53	0.50	1.27	1.79	3.58		
78571282	6.87	1.90	0.02	0.80	0.13	6.86		
78751325	6.41	2.0	0.13	0.88	1.04	8.0		
78601372	5.82	1.56	0.41	1.01	1.55	3.80		
78661375	5.30	1.72	0.37	1.14	1.88	5.09		
75270865	5.12	1.84	0.36	1.12	2.24	6.23		
75300878	7.37	1.73	-0.05	0.84	-0.24	5.18		
75260890	5.12	1.84	0.36	1.12	2.24	6.23		
75480997	7.25	1.67	0.07	0.74	0.33	4.66		
75391064	6.50	1.80	0.34	0.87	2.0	5.83		
75381120	6.54	1.76	0.15	0.92	0.83	5.45		
75201142	7.44	1.83	-0.21	0.82	-1.31	6.13		

74951182	6.12	2.01	0.08	0.83	0.61	8.12		
74951215	5.95	1.80	0.47	1.07	2.72	5.83		
74901362	5.89	2.24	0.10	0.79	1.07	11.24		
75151400	6.17	1.82	0.29	0.87	1.77	6.03		
75231440	7.09	1.55	0.20	0.84	0.76	3.72		
74851625	4.88	2.27	0.53	0.81	6.22	11.70		
74951548	6.56	1.33	0.35	1.02	0.84	2.35		